An inter-comparison of the climate impact of short-, medium- and long-range aircraft

by

J.T. van der Maten

to obtain the degree of Master of Science in Aerospace Engineering
at the Delft University of Technology,
to be defended publicly on Monday August 23, 2021 at 10:30 AM.

Student number:	4279247	
Section:	Aircraft Noise and Climate Effects	
Thesis committee:	Prof. dr. V. Grewe,	DLR, TU Delft, supervisor
	Dr. F. Yin,	TU Delft, supervisor
	Dr. M.F.M. Hoogreef,	TU Delft

An electronic version of this thesis is available at `http://repository.tudelft.nl/`.

TU Delft

Abstract

Aviation has a growing impact on the earth's climate, due to its emissions causing an increase in the global near-surface temperature. In order to better understand the dynamics by which different aircraft types contribute to this global warming and how this can be mitigated, the impact of different aircraft categories is analysed and compared. These categories are constructed by dividing aircraft into groups with a similar number of seats. Two approaches are employed to assess the climate impact of these categories.

First of all, a global aviation emission inventory is used together with a climate response model, to evaluate the temperature change caused by each individual category. It is found that in absolute terms the middle category with 152-201 seats, and the largest aircraft with over 302 seats will cause cause the largest temperature change by the year 2100, compared to 1940. At the same time, per amount of generated capacity in the form of available seat kilometres, the middle category shows the smallest climate impact of all, with the largest aircraft being the second worst.

From historical positional data of aircraft, flight trajectories are identified, to which an aircraft performance model is applied. This leads to the conclusion that the optimal distance in terms of fuel use is ~2500 km, with an increase in fuel burn for both longer and shorter distance flights. The NO_x emission increases for increasing flight distance, due to higher thrust settings and a higher rated thrust of the engines used. Next to being able to fly longer distances, the three largest aircraft categories cruise at a higher Mach number, increasing fuel use and NO_x emission. Additionally, by flying in a less busy airspace, such as above the Atlantic, the impact of contrails is larger for these aircraft, as there is a smaller atmospheric capacity to form contrails in these areas. Another reason that the largest aircraft perform worse is the higher level of comfort provided to the passengers. It is shown that increasing the seating density to maximum capacity leads to a reduction in fuel use and NO_x emission per available seat kilometre especially for the largest aircraft, narrowing the gap with the smaller aircraft categories which already make use of a high density seating.

Based on the outcome it is suggested to adjust the policies dealing with aviation's climate impact, to reflect the differences between the impact of the different aircraft types. Additionally, a direct reduction in aviation's climate impact can be achieved by making use of the most climate efficient aircraft type for a given mission.

Contents

List of Figures

List of Tables

1

Introduction

Global warming is one of the most debated topics of current times, with humanity facing the challenge of stopping the rapid change of the earth's climate. The large amounts of emissions and resulting climate impact of many sectors, including aviation, are under much discussion. The aviation industry has been showing rapid growth, offering large numbers of people the possibility to travel quickly. As a result the aviation industry has been estimated to account for 3.5% of the overall anthropogenic forcing in 2011 [35], with all projections indicating significant growth in aviation's emissions, up to a factor 5 for CO_2 between 2010 and 2050. [10]

In order to reduce the climate impact of aviation in the future, there are various measures that can be taken. Improving an aircraft's fuel efficiency can lead to a reduction in greenhouse gas emissions, such as CO_2, and as it directly benefits airlines from a cost perspective, there is a clear incentive to invest in this area. Historically, throughout the late 90s and early 00s a close to linear improvement in fuel burn per revenue passenger kilometre (RPK) can be seen, as shown in Figure 1.1. Due to physical limitations of the engine propulsive efficiency, and the aerodynamic efficiency of the typical tube and wing aircraft design, future improvements on the overall aircraft efficiency might require high-level changes to the aircraft design. Such high-level changes could for example take shape in a flying wing aircraft design or changing to a hydrogen based fuel system. [60]

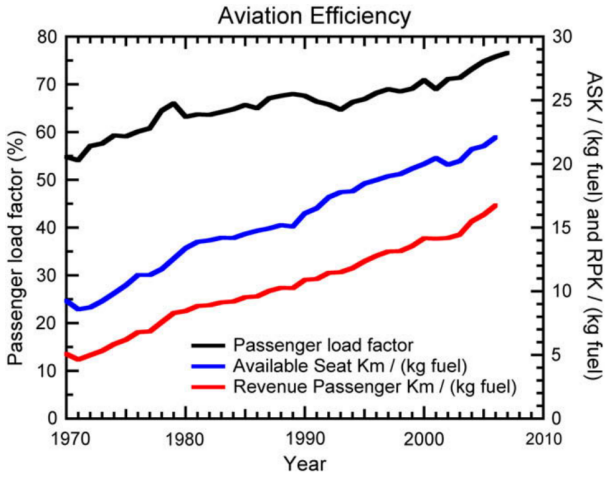

Figure 1.1: Aviation Passenger Load Factor and RPK and ASK per Unit Fuel Burn, taken from [36]

Alternatively, measures can be taken to reduce the climate impact of aircraft, without moving to a radically different design. For the Airbus A330-200 specifically, the climate mitigation potential has been assessed by adjusting the aircraft's operational parameters in both altitude and speed. [6] Adjustments to these parameters showed a potential 42% global reduction in temperature response, at the cost of a 10% increase in cash operating cost, by reducing the cruise altitude and Mach number. Moreover, by also incorporating a design

change a 32% and 54% temperature response reduction was found at a 0% and 10% operating cost increase respectively. This shows that there is significant potential for the reduction of climate impact, both from operational and design changes for this specific long-range aircraft.

In order to effectively take measures aimed at reducing the climate impact of aviation, it is important to understand where this impact originates and where opportunities present themselves in making improvements. The global aircraft fleet consists of a wide range of aircraft, varying, among other things, in age, size and usage. This research aims to answer how the different types of aircraft compare in climate impact, both in absolute and relative terms. This will show what type of flights are currently the most efficient from a climate perspective and which impair overall performance. Ultimately, finding the causes of this difference will aid in formulating a strategy to mitigate the climate impact of aviation. For practical reasons the aircraft are categorised according to size, which directly relates to the range. The resulting research objective is defined as follows:

To contribute to the scientific knowledge on the climate impact of aviation by comparing the impact of different range aircraft, through quantifying their individual contributions, taking into account all relevant emission types and flight operations.

2

Aviation and Climate Change

2.1. Aviation Growth

When looking at air traffic over the past decades, the aviation industry has been showing a rapid growth. Certain events such as the attack on the World Trade Center and the '08 financial crisis have caused the traffic to temporarily dip, but over a longer period aviation has proven to be resilient. Figure 2.1 shows the growth of revenue passenger kilometres over time, indicating the two times doubling of passenger traffic over a 15-year period.

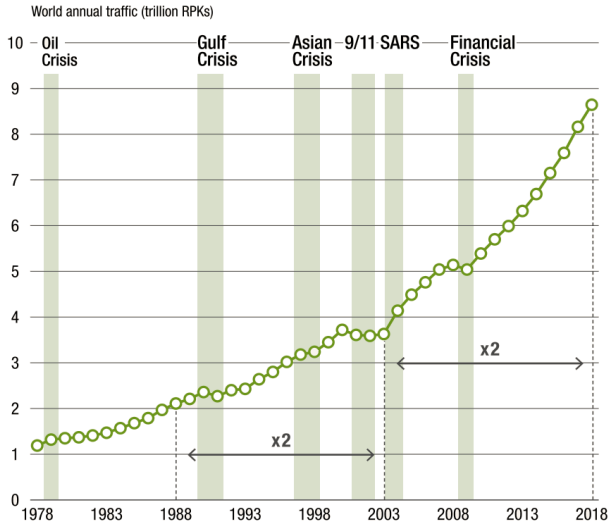

Figure 2.1: Aviation Historical Traffic, taken from [1]

Trying to look forward, the common practice for forecasting the future growth of aviation used within the financial industry revolves around the GDP. Although not scientifically proven, in 2016 it was "widely acknowledged that the number of passengers at airports around the world grow at a rate of about 1.5 times that of the worldwide GDP" [30], albeit with regional variations. This indicates that whenever possible people are wanting to fly more and income is a main factor preventing people to do so. Figure 2.2 shows a traffic forecast made by the ICAO in 2015, which is based on factors including the expected development in GDP, population and travel cost. Without looking much into the exact values of the expected growth, the overall consensus is that the aviation industry has great potential for growth. As long as people are willing to fly and there is no change in the assumed development of factors such as GDP and travel cost, global traffic is likely to show continuous growth throughout the next decades.

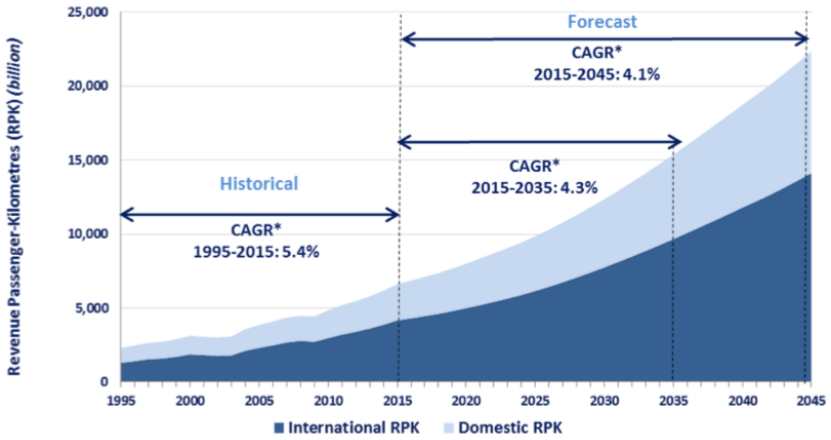

Figure 2.2: ICAO RPK Forecast, taken from [42]

In 2020 COVID-19 caused a major reduction in air traffic, reducing RPKs by as much as 66%, shown in Figure 2.3. This adds to the uncertainty of the industry's size in the future, but does not necessarily affect the long-term potential of the industry if current global conditions are to be temporary. In the short term the main question is how fast the demand could bounce back, as the capacity, for example in airport infrastructure, is still in place. In November 2020 IATA's CEO stated he expects the RPKs to return to the 2019 level by 2024, indicating the expected impact to be short term. [7]

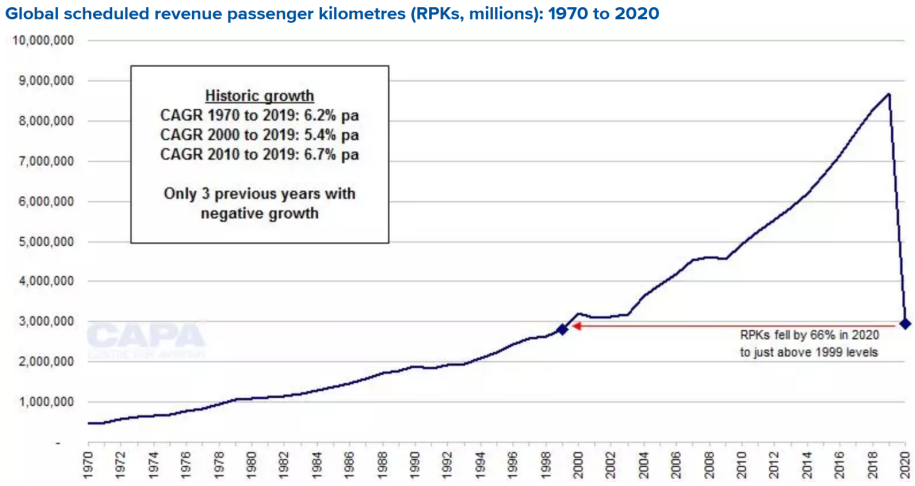

Figure 2.3: CAPA Historical RPKs, taken from [12]

Ultimately, when aiming to address the development of the overall climate impact of aviation, the way in which the size of the industry will change is one of the uncertain factors that play a role. As it stands now, indicators show that there is an ever-growing demand in flights, and the natural growth of the industry as a whole has not slowed down until recently, as COVID-19 struck - potentially a one-time event. Therefore an overall scenario as sketched in Figure 2.2 remains plausible, even though for the next few years the RPKs would be significantly reduced.

What remains true is the currently relevant factor of measures to be taken to reduce the industry's climate impact. Any restriction on flights or increase of the cost base impacts the way in which the industry can grow. For example, French lawmakers have suggested banning short-haul domestic flights that could reasonably be made by train. [3] Such a measure directly reduces the number of flights that are made, and measures taken in the future could significantly change the landscape of the industry. However, how these will affect the industry over the next decades is a case of speculation.

2.2. World Fleet

In 2018 the commercial airline transport fleet consisted of roughly 26,000 aircraft. The global distribution is shown in Figure 2.4. Most of these aircraft are operated in the Americas, followed by Asia Pacific, which is characterised by its recent rapid growth in fleet size. A quarter of the aircraft are based in Europe, and the remainder is taken up by Africa and the Middle East. Within the global fleet there are large variations in aircraft types. A typical classification is dividing the aircraft into narrowbodies, widebodies, regional jets and turboprops. The share of each category is shown in Figure 2.5.

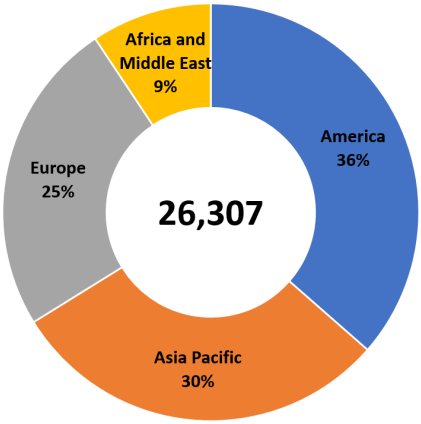

Figure 2.4: Commercial World Fleet by Region, data taken from [4]

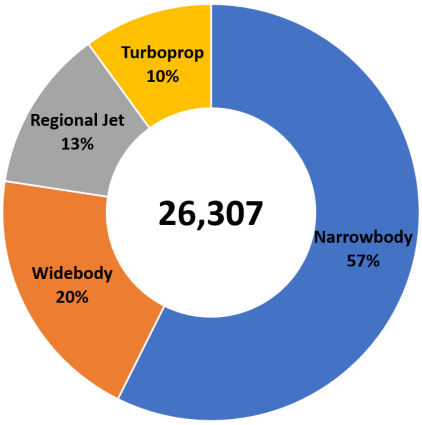

Figure 2.5: Commercial World Fleet by Type, data taken from [4]

Over half of the global fleet consists of narrowbodies. Narrowbody aircraft are defined by having a single aisle seating arrangement, such as the well-known Airbus A320 and Boeing 737. Widebodies have at least 2 aisles and are therefore larger in size. Regional jets are smaller than narrowbodies, and are typically defined by having fewer than 100 seats. Due to their size these aircraft are mostly used for shorter, regional flights. Lastly, as the name suggests turboprops are aircraft driven by propeller engines. Historically airlines have moved to making more use of larger aircraft, as can be seen by the increase in seats per departure in Figure 2.6.

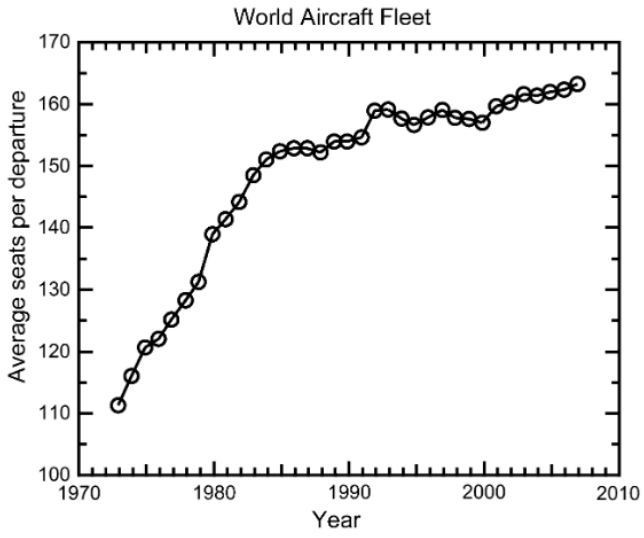

Figure 2.6: Historical Average Seats per Departure, taken from [36]

The seating capacity of an aircraft is not an individual parameter that can be altered without impacting other aspects of the design. Having more seats directly leads to an increase in aircraft size and weight, which in turn affect the fuel that can be carried and the performance parameters, such as the maximum range. In general larger aircraft tend to have a longer range, as can be seen in Figure 2.7, which shows the design range

for a selection of jet aircraft. Note that here the number of seats is described as maximum, assuming a single class configuration, which will give a higher number compared to actual practice. However, this maximum allows for a direct comparison between different aircraft. Particularly for the larger aircraft there is a significant spread in range, seen for example at 440 seats giving a design range between 8000 and 16000 km. For 440 seats specifically, there is a multitude of aircraft variations on the Airbus A340 and Boeing 777, which can carry the same number of passengers but have a different performance. In general it seems that the larger the aircraft, the longer the range is that can be obtained, while also having more design freedom indicated by the larger spread.

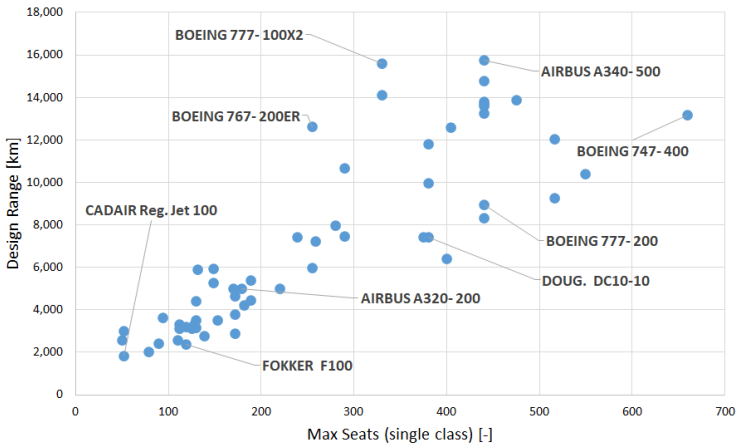

Figure 2.7: Design Range vs Maximum Seat Capacity, data taken from [31]

Figure 2.8 shows how airlines make use of different aircraft sizes for their routes. The figure is based on worldwide air traffic data from 2003 until 2012; it shows the share of each aircraft category for each type of segment defined by distance and monthly passenger volume. Next to showing that larger aircraft are more often used for longer segments, it also shows a different effect, namely that on busier routes larger aircraft are being used. This means that in order to increase the overall capacity on a certain segment, airlines are choosing to increase their equipment capacity, as opposed to solely increasing flight frequency. [32]

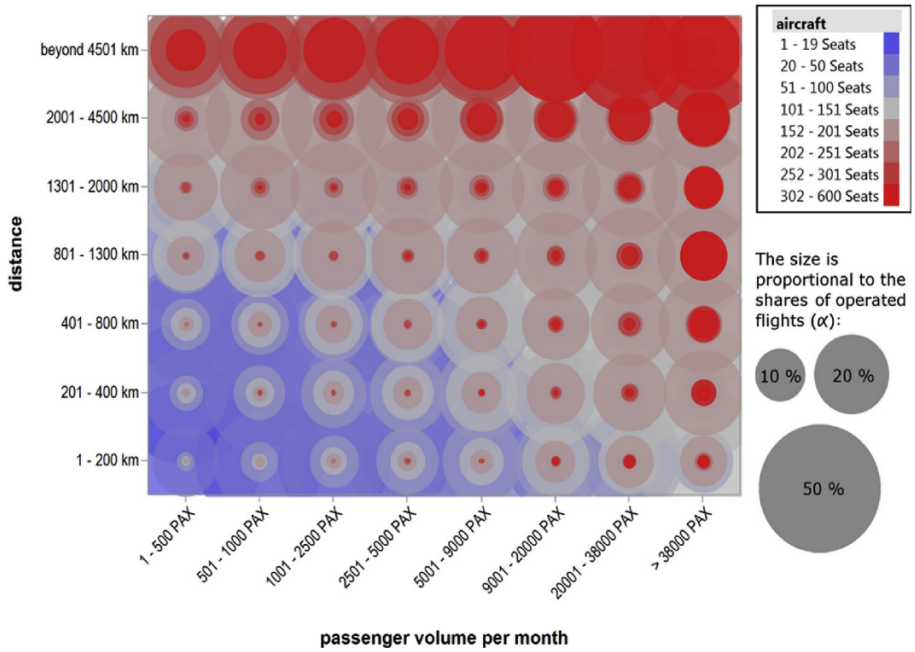

Figure 2.8: Distribution of Aircraft Sizes for Distance and Passenger Volumes, taken from [32]

In fact, the findings suggest a continuous relation, as shown in the example for the ranges beyond 4501 km in Figure 2.9. Curves are defined by a Gaussian function, which resulted in a coefficient of determination above 0.93 on average for the dataset. For smaller passenger volumes there is a clear preference for smaller aircraft, whereas for the busiest routes the largest aircraft dominate. Ultimately, this indicates that airlines do have some freedom in aircraft selection for their different routes and the reason for using larger aircraft is not solely due to being restricted by the required flight range.

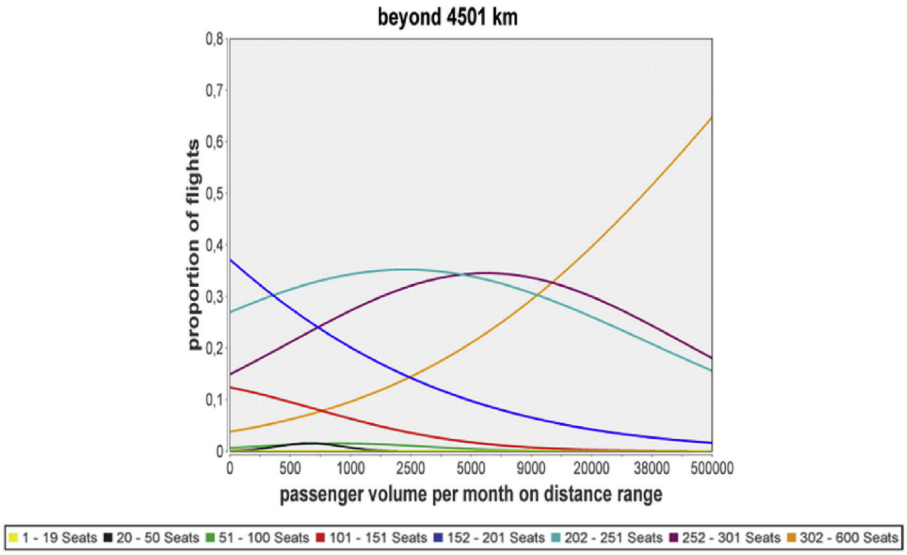

Figure 2.9: Continuous Distribution of Fleet Mix, taken from [32]

2.3. Climate Change

The ever-growing volume of air traffic leads to questions on the climate impact of the aviation industry. By burning jet fuel aircraft emit greenhouse gases and other species affecting the atmosphere at various altitude levels. In 2005 aviation was estimated to represent 3.5% of the anthropogenic forcing [35], a number which could increase taking into account the growth of the industry, and other industries moving to greener solutions. Weight limitations and safety restrictions constrain freedom in aircraft design, which complicates a transition similar, for example, to cars moving to driving electric. Still, there is a need for a cleaner way of flying, with a reduction in climate impact. In order to achieve this, it is first necessary to understand how aviation contributes to climate change, with the focus in this research being on comparing the impact of different aircraft based on their size and range.

As this research aims to address the climate impact of various aircraft types, it is first needed to define what this term entails. As aircraft burn fuel, the resulting emissions enter the atmosphere and what follows is a chain of effects described in Figure 2.10. Whereas the mass of the emitted agents due to the burning of fuel can be calculated with a relatively high certainty, the result has little direct scientific value as it gives no information on the ensuing impact it has on the global climate. In contrast, quantifying the impact or damage as indicated in Figure 2.10 would require an in-depth modelling of the earth's response to climate change, which would increase the uncertainty in the outcome and is not within the scope of this research.

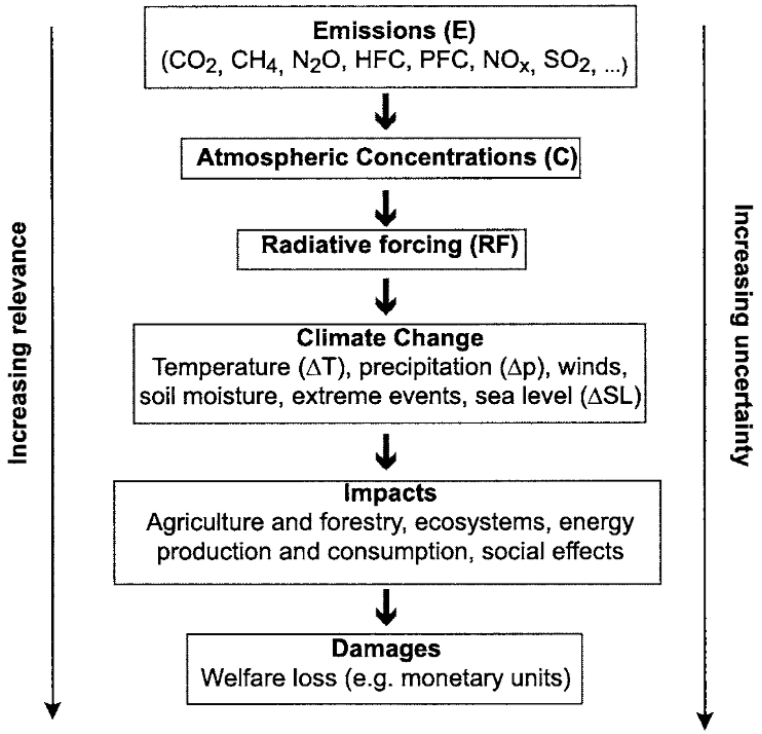

Figure 2.10: Cause-Effect Chain from Emissions to Climate Change and Damages, taken from [13]

Radiative forcing is a widely used climate metric, making results of different research accessible and easy to compare. However, there are different definitions of the term. A commonly used version is the stratosphere-adjusted radiative forcing, defined by the IPCC:

"The radiative forcing of the surface-troposphere system due to the perturbation in or the introduction of an agent (say, a change in greenhouse gas concentrations) is the change in net (down minus up) irradiance (solar plus long-wave; in $W\,m^{-2}$) at the tropopause AFTER allowing for stratospheric temperatures to readjust to radiative equilibrium, but with surface and tropospheric temperatures and state held fixed at the unperturbed values" [52]

This means it describes changes in the radiation balance without taking into account secondary effects on the surface and troposphere. Often concentration changes are calculated from past emissions, which are then imposed on pre-industrial atmospheric conditions. [21] Additionally, radiative forcing is typically shown as globally averaged value, even though spacial fluctuations occur depending on the location of emission for certain agents.

For steady-state conditions the near-surface temperature change is close to the linear product of the RF and the so-called climate sensitivity parameter, λ ($K(Wm^{-2})^{-1}$). [34] Although originally considered to be a constant, it was later found that this sensitivity parameter depends on the type of perturbation, and as such RF cannot be easily converted into a temperature change. [34] Furthermore, as RF is about a single point in time, comparing the RF of different emissions does not take into account the different time periods over which these emissions have effect. For example, it can take decades for CO_2 to be removed from the atmosphere while soot aerosols have a lifetime of about a week. [53]

Additional to RF another term called effective radiate forcing (ERF) has been introduced. [28] Whereas the RF concerns the changes in the tropopause after allowing for a new equilibrium to be found, the ERF term includes rapid adjustments of the earth's surface and troposphere. For greenhouse gases both RF and ERF terms yields similar values, and mainly differences are found when comparing the forcing for example of clouds and aerosols-cloud interactions. In these cases ERF has shown to be the better indicator of the surface temperature response. [28]

Ultimately, in order to find a meaningful answer to address the climate impact of various aircraft types, the associated near-surface temperature change is the main factor of interest, going a step further than the radiative forcing, but not moving into the more uncertain area of impact on an ecosystems scale. This near-surface temperature change will be globally averaged, making it a general term for global climate change, as opposed to giving details on local effects.

2.4. Aircraft Emissions

Aviation is a source of various emissions that alter the composition of the atmosphere, resulting in a change of climate on a global scale. Aircraft engines for example emit the well-known CO_2 which has a long lasting impact, as well as shorter lasting emissions such as NO_x. [34] Another main contribution to climate change is made by contrails and the resulting induced cirrus cloudiness. Combined, the effective radiative forcing of aviation was estimated to be 100.9 mWm^{-2} in 2018. [35] Figure 2.11 shows the ERF estimates for the various species and individual effects of aviation, additionally the 5-95% confidence intervals are given. The last column shows the confidence levels of the different species. Only for CO_2 the confidence level is considered high, and for all other effects the 5-95% confidence interval covers a significant range.

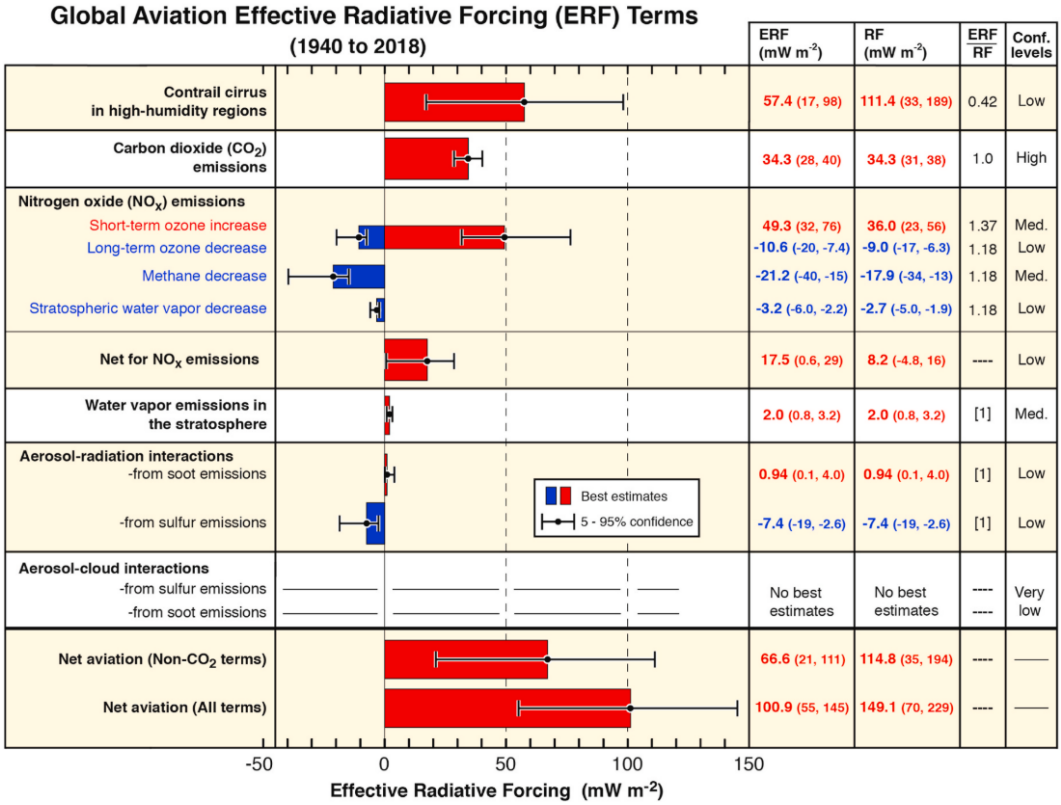

Figure 2.11: Aviation Climate Forcing Best-Estimates, taken from [35]

2.4.1. CO_2

Currently CO_2 is the largest global contributor to radiative forcing; relative to 1750 emissions of CO_2 have caused an RF of 1.68 [1.33 to 2.03] Wm^{-2} in 2011. [28] The largest source of anthropogenic CO_2 emission is fossil fuel burning, next to others such as cement production and deforestation. [28] In 2018 aviation's ERF due to CO_2 was estimated to be 34.3 mWm^{-2}. [35] Over the last decades the atmospheric CO_2 concentration has been increasing rapidly, as depicted in Figure 2.12.

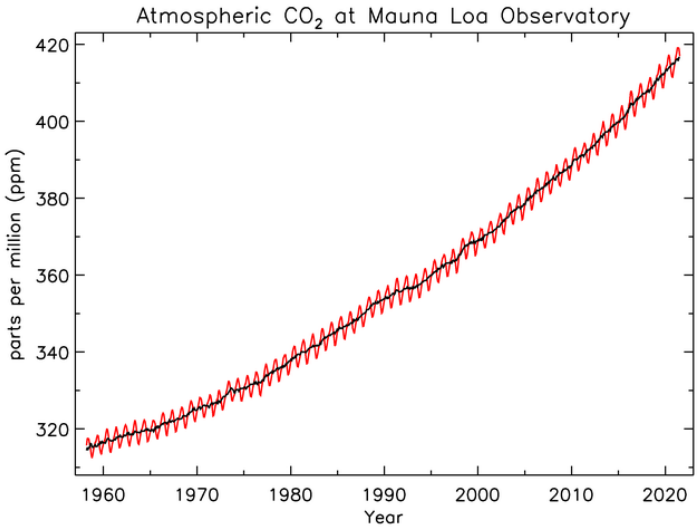

Figure 2.12: Monthly Average Atmospheric Concentration of CO_2 at Mauna Loa (red) and trendline (black), taken from [33]

Only a part of the carbon in the Earth System is represented by atmospheric CO_2. The rest is found in other reservoirs, such as the biosphere, ocean, rocks and sediments. Between these reservoirs carbon is exchanged, described by the carbon cycle. CO_2 in the atmosphere is removed by various natural processes, each with different timescales as shown in Table 2.1. Because of this, the effects of CO_2 do not apply on a single timescale. [28]

Table 2.1: The main natural processes that remove CO_2 consecutive to a large emission pulse to the atmosphere, their atmospheric CO_2 adjustment time scales, and main (bio)chemical reactions involved, taken from [28]

Processes	Time scale (years)	Reactions
Land uptake: Photosynthesis–respiration	$1–10^2$	$6CO_2 + 6H_2O + \text{photons} \rightarrow C_6H_{12}O_6 + 6O_2$ $C_6H_{12}O_6 + 6O_2 \rightarrow 6CO_2 + 6H_2O + \text{heat}$
Ocean invasion: Seawater buffer	$10–10^3$	$CO_2 + CO_3^{2-} + H_2O \rightleftharpoons 2HCO_3^-$
Reaction with calcium carbonate	$10^3–10^4$	$CO_2 + CaCO_3 + H_2O \rightarrow Ca^{2+} + 2HCO_3^-$
Silicate weathering	$10^4–10^6$	$CO_2 + CaSiO_3 \rightarrow CaCO_3 + SiO_2$

In 2018 aviation accounted for 2.4% of global CO_2 emissions due to fuel use and has increased 32% over the previous 5 years. [19] For burning jet fuel a constant emission index of 3.16 kg CO_2 per kg of fuel has been widely accepted [19, 34, 61], allowing for a straightforward translation between fuel and CO_2 mass. Additionally, the atmospheric CO_2 concentration changes caused by aviation are globally uniform [34], making that the location of the emission is of no importance when quantifying CO_2 climate impact.

On the topic of aircraft range and CO_2 emissions, Park and O'Kelly [43] have estimated the average fuel burn per stage length, shown in Figure 2.13. Their approach is based on combining flight schedules for a one-year period within 2012-2013, with a fuel burn model derived from EMEP/EEA aviation inventory data. In general, findings show that flying short distances is fuel inefficient due to the higher frequency of landings and take-offs. However, long-range flights have the downside of having to carry additional fuel during the flight in order to extend the range, which increases the average fuel burn. In the end, the optimal stage length CO_2-wise was found to be 1500-2000 nautical miles, or 2780-3700 km. Here the fuel burn is ~0.04 kg per seat nautical mile, which translates to 68 grams of CO_2 per seat-km using the emissions index of 3.16 kg/kg.

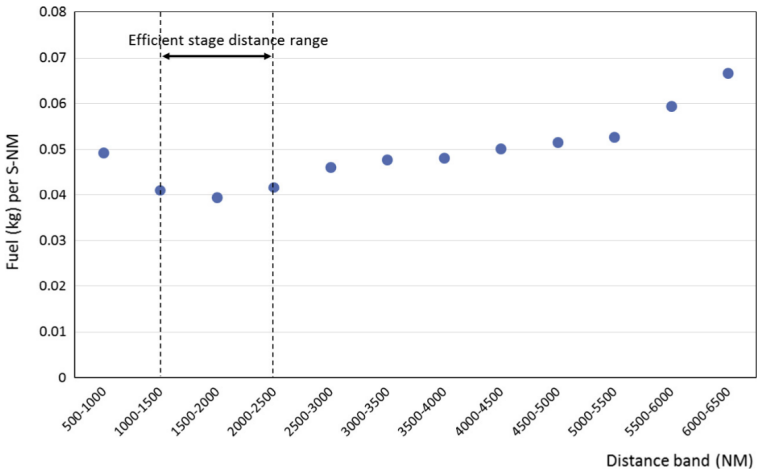

Figure 2.13: Average Fuel Burn vs Stage Length, taken from [43]

Similar work has been done by Graver, Zhang and Rutherford. [19] Again, flight schedule data is used, now for calendar year 2018. In this case 'Piano 5' software was used to estimate the fuel burn, which is based on both private and public sources of aircraft performance data. A graph of emissions vs stage length can be seen in Figure 2.14. The red line indicates the grams of CO_2 emitted per RPK, whereas the bars show the share of total emitted CO_2 mass for each group of flight distances.

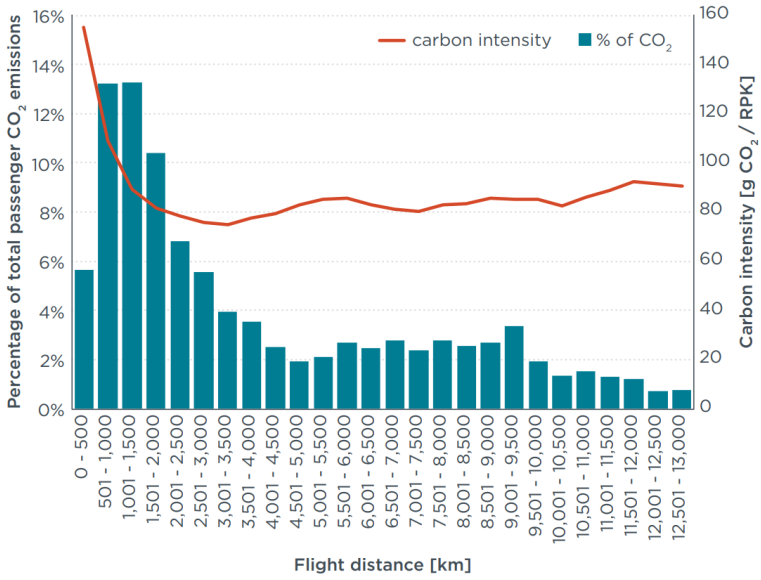

Figure 2.14: CO_2 Emission vs Stage Length, taken from [19]

As opposed to the previous graph results are expressed per passenger rather than per seat, which makes that the results cannot be compared one-to-one. However, the most CO_2-efficient stage length is again found to be between 3000-3500 km, with the lowest being 75 grams of CO_2 per RPK. The biggest difference between the two results is the slope of the fuel/emissions after the optimal point. Over the same range the estimated fuel burn per seat nautical mile increases by more than 50%, whereas the estimated carbon intensity per RPK increases less than 30%. The differences between the two are expected to be largely caused by the different fuel burn modelling approaches, but could also be (partially) due to a change in passenger load factor over increasing stage length, or a change in fuel efficiency between the two time periods.

2.4.2. NO_x

NO_x itself is not a greenhouse gas and as such does not directly lead to a temperature change. It does, however, play a large role in the atmospheric composition, by reaction with other climate agents. It mainly leads to a production of ozone (warming) and reduction of methane (cooling).

NO_x emissions of aircraft consist of NO and NO_2, at varying ratios depending on thrust levels. On a common single-aisle aircraft jet engine the percentage of NO_x represented by NO_2 was measured to be up to 80% at low power settings, reducing to 7% at the highest thrust. [62] Research in 1997 found a best estimate of 0-15% during cruise [50], but this value is engine dependent and could since have changed due to technological advancements. Additionally, the amount of NO_x emitted per kilogram of fuel burned, the emission index, varies with thrust. The NO_x emission index is lowest at engine idle, and increases with increasing thrust setting, as can be seen in Figure 2.15.

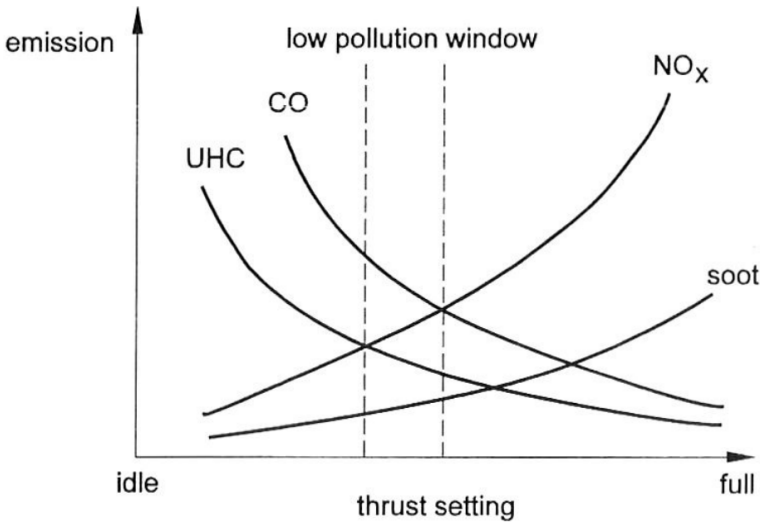

Figure 2.15: Emission Indices vs Thrust Setting, taken from [38]

Additionally, larger engines tend to emit more NO_x per kilogram of fuel. Figure 2.16 displays the emission indices as given by the ICAO engine database [41], which is a collection of aircraft engine data as provided by the manufacturers. Two thrust settings from the database are displayed as an example, showing both the increasing emission index for higher thrust settings and higher rated thrust (larger) engines.

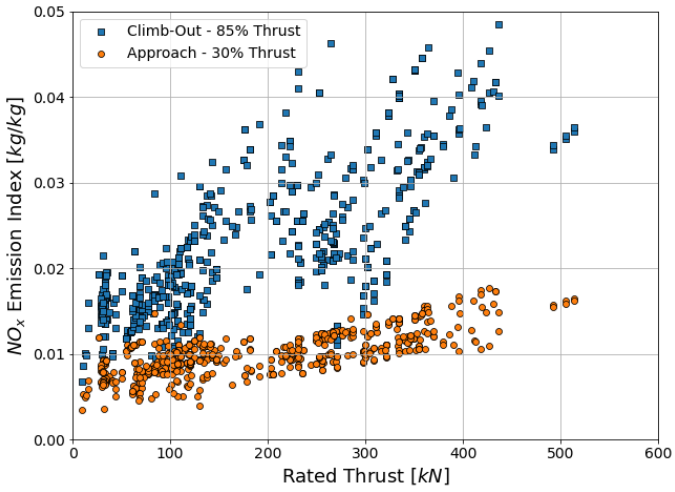

Figure 2.16: NO_x Emission Index vs Engine Thrust by Thrust Setting, data taken from [41]

As opposed to CO_2, the location of the emitted NO_x and the associated atmospheric conditions have a strong influence on the impact of the emission. Where for CO_2 an emission index could be used to quantify the total emitted mass from the fuel usage, doing so for NO_x serves little direct purpose as the total mass cannot be used to directly quantify or compare climate impact. For example, aircraft were estimated to account for 2% of total NO_x emissions from man-made and natural sources in 1997 [37], while it accounted for 30-40% of the NO_x tropospheric burden of the Northern Hemisphere in 1990 [22], indicating the relevance of the location at which emission takes place. The total effective radiative forcing of aviation due to NO_x, including its cooling and warming effects, was estimated to be 17.5 mWm^{-2} in 2018. [35]

The effect of NO_x emissions on ozone levels strongly depends on the altitude of the emission. In the troposphere and lower stratosphere, altitudes at which aircraft typically cruise, under the influence of solar radiation NO_x contributes to the production of ozone through oxidation of carbon monoxide, methane and higher hydrocarbons. Higher in the stratosphere other processes gain importance, and here additional NO_x leads to a decrease of ozone levels rather than an increase. [14] Figure 2.17 shows how the global warming potential of NO_x varies with altitude, with a peak around an altitude of 12 km. The example mentioned is valid at mid-latitudes during summer, which would be different for other locations and seasons. [38]

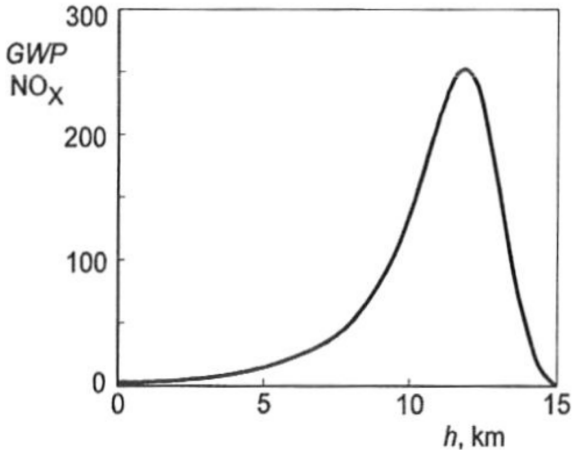

Figure 2.17: NO_x Global Warming Potential vs Altitude, taken from [38]

The formation of ozone is the most important effect caused by NO_x emission. The main O_3-related processes in the troposphere are shown in Figure 2.18. Hydrocarbons are converted into CO, which in turn converts into CO_2 and within this process O_2 is used to create HO_2. Ultimately, this HO_2 together with NO lead to a production of NO_2, which, under the influence of sunlight, leads to a production of O_3. Peroxyacetyl radicals from photolysed NMHC compounds can react with NO_2 to form peroxy acetyl nitrate (PAN), which can be transported over long distances before subsiding and eventually decomposing. [34] The reaction between NO_2 and OH leads to the formation of HNO_3 or nitric acid, which causes removal of nitrogen compounds through rain-out.

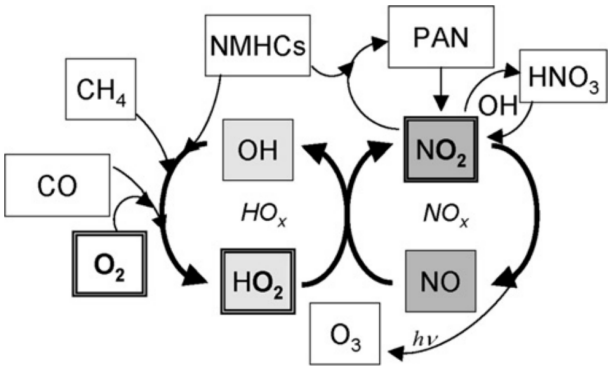

Figure 2.18: Main Tropospheric O3-Related Chemistry, taken from [34]

As can be observed in Figure 2.18 within these reactions there is a destruction of methane as it reacts with OH.

$$CH_4 + OH \rightarrow CH_3 + H_2O \tag{2.1}$$

With ozone and methane being greenhouse gases, the ozone production leads to a warming effect, whereas methane destruction leads to a cooling effect, ultimately with the warming effect being more prominent.

In addition to the direct effect of NO_x, some factors need to be taken into account to estimate its impact. One of these is 'primary mode ozone'; due to methane being part of the reactions leading to the creation of ozone, the destruction of methane leads to decreased background ozone levels. Next to this, the amount of methane entering the stratosphere and decomposing into water vapour and carbon dioxide, is reduced, which together with the primary mode ozone leads to a cooling effect reducing the total radiative forcing caused by NO_x emissions. [24]

2.4.3. Water Vapour and Contrails

Similar to other greenhouse gases, water vapour leads to a direct warming effect when present in the atmosphere. For the year 2018 aviation's H_2O direct radiative forcing was estimated to be 2.0 mWm^{-2}. [35] When H_2O is emitted in the troposphere its residence time is very short, resulting in a relatively small warming effect compared to H_2O emitted in the stratosphere, where water vapour can accumulate longer. [11]

Contrails form during the mixing of hot and humid engine exhaust with the drier and cooler surroundings. As the air saturates with respect to water, droplets are formed, which can freeze under low temperatures, ultimately leading to contrail formation. For known conditions, whether contrails are formed can be assessed through the Schmidt-Appleman Criterion. [2] Because water vapour cannot directly transform into ice, during the mixing a moment is required in which saturation with respect to liquid water is reached. Whether or not this happens depends on the water vapour pressure and temperature of both the air and exhaust. The process of isobaric mixing in shown in Figure 2.19.

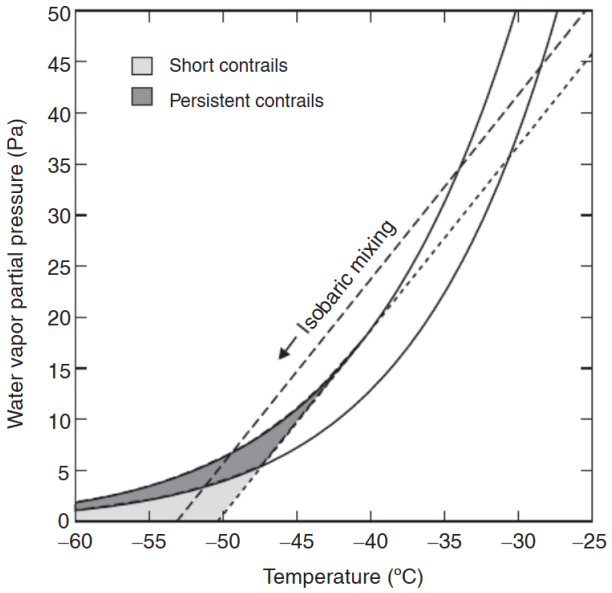

Figure 2.19: Temperature - Water Vapour Partial Pressure Phase Diagram of Contrail Formation via Isobaric Mixing of Hot Exhaust Gases with Cold Ambient Air, taken from [16]

The two curves describe the water saturation partial pressure with respect to water (upper) and ice (lower). The straight lines are examples of mixing trajectories, going from the exhaust (upper right) towards ambient (lower left) conditions. In order for contrails to form this line has to cross the water saturation curve, such that droplets are formed. In addition to the criteria for the formation of contrails, in order for contrails to persist the ambient conditions need to be at a phase point within the dark grey, or so-called ice supersaturated region. On average, flights at cruise level are within such a region about 15% of the time. [16] Persistent contrails can spread out due to the wind, transforming into cirrus clouds, increasing its area of effect.

Contrails and cirrus clouds reduce incoming short wave radiation and outgoing long wave radiation. [15] The total warming effect of linear contrails and especially its induced cirrus cloudiness is highly uncertain. For 2018 their combined effective radiative forcing was estimated to be 57.4 mWm^{-2}, higher than that of CO_2. [35] The effective radiative forcing due to contrails is significantly lower than its conventional radiative forcing, due to the reduced radiative impact of natural clouds in the presence of contrail cirrus. [44] This can be seen in Figure 2.20, as the coverage of natural cirrus decreases for an increasing contrail cirrus coverage. The two sources are effectively competing to condensate the available supersaturated water vapour in the ambient atmosphere. [44] It is suggested that in the context of aviation climate impact contrails play a smaller role than assumed so far.

An important factor affecting the influence of contrails is cloud saturation. Figure 2.20 shows for an estimated 2050 air traffic density, how the cloud coverage at a given altitude changes for an increasing amount of traffic. Whereas the 2050 inventory results in a mean contrail cirrus coverage of roughly 1%, in order to obtain the double amount of coverage air traffic needs to increase by a factor 6. As air traffic increases additional cloud formation is reduced, due to aircraft flying in areas where clouds have already been formed.

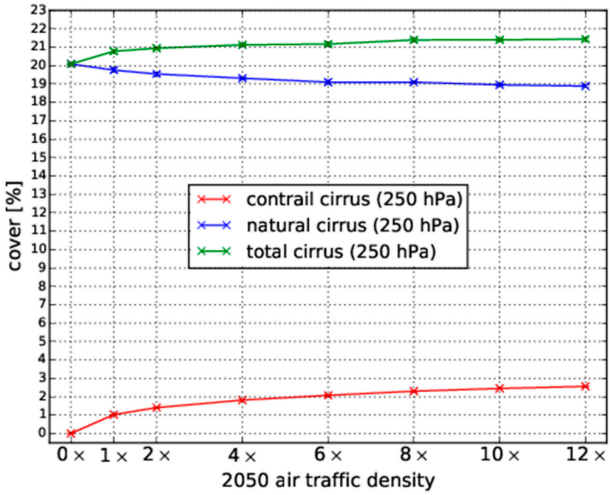

Figure 2.20: Global Mean Coverage of 2050 Aviation Inventory, taken from [44]

2.4.4. Aerosols

Aviation aerosols have both a direct effect due to scattering and absorption of solar radiation and an indirect effect due to their influence on other agents. [34] The direct effects are near zero, with the indirect effects making up the majority of the response. [15] Aerosols indirectly influence cloudiness by acting as ice nuclei, causing the creation of soot cirrus and modifying ambient cirrus cloud properties. [34] The effects of aerosols operate on a timescale of roughly a week.

3

Methodology

In order to assess the climate impact of the different aircraft types, two approaches are used. First of all, an inventory of aviation including the distribution of fuel and emissions is used, in combination with a climate response model to analyse the overall impact of aviation and its subcategories of aircraft. Additionally, an aircraft performance model is applied to flights identified from historical aircraft positional data, so that more details can be provided on the causes of the differences in climate impact between aircraft.

3.1. Climate Assessment of Aircraft Categories

3.1.1. WeCare Inventory

At the basis of the further analysis is a database containing information about the global spacial fuel burn and emissions from aircraft in 2012, constructed by the DLR within their 'WeCare' project. [23] Based on the routes flown that year, a model is applied generating the trajectories and calculating the fuel burn and emissions for each route. The resulting database holds information on the the fuel burned, distance flown and NO_x emitted on a 3D grid, with a resolution of 1 degree in longitude and latitude and 25 altitude levels from sea level to 178 hPa.

Within this database, a distinction is already made between aircraft categories based on their size. Seven different categories are defined, characterised by the amount of seats within the aircraft. The same categorisation will be used throughout the analysis, as it effectively separates the different aircraft of interest within this research. Table 3.1 shows the definition of the different categories, together with examples of commonly used aircraft within each category. Referring to the aforementioned aircraft types, categories 1 and 2 contain turboprops and regional jets, narrowbody aircraft are found within categories 3 and 4, and widebody aircraft are found within categories 4 and up. This means category 4 is a mix of single and twin aisle aircraft. Due to the different seating configurations available for a given aircraft model, it is possible for a certain model to have versions occurring in multiple different categories. Aircraft with fewer than 20 seats are excluded from this research as they are not of interest, the focus being on the aircraft commonly used by airlines worldwide.

Table 3.1: Definition of the Different Aircraft Categories

Category	Seats	Examples
1	20-50	Embraer ERJ140
2	51-100	Embraer ERJ170
3	101-151	Boeing 737-700, Airbus A319
4	152-201	Boeing 737-900, Airbus A321
5	202-251	Airbus A330-200
6	252-301	Boeing 787-900, Airbus A340-300
7	302+	Boeing 747-400, Airbus A380-800

Figure 3.1 displays the total fuel burned by the different categories in 2012. Categories 4 and 7 account for the largest part of the overall fuel burn, while the smallest 2 categories have a fuel burn that is infinitely smaller. This is in line with expectations as Figure 2.5 showed that regional jets and turboprops together make up only 23% of the world fleet, and as they are smaller in size are capable of a smaller fuel burn per aircraft. Furthermore, this indicates that aircraft with the number of seats being between 152-201, are more commonly used than their adjacent categories (or have a significantly higher fuel burn rate), and the largest aircraft have the largest fuel burn overall, given that this comprises all aircraft that have 302 or more seats.

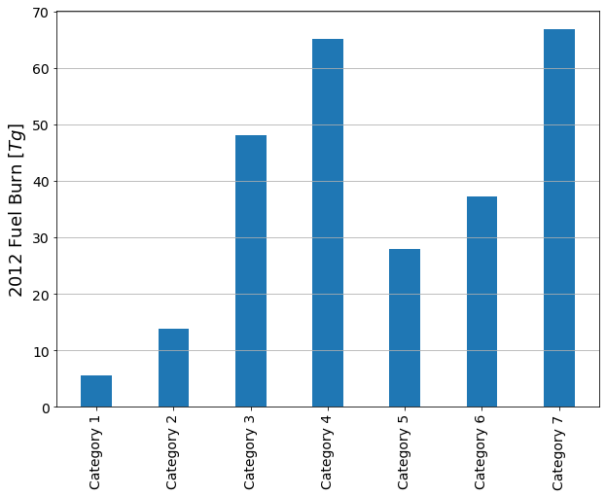

Figure 3.1: 2012 Fuel Burn by Category

The distribution of the fuel burn globally can be seen in Figure 3.2. Due to the large differences in fuel use per area, a logarithmic scale is applied. Three main areas show a high density of fuel use, which are the US, Europe and Southeast Asia. High frequency routes can also be distinguished, such as the Cross-Atlantic flights between Europe and the US. Ultimately, the global fuel use of aviation is far from evenly distributed and a few hot-spots make up the majority of air traffic.

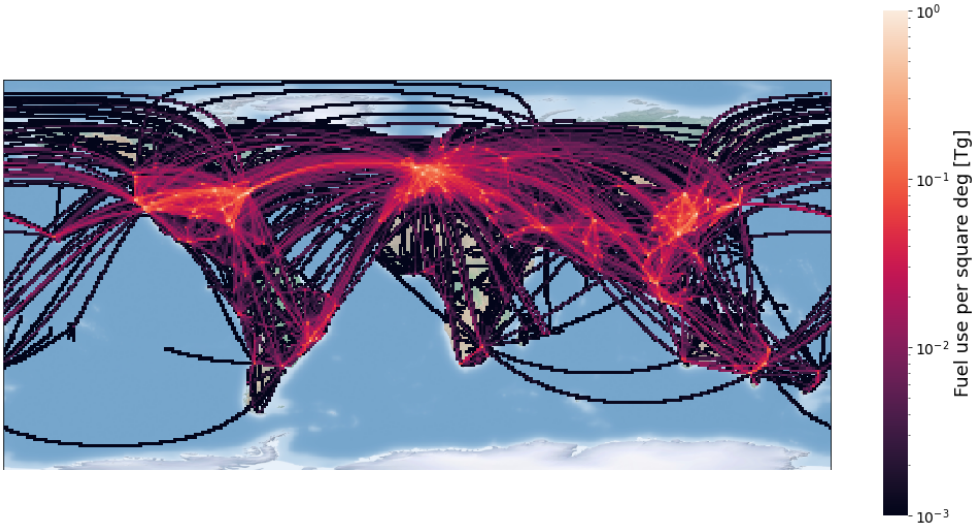

Figure 3.2: 2012 Global Aviation Fuel Distribution

Figure 3.3 shows the fuel distribution versus altitude for the 3 of the 7 different categories. As one would expect, the majority of fuel is burned at cruise level, as well as a slight increase at ground level due to the high

thrust take-offs. The relative difference between the cruise level and ground level peak is largest for the categories with the largest aircraft. This is related to the range increasing with aircraft size, as shown in Figure 2.7. As the highest categories typically have a longer range, the cruise section makes up a larger portion of their flights, which is the reason for this cruise level peak to be larger relatively.

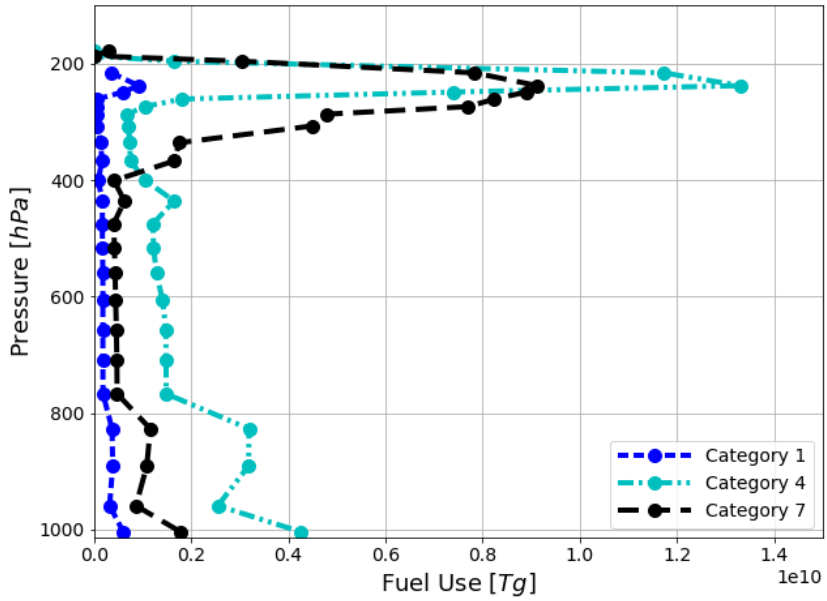

Figure 3.3: 2012 Fuel vs Altitude by Category

The emission indices found in Figure 3.4 show how many grams of NO_x is emitted per kg of fuel burned overall for each category. The smaller aircraft have a slightly lower emission index than the largest. One clear difference is found in the NO_x emission index of category 3. Potentially, this could be due to flying at higher thrust levels or the engines used having high NO_x emissions as standard. Figure 3.5 shows the average amount of fuel burnt per kilometre flown. Since larger aircraft fly at a higher absolute thrust, it makes sense that as the size increases, so does the fuel required to fly a certain distance. Notable is the rather slight increase from category 2 to 4, where even though the size is significantly increased, the fuel burn is close to equal. This can be a result of both the engine efficiency as well as operational differences.

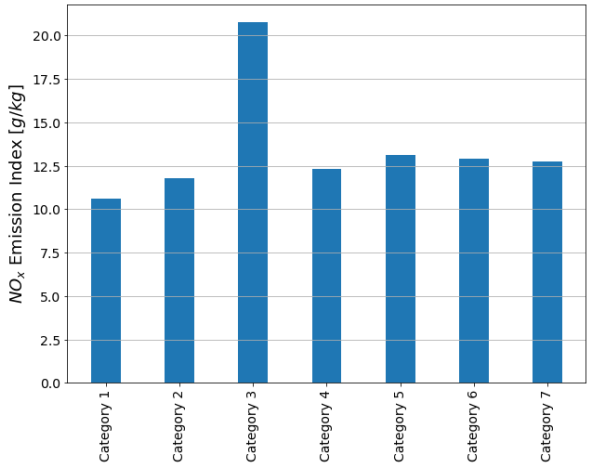

Figure 3.4: 2012 NO_x Emission Index by Category

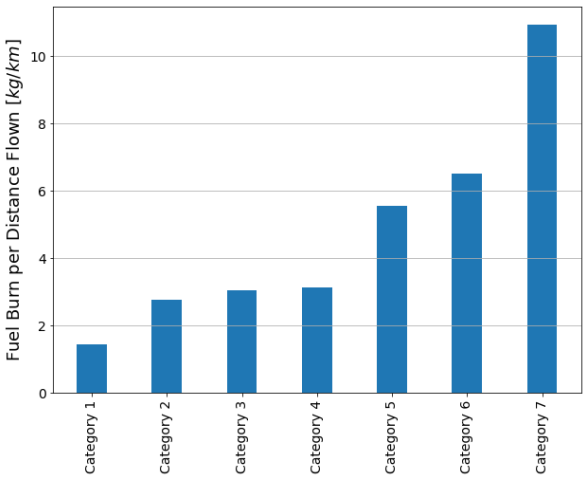

Figure 3.5: 2012 Fuel Burn per Distance Flown by Category

3.1.2. AirClim

In order to assess the climate impact of aviation emissions, AirClim [20] is used. AirClim is a climate response model, extended from a linear response model constructed by Sausen and Schumann. [46] A main difference is that AirClim resolves the effects of emission on a 3D grid, as opposed to the approach of using global mean values. After the initial introduction of the model, it has been adopted to include effects of long-term ozone depletion and contrail cirrus. [5]

At the basis of the AirClim model are pre-calculated atmospheric data, derived from steady-state simulations performed using the E39/C climate-chemistry model [25], which comprises a combination of a chemical and circulation model. This data contains chemical perturbations and radiative forcing of ozone, methane, water vapour and contrails, calculated for the predefined emission regions with a normalised emission strength. [20] In essence, this describes the sensitivity to a certain perturbation, which, combined with a set of emissions, is used to obtain the radiative forcing of this input. The development of radiative forcing in turns leads to a temperature response, using the approach by Sausen and Schumann [46], where RF^* is the normalised radiative forcing with respect to CO_2, and G represents the Green's function for near-surface temperature response.

The temperature change in Equation 3.1 is given by the convolution integral combining the normalized radiative forcing of a species with the Green's function. This function, shown in Equation 3.2, describes the impulse response of the earth's surface to a given forcing. Here α and τ are constants, describing the response time and temperature change over this time respectively. The values used are 36.8 years and 2.246/36.8 K/year. The normalised forcing in Equation 3.3 is found by summing the components of the individual species. This component is found by dividing the radiative forcing by that of CO_2, which is then multiplied by the climate sensitivity parameter λ, which has also been normalised by that of CO_2. The climate sensitivity parameter for the different species is shown in Table 3.2. Lastly, this is multiplied by the mixing ratio divided by the global mean.

$$\Delta T = \int_{t_0}^{T} G(t-t')RF^*(t')\,dt' \tag{3.1}$$

$$G(t-t') = \alpha e^{-\frac{t-t'}{\tau}} \tag{3.2}$$

$$RF^*(t) = \sum_{species} \frac{RF^{species}}{RF^{CO_2}} \lambda^{eff}_{species} \frac{\Delta C_i(t)}{\overline{C^{species}}} \tag{3.3}$$

Table 3.2: AirClim Climate Senstivity Parameters

Species	λ
CO_2	0.73
H_2O	0.83
O_3	1.00
CH_4	0.86
Contrails	0.43

For verification purposes, AirClim has been compared to the more detailed E39/C model, in both a supersonic and subsonic test case, of which the subsonic case is relevant to this research as this concerns similar aircraft. In this case, the effect of air traffic as a whole is compared to a scenario without any air traffic. In the subsonic test case it was found that the radiative forcing from various climate agents, except for water vapour, are reproduced within 15%, making the model applicable to subsonic air travel. [20]

As one of the inputs for the model, background levels of methane and CO_2 are needed for the entire period over which calculations will be performed. As this includes the atmospheric changes in the future, a certain scenario needs to be assumed. For example, the IPCC has published the so-called SRES scenarios, which include the development of emissions based on the anticipated changes in demographics and technology. [27]

Similarly, IPCC's Representative Concentration Pathways (RCPs) [29] are projections of greenhouse gases up to the year 2100, but with a larger focus on the global warming targets and impact of different measures, rather than the socio-economic model. The concentration development of the different RCPs is shown in Figure 3.6.

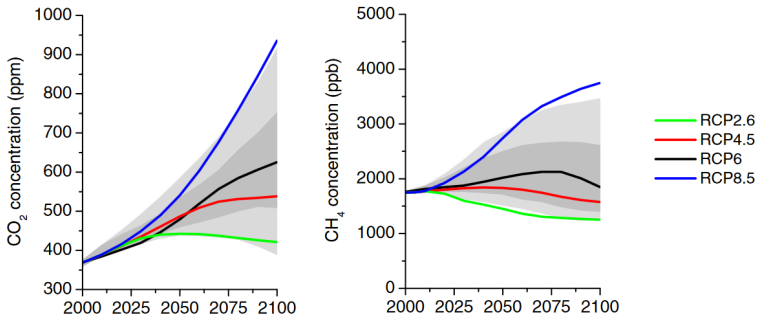

Figure 3.6: RCP Concentration Development Scenario's, taken from [59]

As the future is unknown, it is difficult to say which scenario is most realistic. The reason for the need for different scenarios, and their havings significant differences, is the considerable uncertainty in the future development of emissions. For this analysis the RCP4.5 scenario is applied for the assumed background concentrations, as it compromises the short-term growth of emissions and the effect of possible mitigation effort decreasing the emissions rates over time. This scenario is viewed as a middle-of-the-road approach, whereas the RCP2.6 is described as having "a very low forcing level" [29], and the RCP8.5 is assumed to have "very high greenhouse gas emissions". [29] For the chosen RCP4.5 scenario, radiative forcing stabilises by the year 2100. [29] The influence this assumption of background concentrations has on the findings is addressed in chapter 5.

With the assumption in place accounting for global atmospheric concentrations, the emissions originating from aviation need to be resolved. This is where the WeCare inventory comes into play, which holds all needed parameters for the year 2012. Because this database contains information for a single year, an additional assumption needs to be made for the development of the emissions over time. This is because the aim is not to see the effects of an isolated year of aviation emissions, but rather to address the impact of the aviation industry as a continuously developing entity. The way this is done within AirClim is by providing the temporal development of the aviation fuel use. The resulting emissions and flown distance are then scaled with the change in fuel use over time, assuming there are no changes in the global distribution patterns. The assumed fuel development scenario is the so-called 'business-as-usual scenario', in which the assumption is that current aircraft technology level is maintained. [23] The temporal fuel development is shown in Figure 3.7. Additionally, it is assumed that no bio-fuels are used, the use of which would potentially decrease certain emissions in the future. The influence of this assumption is also addressed within chapter 5.

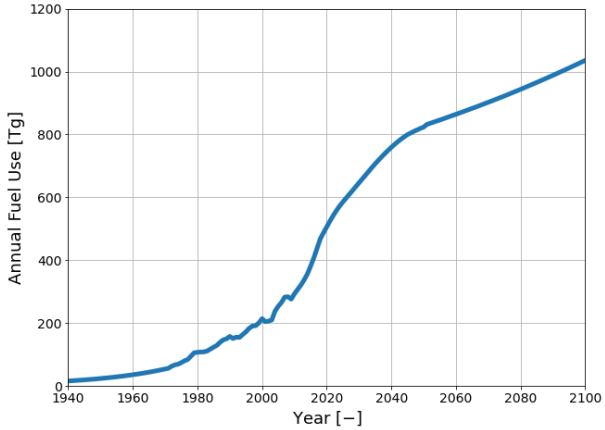

Figure 3.7: Business-As-Usual Fuel Scenario

In order to set a baseline, a simulation is performed using the WeCare database as a whole, thus including all aircraft categories. This database represents the year 2012 and is scaled using the fuel scenario shown in Figure 3.7 to account for changes over time. The considered timeline runs from 1940 to 2100. Figure 3.8 and Figure 3.9 show the resulting radiative forcing and near-surface temperature over time, for all included species.

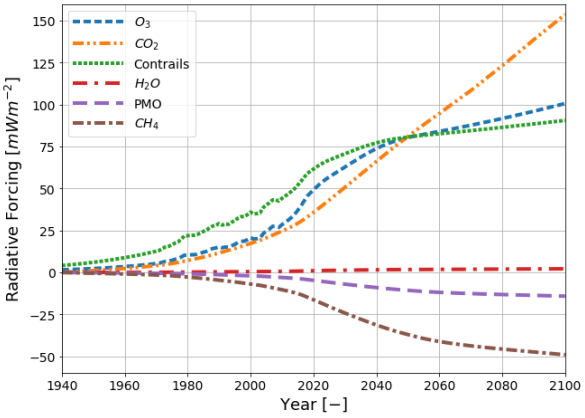

Figure 3.8: Basecase Radiative Forcing by Species

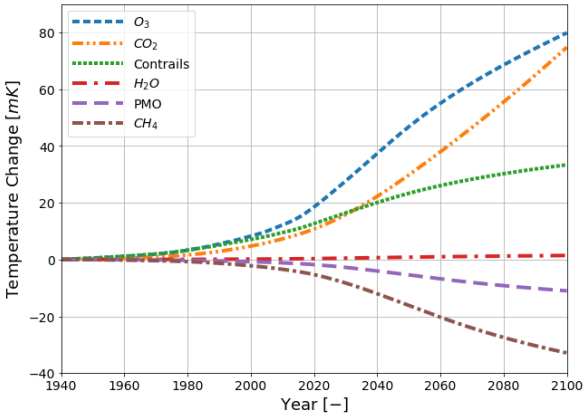

Figure 3.9: Basecase Temperature Change by Species

By the year 2100, the total change in temperature due to aviation is found to be 145 mK. The largest contribution is made by ozone, which together with the cooling effect by methane destruction, and the effect of primary mode ozone, ranks the contribution of NO_x second behind that of CO_2. The temperature change caused by contrails is expected to be roughly half that of CO_2 by 2100, keeping in mind the relatively higher uncertainty of contrails' effects. Contrails' relative share in temperature change decreases over time, due to the effect being short-lived, and saturation in cloudiness causing the effect of a single trail decreasing as air traffic increases. In contrast, the slope of the temperature change caused by CO_2 keeps increasing over time, as the concentration keeps increasing as long as CO_2 is added to the atmosphere faster than it is being removed. The differences between the radiative forcing and temperature graphs are caused by the different climate sensitivity parameters of the species.

In order to assess the effect of an individual aircraft category, several steps are taken. In the basecase the summed fuel, flown distance and emissions of all categories were used to find the overall impact of aviation. Now a sensitivity approach is used to find the impact of each category individually. This means that additional runs are performed in which the total emission inventory used as input is adjusted by the contribution of a single category. This is done in two ways, firstly by applying a negative change: the input emission inventory consists of the summed values of the 6 other categories excluding the one of interest. Secondly, a positive change is assumed: the input emission inventory consists of the summed values of the 6 other categories together with the considered category times 2. This makes that an additional 14 runs of the model are performed in which the input inventory is adjusted. The changes in radiative forcing and temperature change with respect to the basecase are recorded.

By summing the changes in temperate and radiative forcing of the 7 positive or 7 negative runs, again one finds a theoretical total impact of aviation as these describe the impacts of the 7 individual categories. In practise, the impact of the 7 categories summed, either negative or positive, does not match the outcome of the basecase which describes aviation's total impact. This is because the effects of a given amount of emissions or flown distance depends the emissions of the other categories that are included. For example, it was discussed that in terms of cloud formation a form of saturation occurs as air traffic increases. By employing a sensitivity approach the effects of contrails are reduced for all categories, as only a situation is considered in which the other air traffic is also present. Because of this, a scaling is applied.

The scaling that is applied makes that ultimately the summed effects of the individual categories matches the overall effects as described in the basecase. The 7 effects in the negative scenario are summed and the scaling

factor is defined by the ratio of the basecase outcome divided by the summed values. This scaling factor is different for each species and changes over time. The same is done for the positive changes, leaving 2 outcomes of the radiative forcing and temperature change for each category. The final step is averaging these 2 outcomes, resulting in the the estimated influence of each individual category.

The reason for using this approach is that the impact of the different categories together need to match the overall impact for a consistent outcome. By considering both a positive and negative adjustment, the influence of the changes in climate sensitivity is reduced.

Figure 3.10 indicates the relevance of the centroid approach, using the temperature change due to contrails of category 4 as an example. By assuming a positive change (adding the category onto the base case) the found effect of contrails is lower due to a higher saturation. Similarly, the opposite is found when the category is subtracted from the base. The mean of the two simulations is taken as the actual result, which is done for all categories and species.

The scaling factor is shown in Figure 3.11. This example shows the scaling factor regarding the temperature change caused by contrails. The factor is defined as the ratio between the values from the base case divided by the summed values of the 7 different categories. For contrails specifically, the scaling factor deviates much from a value of 1 due to the high importance of cloud saturation, of which aviation is the main contributor. Because the simulations for the individual categories are all based on a deviation from a situation including all aircraft, the effects found already assume a saturation to be present, which does not include the effective increase in saturation due to the added flights. If a flight was performed without any other aviation presence, the effect of its contrails would be significantly increased. Thus, in order to account for this the results of the individual categories are scaled to match the overall base case simulation when joined together.

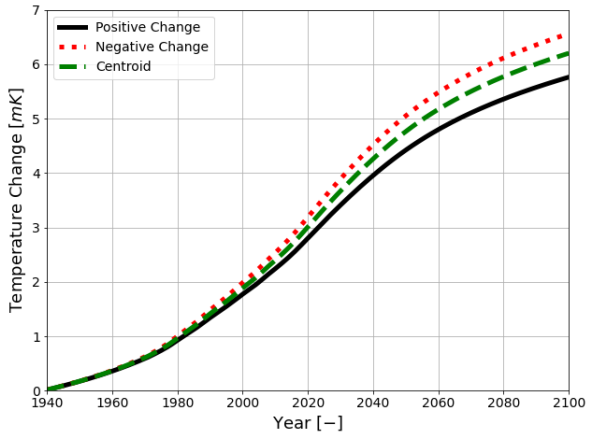

Figure 3.10: Category 4 Contrail Temperature Change

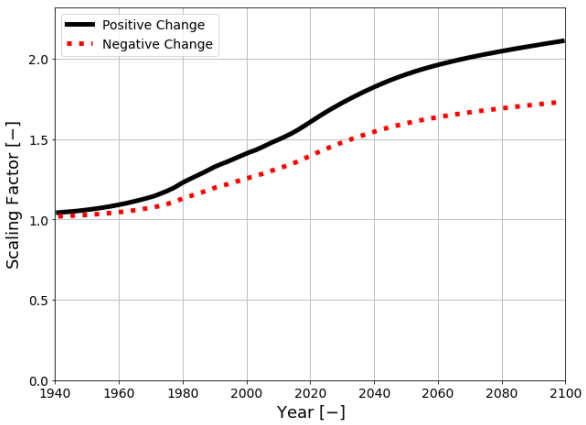

Figure 3.11: Contrail Temperature Change Scaling Factor

3.2. Flight Analysis

3.2.1. OpenSky

In order to model an aircraft's behaviour in flight, positional aircraft data is used, constructed by means of ADS-B data. ADS-B (Automatic dependant surveillance - broadcast) is a technology by which the position of an aircraft is repeatedly determined and broadcast. Over the last few years the equipment has started to be incorporated in most aircraft, and the equipment can be mandatory dependant on location and aircraft. There are various instances continuously collecting and storing the transmitted data, one of which is OpenSky Network [47], which has the advantage of providing open access to their air traffic data.

OpenSky makes use of crowdsourcing in order to obtain a large global coverage. People or organisations can individually set up receivers and share their data with the overall database. This does have downsides, as the network of receivers is not necessarily well structured, with varying levels of coverage as well as challenges concerning the data integrity. There are various causes for invalid data being recorded, such as environmen-

tal noise and software bugs. It was shown that the most common sensor type in the network on average misreported the aircraft ICAO ID 2.4% of the time [48], indicating there is a substantial amount of invalid data in the database.

For this research, flight data is used from a single day, September 1st 2019. One reason for choosing this period was that this data was readily available due to it formerly being used for other research. As this was before the occurrence of Covid-19, global traffic was operating 'per usual', and the date is relatively recent. Because the data is used to construct typical flight trajectories of various aircraft types, rather than investigating the global traffic network and schedules, the fact that not all flights performed that day are recorded is of no direct concern. Additionally, even though patterns in flight schedules change over a year, it is expected that typical distances, speeds and altitudes flown by a certain aircraft model remain the same over time, making that a single day sample properly represents typical flight patterns. Due to the high density of the raw data and the associated processing time needed, the considered period is limited to a single day; additionally the data used is sampled for a 2-minute period every 10 minutes of the day, at a sampling frequency of 1 point every second.

The recorded ADS-B data contains a number of parameters that are of interest. Mainly, the position of the aircraft, defined by latitude, longitude and barometric altitude is used, together with the time of transmission. Additionally, the aircraft model is identified from its ICAO 24-bit transponder ID, which is linked to a single airframe. Extra parameters that are used are the recorded heading and vertical rate of the aircraft. Even though these are not needed for constructing the flight trajectories, they are used in filtering to check whether a potential flight identified from the raw data shows no abnormalities.

After filtering out faulty records, all recorded 2-minute periods for every airframe are condensed into single data points. Within this process, first is the removal of outliers, which are defined as showing a barometric altitude which is over 2 standard deviations from the 2-minute median. Then the condensed point consists of the mean of each parameter for the remaining points of the 2-minute period. As a requirement, at least 20 points should have been left after removing outliers for the outcome to be included, representing 17% of the maximum recorded 120 points. Figure 3.12 shows an example of a 2-minute segment for a single airframe, in barometric altitude versus time. The outliers (red) are removed and the remaining (blue) points are condensed into a single one (green), which is later used to construct the trajectory of the flight.

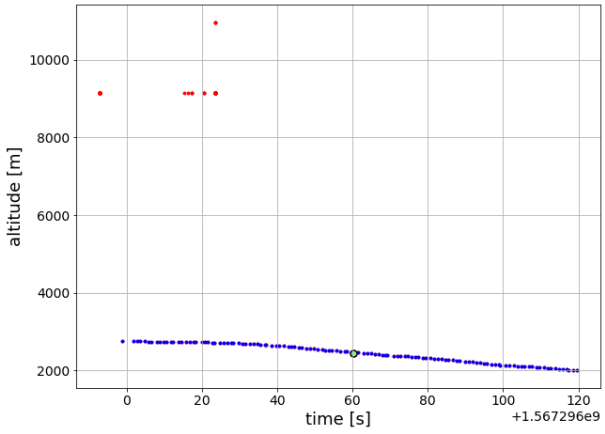

Figure 3.12: Filtering of Points Within 2-Minute Segment

The condensed points are then used to find valid flight trajectories. Per airframe all points are divided into clusters which are separated by periods of climbing or descending below a threshold altitude. Each cluster is then checked against a set of requirements that define a valid flight trajectory. The cruise phase is assumed to be the period between the first and last point where the vertical rate is near zero. Within this cruise phase there should be no significant drop in altitude or change in heading; if there is, the cluster of points is disregarded. It is possible for a flight to have a significant part not recorded due to a loss of signal, for example above the Atlantic Ocean. As long as the start and end of the cruise phase together with a period of climbing and descending is properly recorded, the flight will still be included and the lost part of the trajectory is

assumed to be a straight trajectory connecting the surrounding points by the shortest distance, at a constant altitude. Due to the condensed data being sampled at a rate of once every 10 minutes, the details of the exact take-off and landing procedures are not captured, but the aim of this process is to capture the general trajectory and in particular the cruise section, from which later a mission profile is constructed. Figure 3.13 and Figure 3.14 show an example of a trans-Atlantic flight from Europe towards the US. Each point represents a summarised 2 minute period, 10 minutes apart. The final trajectory is made simply by connecting all these points, showing a filled gap when connection is lost.

Figure 3.13: Example Trans-Atlantic Flight Trajectory Map

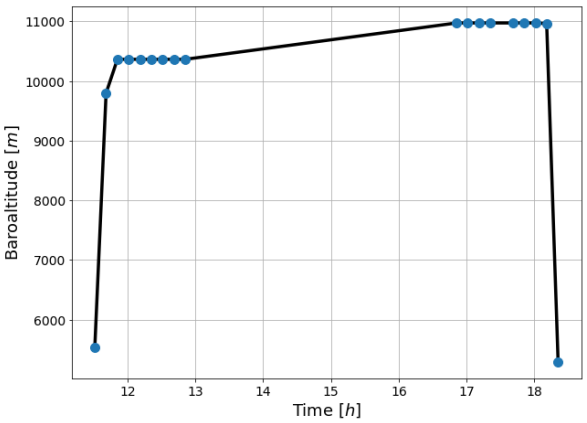

Figure 3.14: Example Trans-Atlantic Flight Trajectory Altitude

The airspeed of the aircraft is not registered within the ADS-B data, so that only the ground speed can be found making use of the location and time data. Depending on the speed and direction of the local wind in flight, the airspeed, which is the relevant parameter needed for drag and fuel calculations, will deviate from the speed of the aircraft with respect to the ground. Figure 3.15 shows the distribution of the Mach number of the Boeing 737-800 for all points in cruise, assuming no wind conditions, so that the airspeed matches the ground speed. The calculation also assumes ISA conditions. It is clear that in reality the wind significantly distorts the airspeed of the aircraft and cannot be ignored. Assuming there to be no wind would lead to a number of points within cruise in which almost supersonic speeds are reached, which is impossible for this aircraft. The actual airspeed of the aircraft cannot be reconstructed accurately without precise wind speed information at the time and location of the aircraft. Because of this, in further analysis it is assumed that the Mach number in the cruise phase is a constant for each aircraft model, and is equal to the mean value of all Mach numbers calculated using the ground speed for that specific aircraft model.

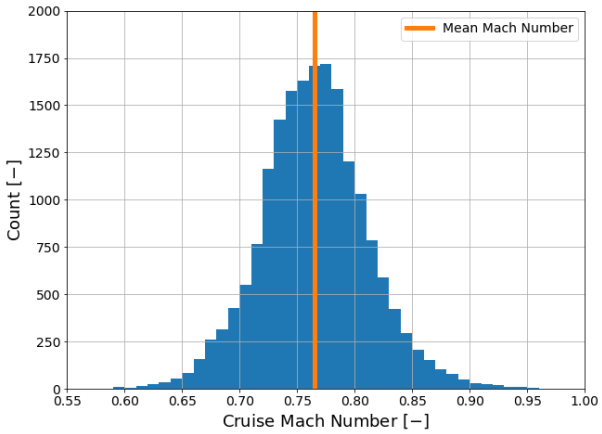

Figure 3.15: No Wind Boeing 737-800 Cruise Mach Number

3.2.2. OpenAP

Having collected information on flight trajectories, the fuel flow and ultimately the amount of emissions can be assessed. The performance model used for this is OpenAP [55], due to it being openly distributed. The model has been presented as an alternative to Eurocontrol's BADA [40], with similar functionalities but without the strict licence agreements. One difference is that OpenAP employs a nonlinear relationship between aircraft speed and thrust, whereas BADA's maximum thrust is independent of airspeed. This makes OpenAP's approach more realistic for lower altitudes at low speed. [55] The functionality relevant to this project is supplying the fuel consumption for a given aircraft and flight trajectory. Additionally, the model has recently been extended to include various emissions.

As a starting point for OpenAP, aircraft kinematics are based on a statistical model WRAP [54], which has been developed by the same author. Within this model flight trajectories are divided into main flight phases, each defined by a set of associated parameters, such as altitude, initial altitude, range and Mach number for the cruise phase. The dynamic performance, which is based on literature and flight data, can be applied to the assumed conditions, resulting in the fuel flow of the engines. Drag polars for the different aircraft models have been estimated from flight data. [56] For the fuel flow, OpenAP makes use of ICAO's engine database [41], which holds information of the performance parameters of the most common aircraft engines, such as fuel flow and emissions in varying operating conditions. These conditions are takeoff, climb-out, approach and idle, defined as 100%, 85%, 30% and 7% thrust respectively. Within OpenAP these points are fitted with a third degree polynomial to obtain a continuous profile. This is done both for the fuel burn rate and the emission index. A linear factor is applied to transform sea-level thrust specific fuel consumption into that at altitude. The model assumes a standard atmosphere (ISA), as well as no wind conditions.

Using this model, standard engines are assumed to be fitted to the aircraft. The exact engine type fitted to an aircraft within the ADS-B data is not known and aircraft are not limited to using a single engine type, with engines occasionally being replaced with other types. Moreover, engines degrade over time and the performance after several years of use is different compared to new. Degradation is out of scope, as the available engine data is limited to ICAO's database, which is a collection of data provided by the engine manufacturers.

OpenAP includes a number of aircraft, which will be used to represent aviation as a whole. Table 3.3 shows the aircraft for which both the fuel model and WRAP model are available within OpenAP and are thus used to represent each category. As no regional aircraft from category 1 and 2 are present, their flights are not analysed using this method. For each other category there are 3 or 4 included aircraft, so that the outcome is not solely dependent on the performance of 1 specific model.

Table 3.3: OpenAP Aircraft by Category

Category	**Aircraft**			
1	-			
2	-			
3	E190,	B737-700,	A319	
4	B737-800,	B737-900,	A320,	A321
5	B757-200,	A330-200,	B787-800	
6	B787-900,	A330-300,	A330-400	
7	B777-300ER,	B747-700,	A380-800	

Whereas the ADS-B information was used to get the overall flight trajectories, using data on 10-minute intervals makes that the climbing and descending phases are not captured in high detail. Because of this, these parts of the flight trajectory are constructed using the WRAP model encompassed within OpenAP. For a number of aircraft the patterns in the take-off and climbing as well as descending and landing phase have been analysed in constructing this model, and the average trajectory from this is used to couple with the cruise phases identified from the Opensky data.

For validation purposes, the OpenAP model has been compared to a real flight performed using a Cessna Citation. The onboard data is used to reconstruct the net engine thrust, and the fuel flow is known. Figure 3.16 shows the fuel flow over time from OpenAP, together with the actual flow and that calculated using BADA. In

this case not the actual thrust is used, but rather that as estimated by the respective models. OpenAP's fuel flow is close to that calculated in BADA, but is lower at the start of climb at high thrust. During cruise the estimated fuel flow for both models is significantly higher than that measured. In Figure 3.17 the fuel flow is shown again, now using the actual thrust as input. Both models now show a better matching fuel flow, with larger fluctuations due to using the actual engine thrust.

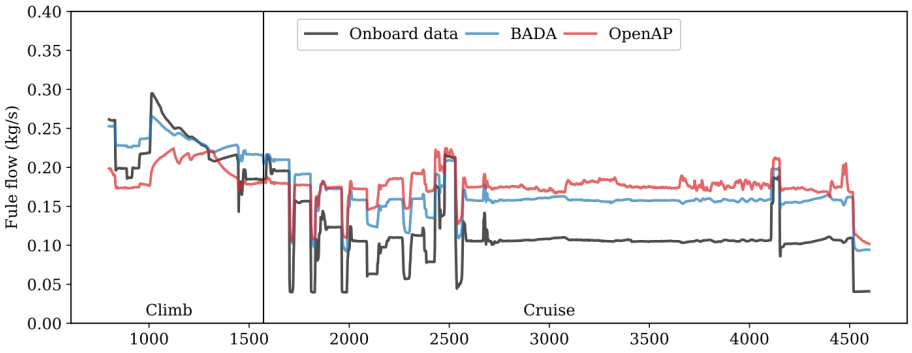

Figure 3.16: Fuel Flow Based on Estimated Thrust, taken from [55]

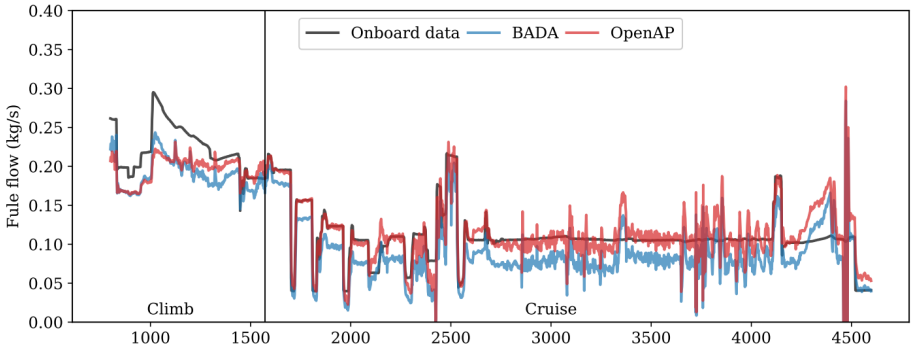

Figure 3.17: Fuel Flow Based on Actual Thrust, taken from [55]

From the considered flight it appears that the fuel flow from OpenAP and BADA can differ significantly from reality. During cruise the estimated fuel flow from OpenAP is higher than that from BADA, while both overestimate this fuel flow. When using the actual thrust of the engines the fuel flow in OpenAP is closer to matching reality, with an underestimation using BADA. The author of OpenAP mentions that lack of access to accurate flight data is a limiting factor for validation of the model. [55] The accuracy of the model will differ per aircraft model, and the lack of data makes that only the performance of the aircraft shown in Table 3.3 can be used in this analysis. The comparison of the considered flight showed that the modelled fuel flow can deviate from reality, but the performance appears to be similar to that of the popular BADA model.

3.2.3. Aircraft Mass Estimation

Flight trajectories can provide most needed parameters, such as the altitude and climb rate, in order to calculate the fuel flow using OpenAP. However, to calculate the thrust and ultimately the fuel flow, it is required to know the current mass of the aircraft. As fuel is being burned during the flight, the aircraft mass is a constantly changing variable. Additionally, the mass with which the aircraft takes off is not only a function of the aircraft model, but also the carried payload and fuel weight, which depend on the current mission. As such, for each flown trajectory the development of the aircraft mass over time needs to be estimated.

The take-off weight of the aircraft can be divided into three main components: the operating empty weight, payload weight and fuel weight. For each aircraft included within OpenAP, the operating empty weight is given and can be used as the starting point for the takeoff weight estimation. The payload weight is made

up by the passengers (including their baggage) and cargo. Because for the flights identified from the ADS-B data it is unknown whether it holds any cargo, the payload it carries is estimated based on the passenger capacity of the aircraft. First of all, a number of seats for each aircraft model needs to be assumed. Based on the available space, information on the maximum number of seats in a one-class configuration can be found. [31] However, in practice airlines deviate from this theoretical maximum and operate aircraft with fewer seats. In order to find a fair estimation on the number of seats, the average of the found configurations of different airlines for each specific aircraft model is used. [51] As aircraft are not always completely filled, the total mass depends on how many seats are actually filled, defined by the load factor. Detailed information on the load factor for individual flights is not freely available and as such an estimate of 0.826 is applied for all flights, which was the industry-wide load factor in 2019. [26] Finally, the mass of a single passenger including baggage is assumed to be 100 kg, which matches the standard passenger weight of 190 pounds (including carry-on), with an additional 30 pounds for checked bags. [9]

The final weight component is the fuel weight, which depends on the mission that is performed. The fuel that is expected to be used throughout the mission is taken on board, with a reserve in case of a deviation. As the fuel flow is one of the outputs of OpenAP, this can be integrated over the duration of the flight to find the fuel mass required. This leads to a circular relation, where the the takeoff weight is required to estimate the aircraft mass and fuel flow during the flight, which is then needed to estimate the fuel and ultimately the takeoff weight. This can be solved by assuming an initial fuel weight, and iterating until the assumed fuel weight matches the required fuel weight plus reserve. Making use of this method assumes that the fuel required to perform the flight is equal to that assumed by the operator beforehand, regardless of unexpected changes in fuel use, for example due to changing wind speeds during flight. Additionally, it is assumed that no deviation is made and the reserve fuel is still there at the end of the flight. Any error in assumed takeoff weight leads to a different fuel flow throughout the flight, making that the resulting outcome is expected to be sensitive towards this parameter.

3.2.4. Fuel and NO_x Calculation

Starting from an assumed mass at the start of the flight (including the assumed carried fuel) there are several phases during which fuel is burned. First of all, while on the ground fuel is used during startup and taxiing. Roskam [45] defines the typical values for fuel burn for these phases in a fuel fraction; the fraction between the total mass before and after these phases. A fraction of 0.99 is assumed for both the startup and the taxi phase, meaning that two times 1% of the current aircraft mass is lost in fuel burn. The thrust setting during these phases is unknown and to estimate the NO_x emission during these periods, the emission index of the idle thrust setting of the engine is applied to the amount of fuel burned.

The takeoff is modelled as a short period at maximum thrust. The WRAP model gives the mean takeoff acceleration and speed at which the aircraft takes off. Assuming the acceleration to be constant leads to the take-off time during which fuel is burned at maximum thrust. The NO_x emission index of maximum thrust is applied.

The climbing phase is constructed by the trajectory model in OpenAP, which gives the mean performance based on historical flights. The trajectory is made up by points at a 1-second interval and the result contains the altitude, true airspeed and vertical rate, up to the cruise altitude. These are then used to find the fuel burn and NO_x emission for each point for which the thrust is calculated within OpenAP. The thrust is made up by the drag coming from the aircraft's drag polar and the component due to the non-zero flight path angle and the aircraft mass. From the engine thrust setting both the fuel burn and NO_x emission is found from the constructed polynomial mentioned before.

Once the cruise altitude is reached, the actual trajectory with the 10-minute intervals is used. In order to increase resolution, the intervals are linearly interpolated to obtain points at a 1-minute interval. This is done to prevent an over-estimation of the aircraft mass as the mass does not change in-between points. Because gaps in the trajectory data occur, this would mean a constant aircraft mass lasting up to hours, which would wrongly increase fuel burn. The same method applies in obtaining fuel burn and emission based on the required thrust.

For the descent phase again the trajectory is formed by OpenAP, starting at the final altitude of the cruise phase. The same method applies for obtaining the fuel and emissions.

Once on the ground, a fuel fraction of 0.99 is again applied for the taxiing, with an assumed idle setting for the thrust. This is where the actual fuel burn and NO_x emission ends, and summing up the results for all phases gives the values of the entire flight. However, additional fuel calculations need to be done for the fuel that is taken on as reserve at the start of the flight, as this, combined with the fuel used, needs to match with that assumed at the start. If it does not match, the assumption is adjusted and the process is repeated until convergence. Only once convergence is achieved are the results used for interpretation.

There is a standard for the additional fuel that is taken on board, consisting of 3 parts. [9] The first is the contingency fuel, which is described as 5% of the fuel needed to perform the trip. The other part consists of diverting to an alternate destination. It is assumed the aircraft starts at sea-level at the initial aircraft mass minus the trip fuel. Another climb is performed up to cruise altitude, after which 200 miles of cruise and finally the descent. The last part is 30 minutes of loiter, for which the aircraft mass is assumed to be the estimated mass on arrival of the alternate destination [9], equalling the initial mass reduced by the trip and alternate fuel. This loitering takes place at 1500 feet altitude, at holding speed, which is assumed to be 230 knots. [8]

For the shown trans-Atlantic flight performed with the Boeing 777-300ER, the final components of the take-off mass are displayed in Table 3.4. Of these components the trip fuel is the only fuel assumed to be burned over the flight, which is used when analysing the results. The breakdown of trip fuel and resulting NO_x for this flight is shown in Table 3.5

Table 3.4: Example Flight Mass Distribution

Component	**Mass** [$10^3 kg$]	**Share of Total** [%]
Operating Empty	168	55
Payload	27.7	9.0
Trip Fuel	94.7	31
Contingency Fuel	4.74	1.5
Alternate Destination Fuel	10.6	3.4
Final Reserve Fuel	2.01	0.66

Table 3.5: Example Flight Trip Fuel and NO_x Mass Distribution

Flight Phase	**Fuel Mass** [$10^3 kg$]	**Share of Total** [%]	NO_x **Mass** [kg]	**Share of Total** [%]
Start-up & Taxi	6.1	6.5	47	2.1
Take-off & Climb	6.0	6.3	179	8.1
Cruise	77	81	1911	86
Descent & Landing	3.6	3.8	67	3.0
Taxi & Shutdown	2.1	2.3	17	0.75

4

Results

4.1. Climate Impact

The near-surface temperature change of the 7 aircraft categories differ clearly, as can be seen in Figure 4.1 and Figure 4.2. These figures show the temperature change of the individual categories, as calculated using the AirClim model. The 2 categories with the smallest aircraft carrying up to 100 seats together are estimated to cause a temperature change of 9.4 mK by 2100, only 6.5% of the total. At the very top is category 7, which includes the largest aircraft with over 300 seats. In-between the smaller aircraft categories 3 and 4 have a larger impact than the larger aircraft in categories 5 and 6. In the long term there is no significant shift in the share that each category contributes, but recently category 7 has overtaken category 4, indicating the shifting of most important factors affecting the climate impact of aircraft. As this shows the overall impact of the category, this is not only about the performance of the aircraft climate-wise, but simply the fleet size and the frequency at which the aircraft are operated are a large factor.

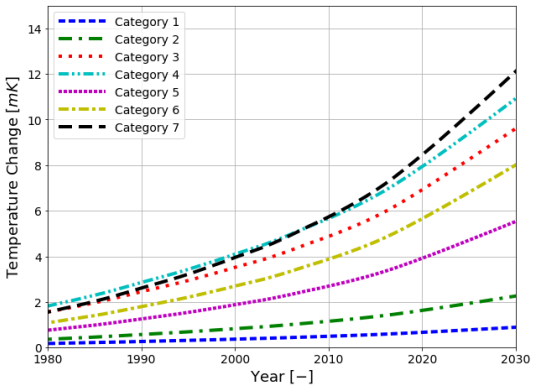

Figure 4.1: Short-Term Temperature Change by Category

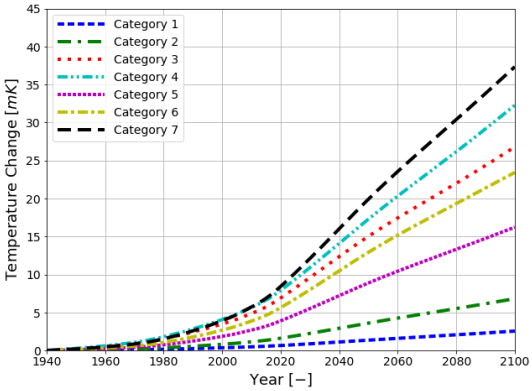

Figure 4.2: Long-Term Temperature Change by Category

In order to better compare the different categories, the impact can be quantified as temperature change per capacity that is being generated. This capacity can be defined as available seat kilometres or ASKs, which is the product of the distance flown and the seats carried. In this case the ASKs generated by each category is known as a result from the WeCare project, the source of the emission inventory. ASKs are known for the year 2012 only, and as such, results of each category are normalised to their generated ASKs in this year.

The resulting normalised climate impact or climate efficiency is displayed in Figure 4.3. It is important to realise that this does not capture the change (increase) in ASKs over time, and thus an increase in temperature change per ASK in 2012 is partially caused by an increasing amount of overall capacity. This method of normalising allows to directly compare the climate efficiency in terms of temperature change per ASK of the different categories, and captures the change of overall impact over time. This does not compare the climate

efficiency of a single category at different points in time, which would require a normalisation with respect to the ASKs in those specific years.

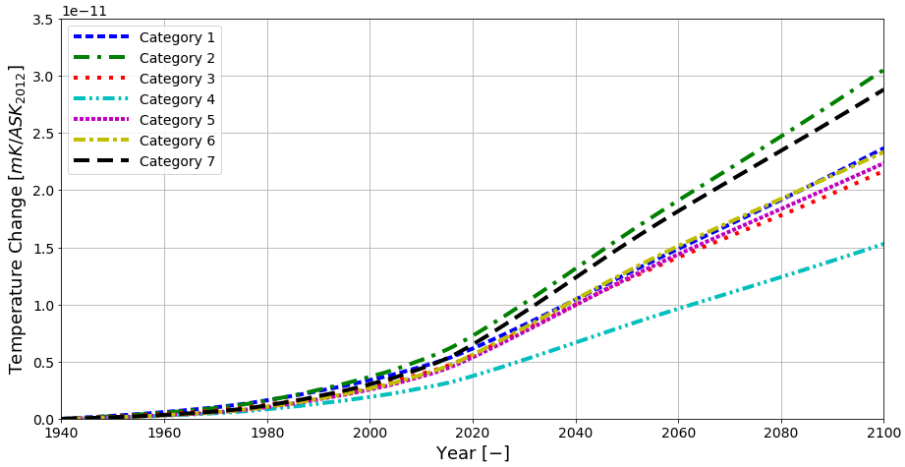

Figure 4.3: Temperature Change per ASK in 2012 by Category

Whereas the overall climate impact of category 2 was near the bottom, it actually shows the worst efficiency in term of climate change. Looking at the temperature change, three distinct groups can be made: category 4 performs best by far, at roughly half the generated temperature change per ASK by 2100 when compared to category 2 or 7. In-between the remaining categories are close together, despite the significant differences in aircraft size.

Figure 4.4 displays the same result in a different way. The average temperature response or ATR is calculated on a timescale of 50 and 75 years from 2012, again normalised against ASKs. The horizontal axis essentially represents the aircraft size, increasing towards the right. There appears to be a 'sweet spot' at category 4, from which both increasing and decreasing the aircraft size negatively affects the climate performance. This is true both for the considered 50- and 75-year time frame.

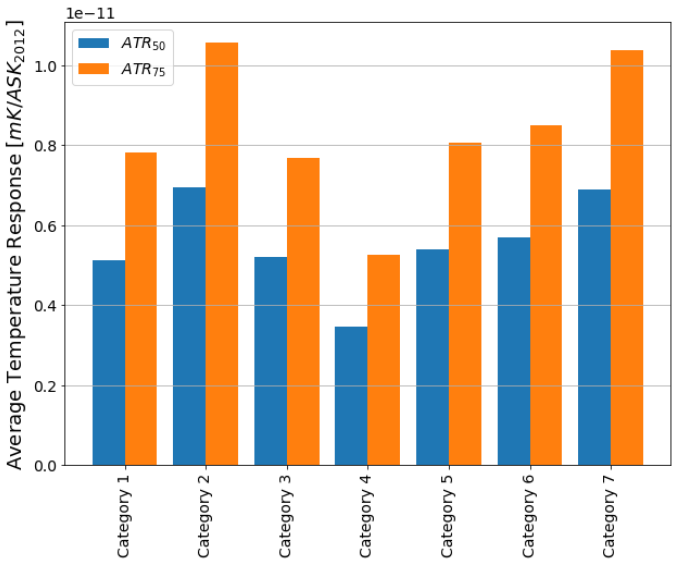

Figure 4.4: Average Temperature Response per ASK in 2012 by Category

One factor that can be assessed directly is the difference in contrail sensitivity of each category. As this is a short-term effect, the development of the contrail radiative forcing directly indicates how the resulting cli-

mate impact is influenced. Figure 4.5 shows the radiative forcing as a result of contrail formation per kilometre flown by each category. First of all, this divides the categories into two groups: aircraft with long ranges able to cross large seas and oceans, and aircraft that cannot. The three largest aircraft categories have a distinctly higher sensitivity to contrails per distance flown, which is caused by spending a larger portion of their flights in areas with a low cloud saturation. In contrast, the smaller aircraft tend to be operated in areas with a higher flight density, as will be shown further on in this chapter.

Over time a decrease in contrail sensitivity can be observed. As air traffic increases, the mentioned saturation effect becomes more apparent. The decline for smaller aircraft is steeper and starts earlier, as the amount of traffic required for a meaningful saturation is achieved earlier in the high frequency areas. The assumed air traffic follows the assumed fuel development scenario, and as this starts to level out towards the year 2100, so does the change in contrail sensitivity.

What becomes clear is that the effect of a certain contrail distance is higher for the largest aircraft categories. However, it is important to keep in mind the matter of scale. Even though the effect of a single contrail created by a category 7 aircraft could be double that of a much smaller category 2 aircraft, the difference in capacity is closer to a factor 5, which means that for a category 2 aircraft contrails will carry a higher relevance.

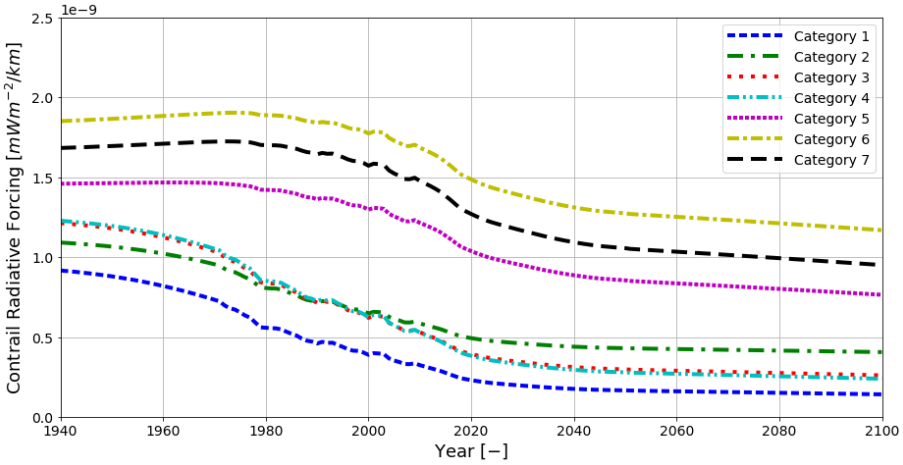

Figure 4.5: Contrail Radiative Forcing per Kilometre Flown by Category

4.2. Flight Analysis

In order to investigate what causes the difference in climate impact between categories, a flight analysis is performed. As larger aircraft are linked to flying longer distances, first the effect of flight distance on several parameters is investigated.

Figure 4.6 shows the average barometric altitude from flights with varying distances. Each dot represents a single flight, which was identified from an analysis of flight data on 01-09-2019. There is no clear direct difference in altitude between long and short distance flights. A small number of flights shorter than 2000 km are at a significantly lower altitude, but these are a small portion of the roughly 5000 flights included in total. As one would expect, there is a high density of short flights recorded. This is partially a result of the limited coverage of the ADS-B database, as gaps in the data make it harder to identify a flight, and the longer a flight takes, the larger the chance of missing information.

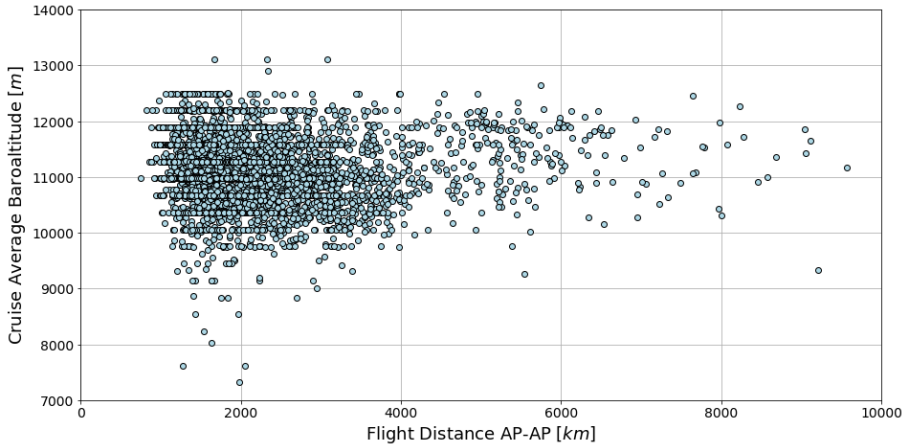

Figure 4.6: Cruise Altitude vs Flight Distance

Next is fuel use. In order to directly compare the fuel use of different aircraft the fuel use is divided by the ASKs, in this case directly calculated from the flown distance and the assumed number of seats in each aircraft model. The fuel use is the result from the trajectory combined with the aircraft performance model. Figure 4.7 shows the normalised fuel use for all identified flights. There is a significant spread, but still a clear pattern can be recognised. A quadratic curve is fitted to the data, which results in a coefficient of determination of 0.89, indicating high predictability. The optimal distance for minimising fuel use shows to be around 2500 km. The higher frequency of takeoffs adversely affects the fuel use for shorter flights, and for longer flights the extra fuel carried to perform the flight increases overall fuel use. After 4000 km a jump in fuel use is seen, which matches the maximum range of the aircraft within category 4. Larger aircraft are required to fly longer distances, this shows that these aircraft have a higher fuel consumption per ASK.

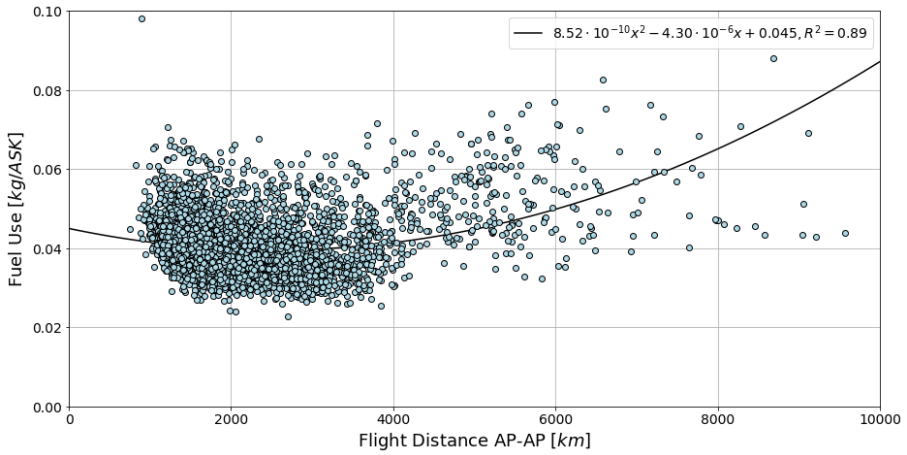

Figure 4.7: Fuel Use vs Flight Distance

The NO_x emissions follow from the same method, results are displayed in Figure 4.8. The emitted NO_x increases with increasing flight distance. This can be seen in the overall NO_x emitted per ASK, but even more so in Figure 4.9, which shows the emission index in kg of NO_x per kg of fuel. The emission index shows an almost linear relation between emission and distance. It has been shown that the NO_x emission index increases with thrust setting, which is one cause of this relation. For the same aircraft flying a short and long distance flight, the aircraft will start off with more fuel in the long flight, increasing weight and drag, ultimately leading to a higher thrust setting and NO_x emission index. Additionally, for a given thrust setting a larger engine tends to have a higher NO_x emission index, as shown previously.

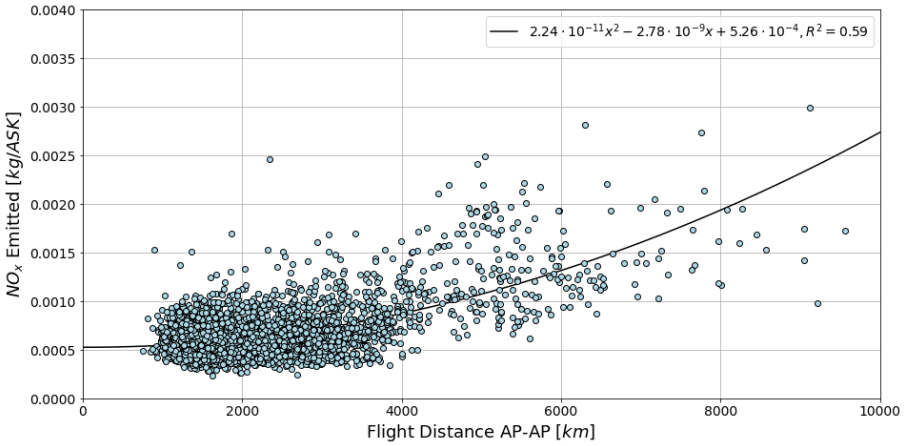

Figure 4.8: NO_x Emission vs Flight Distance

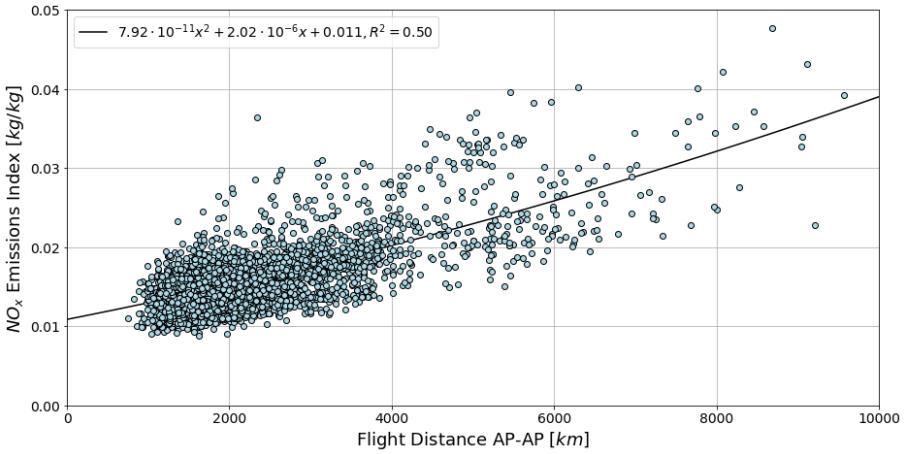

Figure 4.9: NO_x Emission Index vs Flight Distance

The average Mach number during cruise shows clear differences between the smaller and larger aircraft categories. Figure 4.10 shows the cruise Mach number originating from the flight analysis for the aircraft ordered from small to large, starting at category 3. The dashed lines separate the different categories. The aircraft in categories 3 and 4 all fly at roughly the same speed, at a Mach number of 0.77. Almost all larger aircraft have a cruise Mach number above 0.8, with some exceeding Mach 0.85. At subsonic speeds a higher Mach number increases the drag coefficient of the aircraft, by means of drag creep and drag divergence. [57] The overall drag is thus increased, both by this higher drag coefficient and increased velocity directly. The result is that a higher amount of thrust is required from the engines, increasing fuel flow as well as the NO_x emission index. However, this does not mean that flying more slowly would directly reduce fuel burn and NO_x emission. A flight takes longer at slower speeds, increasing the duration at which fuel is burned. Airlines benefit from operating aircraft at the most fuel efficient speeds, which implies that the larger aircraft have been designed to fly at a higher cruise Mach number. Analysis of the climate mitigation potential for the A330-200 has also shown an increase in fuel burn when reducing the cruise speed. [6]

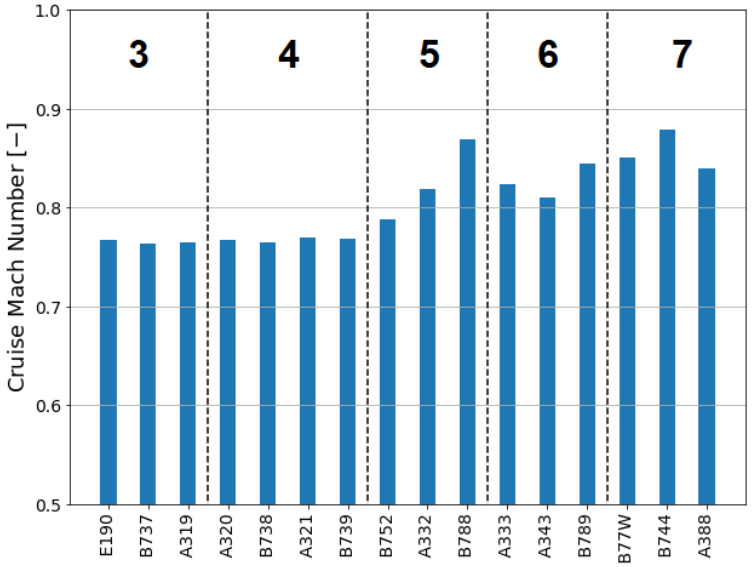

Figure 4.10: Cruise Mach Number by Aircraft

4.3. Category 1

Category 1 is the category with the smallest aircraft, with up to 50 seats. The overall temperature change linked to this category is the lowest of the categories, at 2.6 mK by 2100 i.e. 1.8% of the total. Per ASK however, the category shows an average performance climate-wise, as can be seen in Figure 4.11. Figure 4.12 and Figure 4.13 show the radiative forcing and temperature change due to individual species respectively. Compared to the effect of different species for aviation overall, the main difference is a much smaller relative impact of all NO_x related effects (ozone, methane, PMO). This is in line with the increase of NO_x emission with distance discussed in the previous section.

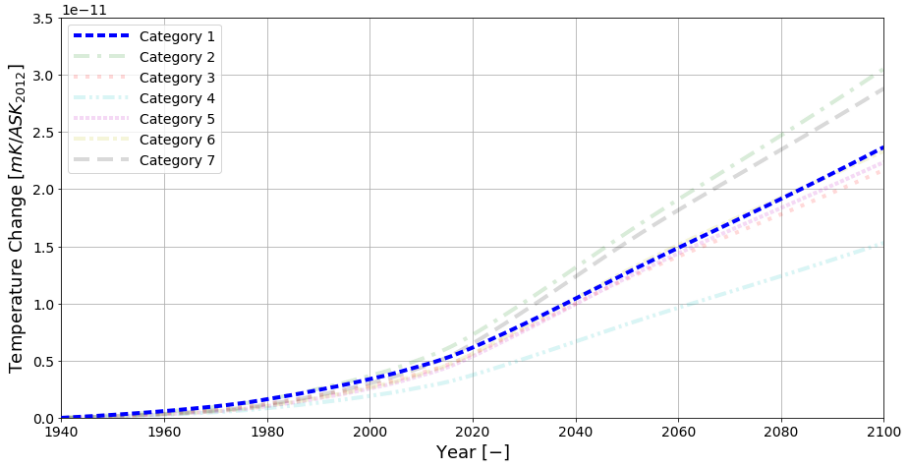

Figure 4.11: Category 1 Temperature Change per ASK in 2012

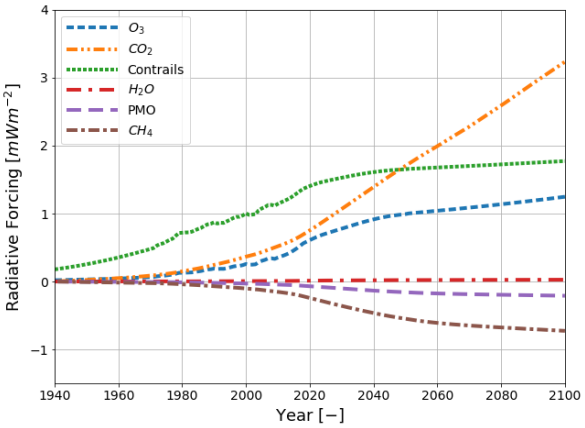

Figure 4.12: Category 1 Radiative Forcing by Species

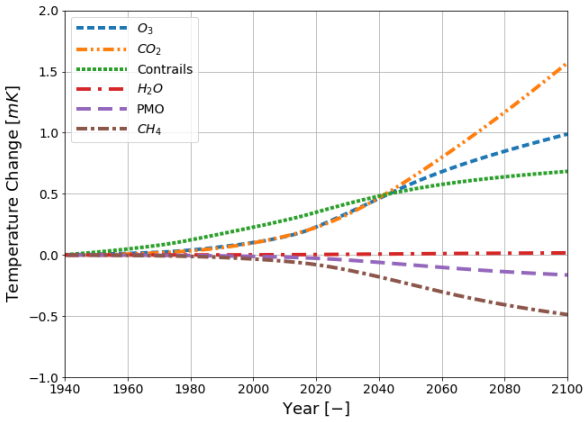

Figure 4.13: Category 1 Temperature Change by Species

Figure 4.14 shows the global distribution of fuel for category 1 constructed from data from the WeCare project. There are 3 clear areas with high activity, namely the east side of the US, Europe, and Eastern Asia. Note that a logarithmic scale has been applied, indicating the large difference between high and low fuel areas. A result of flying in such high-density areas is that there is a large saturation with respect to contrails, which reduces the effect of additional trails. At the same time, the overall effect of contrails for this category is not lower than average. This is due to the calculation of the contrail effects not being affected by aircraft size. Because of this, small aircraft show a large effect per seat, by being smaller in size and this negative effect counters the positive effect of flying in high density areas, resulting in an average contrail contribution.

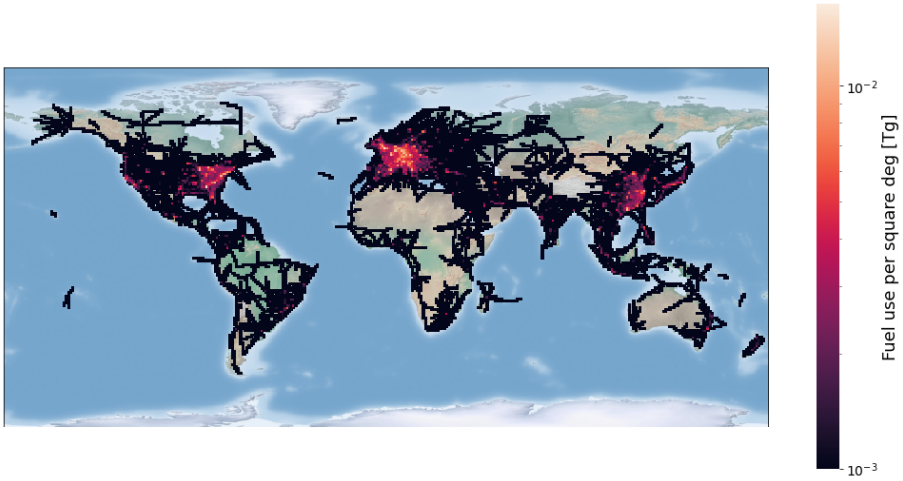

Figure 4.14: Category 1 Global Fuel Distribution in 2012

4.4. Category 2

Category 2 carries 51-100 seats. The overall impact is behind that of category 1, but at a distance from the larger categories. However, it is at the top of temperature change per ASK, showing worst performance, as shown in Figure 4.15. In many ways this category is similar to the smaller aircraft category when looking at the individual species' contribution in Figure 4.16 and Figure 4.17. A small increase in the relative contribution of ozone can be seen compared to CO_2, but this is not the main cause of the difference, but in fact it is the larger contrail effects, seen both in RF and temperature.

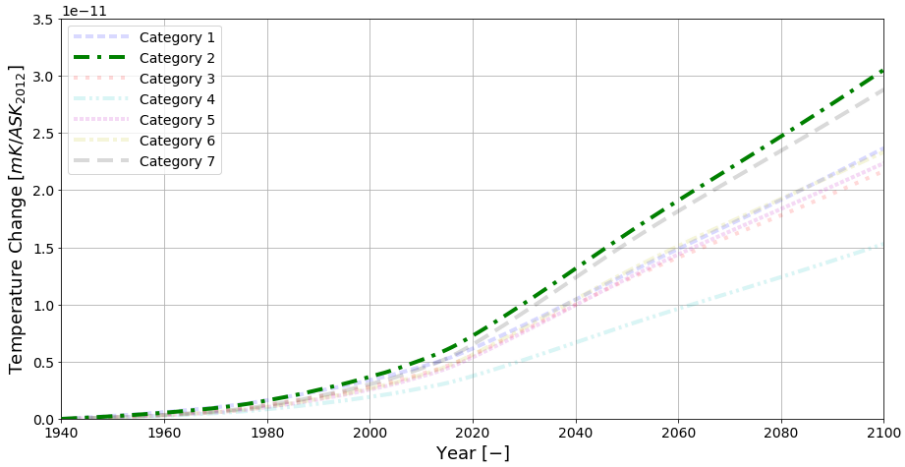

Figure 4.15: Category 2 Temperature Change per ASK in 2012

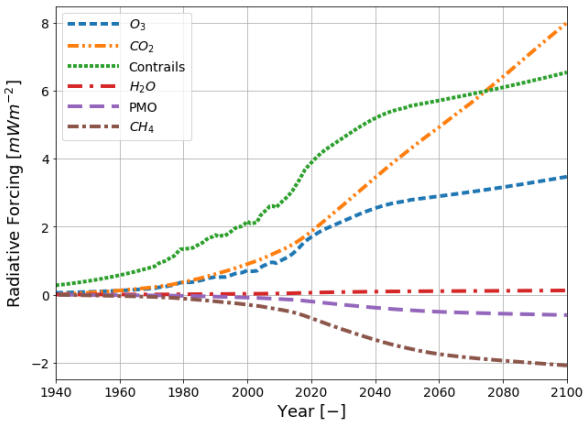

Figure 4.16: Category 2 Radiative Forcing by Species

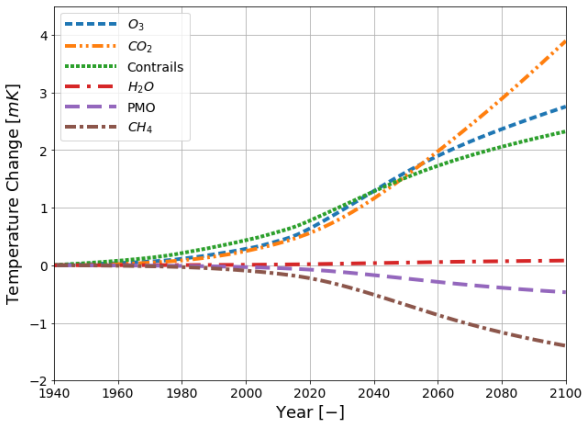

Figure 4.17: Category 2 Temperature Change by Species

By 2100 34% of this category's temperature change is due to contrails, compared to 27% for category 1. This increase can be explained by looking at the global fuel distribution. For category 1 aircraft are flown in three main areas, in which there is a large contrail saturation effect. For category 2 the peaks in fuel use are in the same place, but the distribution globally is much more even, as displayed in Figure 4.18. Other areas, such as the West US, South Asia and Brazil show a much higher relative fuel use, meaning that this category flies more in these areas. Such areas have a lower contrail saturation due to having less traffic overall, which ultimately leads to a higher climate impact caused by category 2. Additionally, as the small aircraft within categories 1 and 2 are typically used for short distance flights, and as such is is expected to adversely affect fuel use by deviating from the optimal distance.

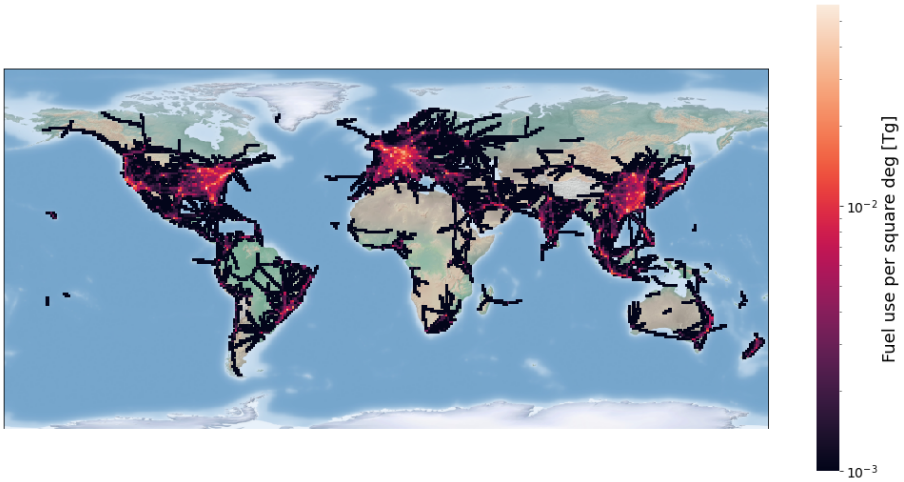

Figure 4.18: Category 2 Global Fuel Distribution in 2012

4.5. Category 3

Category 3, comprising aircraft with 101-151 seats, is one of the better performing aircraft categories. The total temperature change is third overall, but in terms of efficiency is second only to category 4, albeit at a significant distance as can be seen in Figure 4.19. The impact of individual species, displayed in Figure 4.20 and Figure 4.21 show that compared to the smaller aircraft categories, the NO_x effects are much larger and contrails play a smaller role.

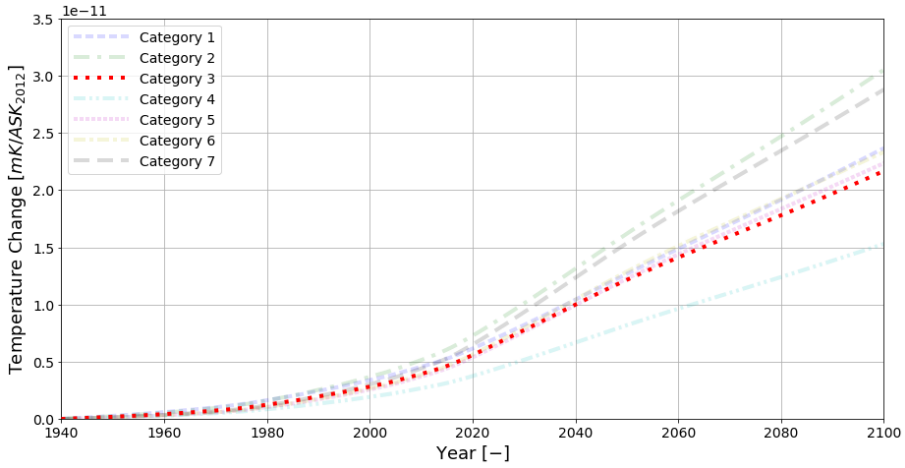

Figure 4.19: Category 3 Temperature Change per ASK in 2012

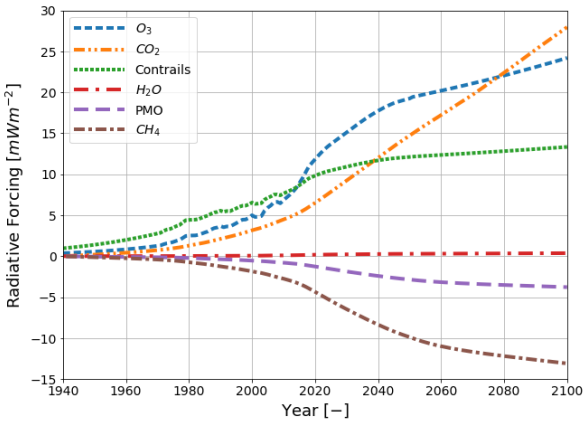

Figure 4.20: Category 3 Radiative Forcing by Species

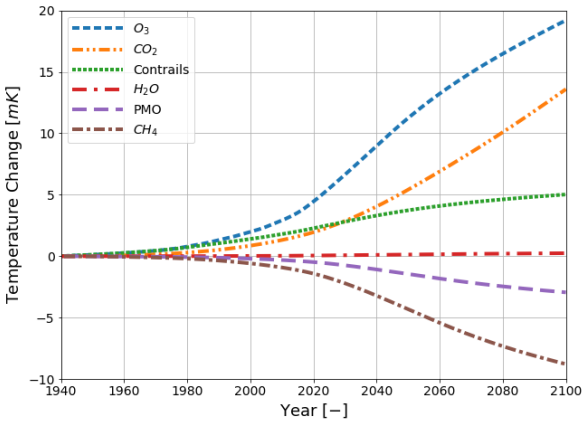

Figure 4.21: Category 3 Temperature Change by Species

In total 806 flights have been identified for this aircraft category, shown in Figure 4.22. Blue dots represent the recorded ADS-B data and the red lines are the resulting trajectories. Almost all identified flights are performed within Europe and the US, as a direct result of limited coverage in the ADS-B data.

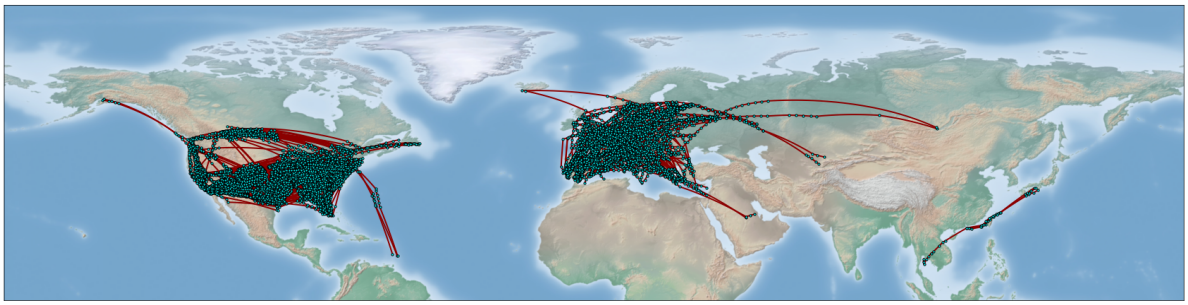

Figure 4.22: Category 3 01/09/2019 Identified Flights

This aircraft category shows flights up to a distance of 4000 km, indicating this is the maximum range of the aircraft included. Compared to other flights at the same distance (mainly done by category 4), flights are performed at a higher altitude. Figure 4.23 shows the different category 3 flights. The faded points represent the other categories. This altitude difference affects the impact of NO_x, as discussed in subsection 2.4.2. The given example showed a maximum global warming potential for NO_x emitted around an altitude of 12 km, just above the average cruise altitude of these aircraft. This is one of the reasons why this category shows a much higher relative NO_x impact.

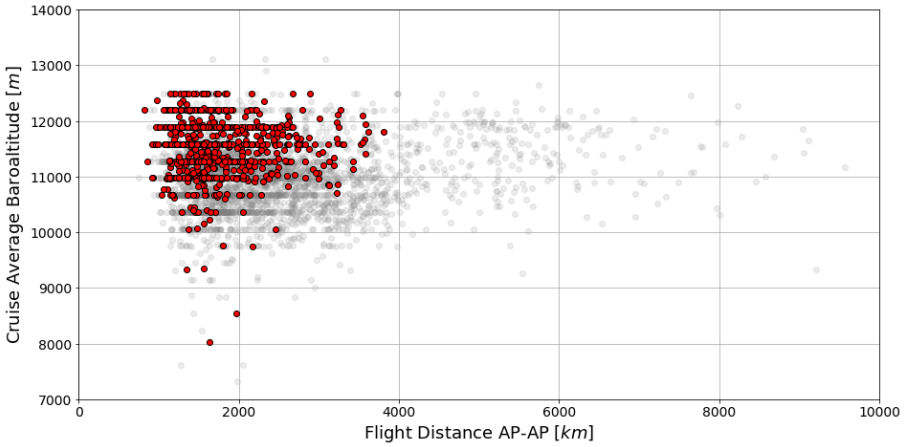

Figure 4.23: Category 3 Flight Distance vs Cruise Altitude

The fuel per ASK versus flight distance is shown in Figure 4.24. Compared to category 4 flying the same distances, the fuel use per seat is slightly higher. At the same time, the fuel burn is calculated to be lower than that of the largest categories flying the same distances. The optimal flight distance fuel-wise for this category is around 2000 km. Shorter distances result in a higher relative fuel burn, which is expected to be caused by the fuel-intense takeoff and climbing to make up a larger part of the flight. Flying longer than 2000 km causes the increased amount of fuel carried during the entire flight to increase the overall fuel burn.

The horizontal black line represents the average fuel burn per ASK based on the WeCare data for this category. The points all lie around this average, indicating that the fuel burn calculated from the set of identified flights roughly matches the overall average calculated with a different method. In general, the fuel burn using this method results in a higher fuel burn for this category.

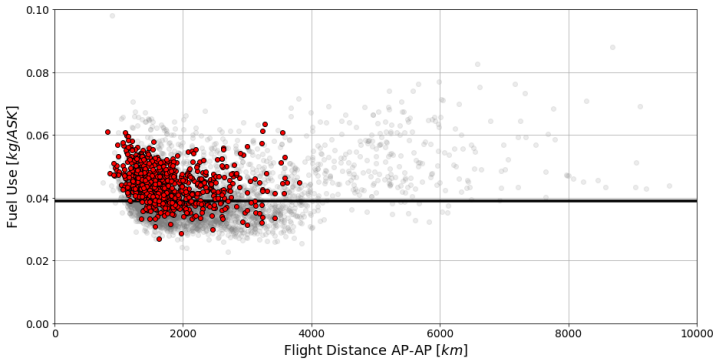

Figure 4.24: Category 3 Flight Distance vs Fuel Use

Figure 4.25 shows the NO_x emission per ASK for the identified flight. For category 3 the amount of NO_x emitted is similar to other aircraft flying similar distances. Compared to the WeCare database this method results in lower NO_x emissions, with the majority of points being below the database average. This can be a result both of different calculation methods and of as a different selection of aircraft used to represent the different categories. Whereas the calculated temperature change is based on the WeCare NO_x values, this approach does not yield the same results in terms of NO_x emission. Because of this, the relatively high contribution of ozone for this category might have been overestimated. The influence of the uncertainty in NO_x emissions for all categories will be addressed in chapter 5.

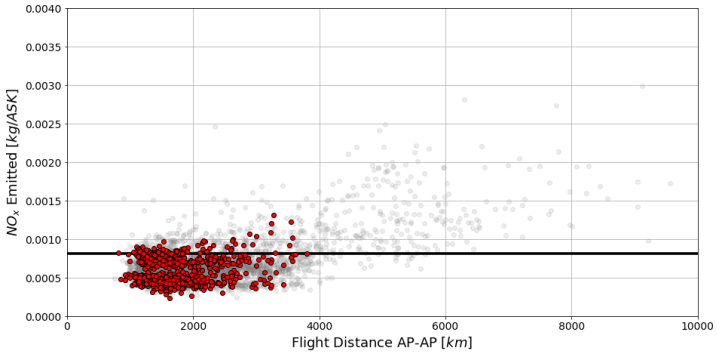

Figure 4.25: Category 3 Flight Distance vs NO_x Emission

Similar to how category 2 showed a more even distribution in fuel use than category 1, the global differences are even smaller for category 3, as can be seen in Figure 4.26. The global activity is more spread out and several regions with no presence of smaller aircraft show some category 3 fuel use, such as Africa, Australia and large parts of Central Asia.

Figure 4.26: Category 3 Global Fuel Distribution in 2012

4.6. Category 4

Having 152-201 seats, category 4 aircraft are the most commonly used globally. Whereas it shows to have one of the largest impacts overall, it is the category with the lowest temperature change per ASK as shown in Figure 4.27. By 2100 its impact per ASK is roughly half that of the worst categories. The variation between the effects of individual species of category 4 is very similar to that of the overall distribution, one difference being a slightly lower relative impact of ozone. Whereas category 3 had a higher impact due to higher cruise altitudes, for this category the impact is lower.

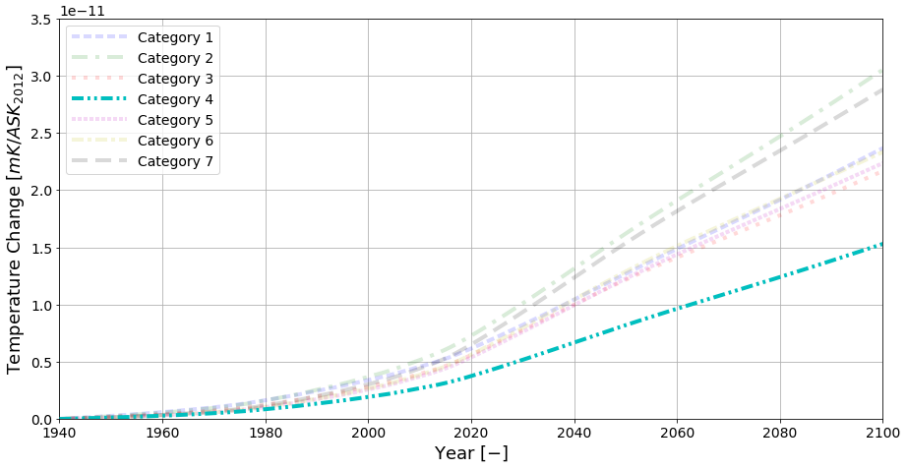

Figure 4.27: Category 4 Temperature Change per ASK in 2012

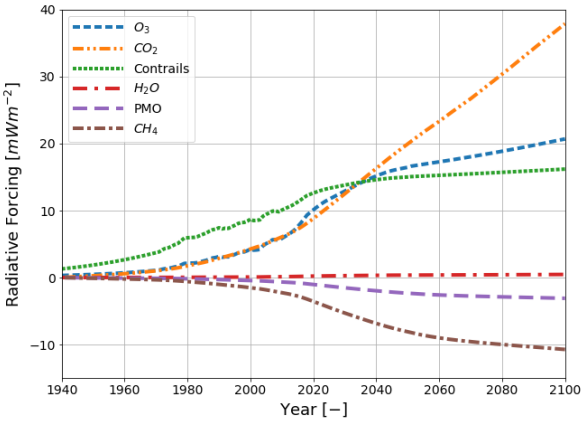

Figure 4.28: Category 4 Radiative Forcing by Species

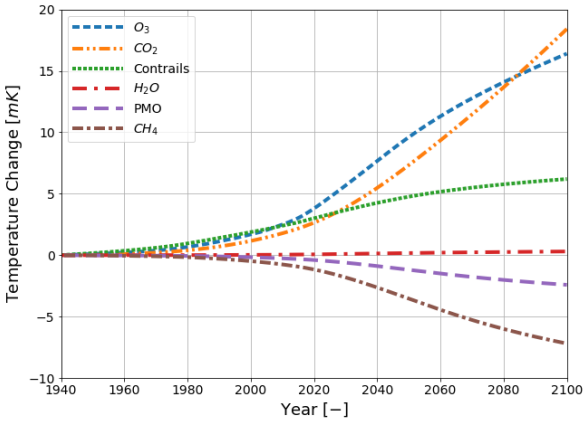

Figure 4.29: Category 4 Temperature Change by Species

The majority of all identified flights are from this category, making up 3819 flights in total. The overall distribution is very similar to that of category 3, but the same routes are flown at a higher frequency. The range limits the aircraft to mostly fly within a continent, as can be seen in Figure 4.30.

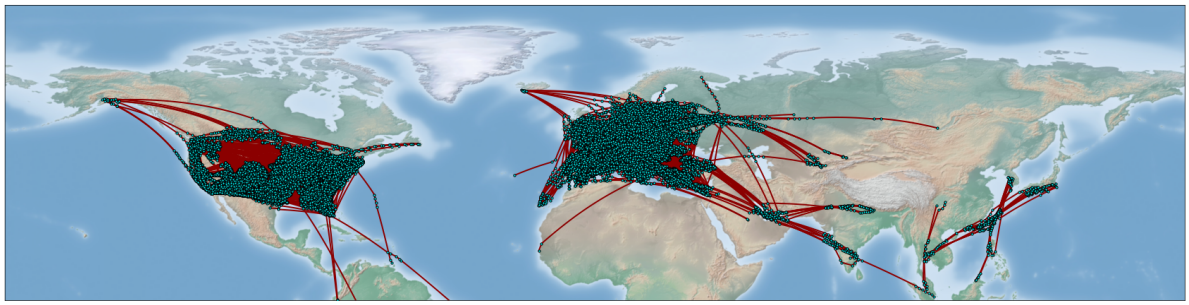

Figure 4.30: Category 4 01/09/2019 Identified Flights

Figure 4.31 shows the flight distances and altitude for flight of aircraft within category 4. With a few exceptions the flights do not exceed a 4000 km flight distance. The ranges covered by this category completely overlap those of category 3, as the very shortest flights are also performed with these aircraft. The average cruise altitude is notably lower.

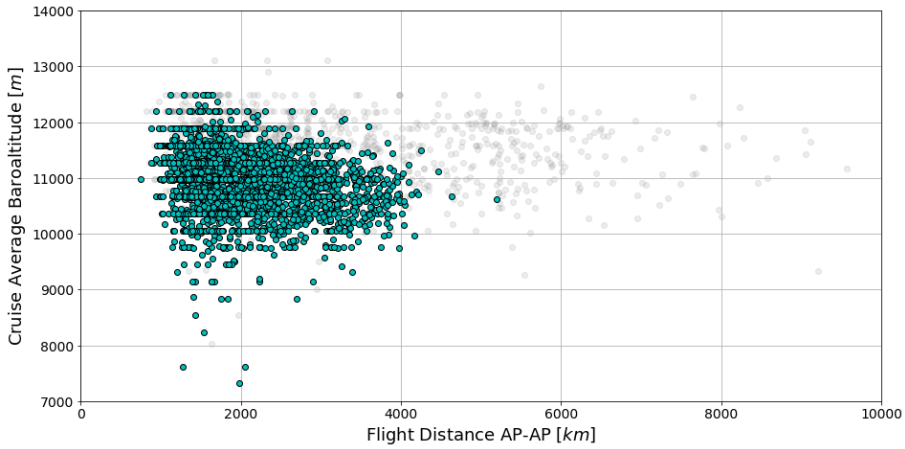

Figure 4.31: Category 4 Flight Distance vs Cruise Altitude

In terms of fuel use, this category is slightly more efficient than category 3, which can be seen in Figure 4.32. The fuel use per ASK is rather flat over distance, with the average slightly above that found in the WeCare project data. For the same routes, using the aircraft sized for 152-201 seats is the most fuel efficient, with a reduced efficiency both when using smaller and larger aircraft.

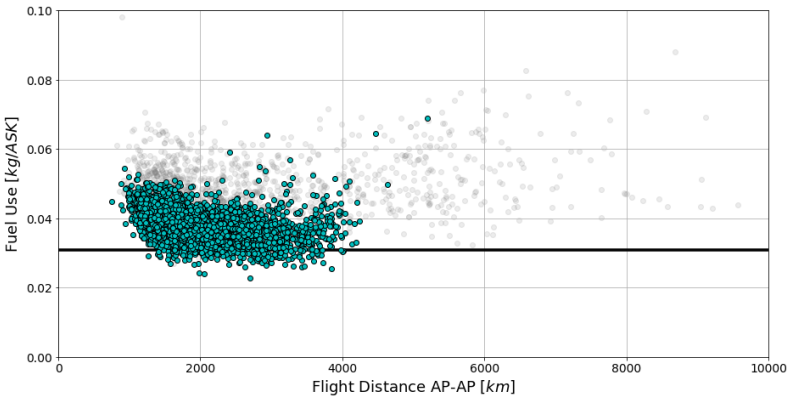

Figure 4.32: Category 4 Flight Distance vs Fuel Use

Whereas category 3 showed a lower amount of NO_x emissions compared to the inventory average, for this category the emissions are much higher, with only few points below the average, displayed in Figure 4.33. Directly compared to category 3 the emitted NO_x calculated is roughly equal for similar flight distances. Possibly, part of the performance of this category is due to the NO_x emissions being underestimated.

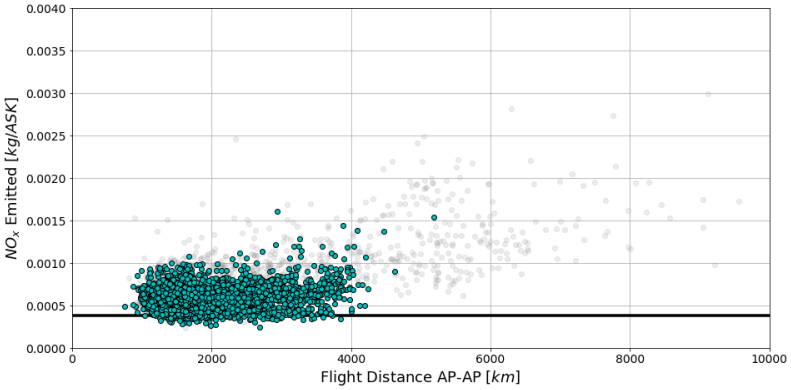

Figure 4.33: Category 4 Flight Distance vs NO_x Emission

Comparing the global fuel distribution to the previous category, there are only very minor differences. The only difference is the higher frequency at which these aircraft are operated, resulting in a total fuel use that is 35% higher than the previous category.

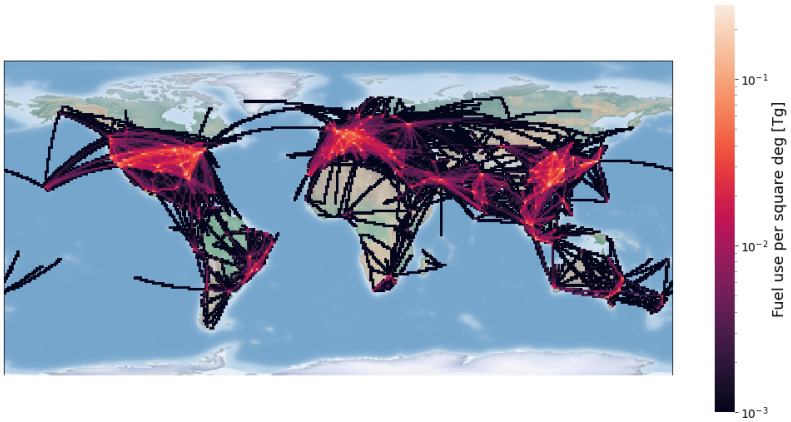

Figure 4.34: Category 4 Global Fuel Distribution in 2012

4.7. Category 5

Category 5 is about aircraft carrying between 202-251 seats. Its overall impact ranks third only behind the two smallest categories. By temperature change per ASK this category is in the middle of the group as shown in Figure 4.35. From the individual species' contribution, shown in Figure 4.36 and Figure 4.37, one can see that the impact of contrails is relatively high for these aircraft. In comparison the relative impact of CO_2 to that of O_3 closely matches that of aviation overall, both at a lower share due to the increased contrail's magnitude.

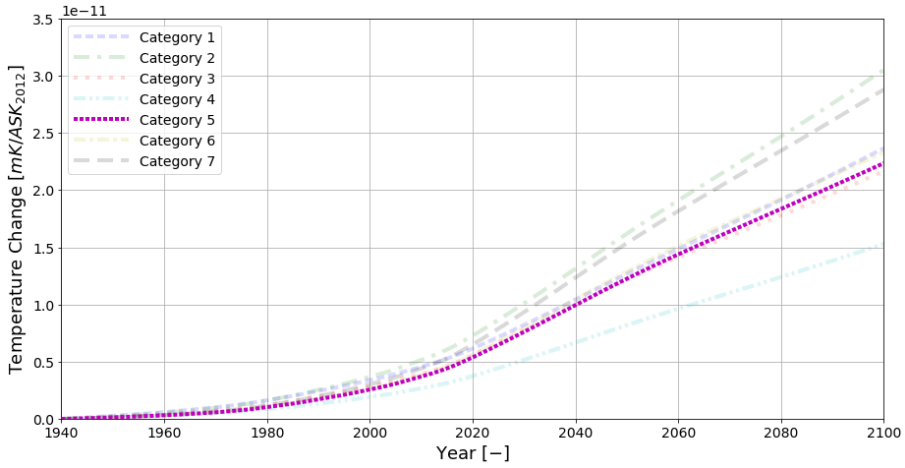

Figure 4.35: Category 5 Temperature Change per ASK in 2012

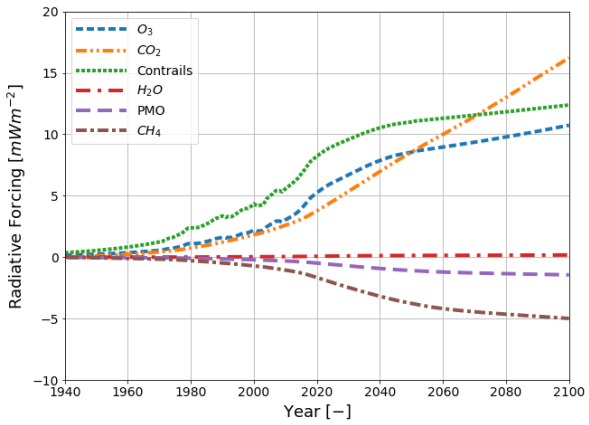

Figure 4.36: Category 5 Radiative Forcing by Species

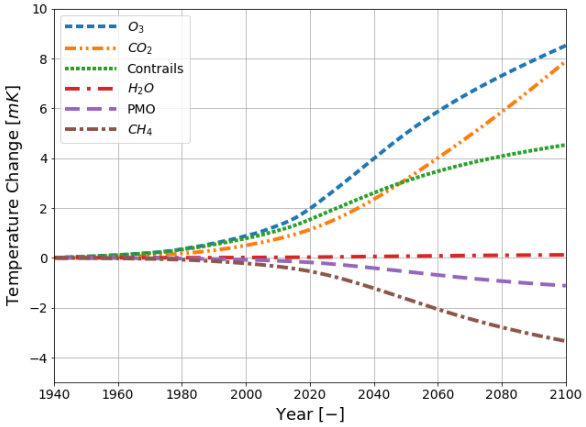

Figure 4.37: Category 5 Temperature Change by Species

From the flight data 288 flights have been found. These immediately show why this category is different from the previous, in that the range allows much longer flights to be made, resulting in flights going overseas and all the way from Europe to Japan as can be seen in Figure 4.38.

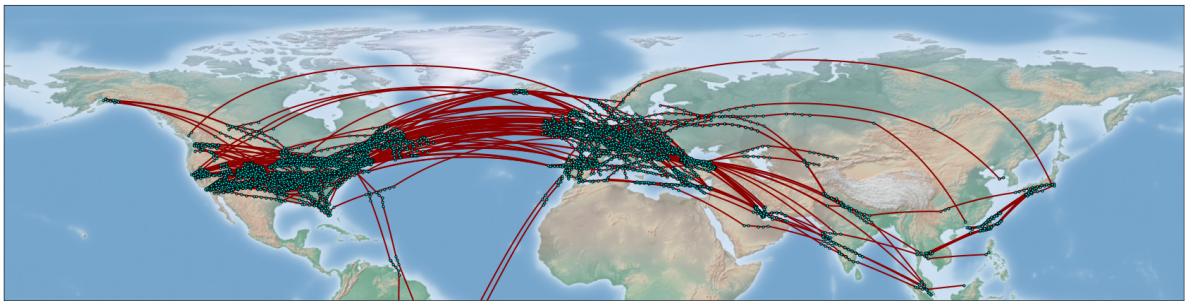

Figure 4.38: Category 5 01/09/2019 Identified Flights

Whereas the previous category mostly flew missions below 4000 km, slightly increasing aircraft size results in a big jump with ranges up to 9000 km. The average cruise altitude is close to 12 km, covering the highest flown flights of the overall flights found, as can be seen in Figure 4.39.

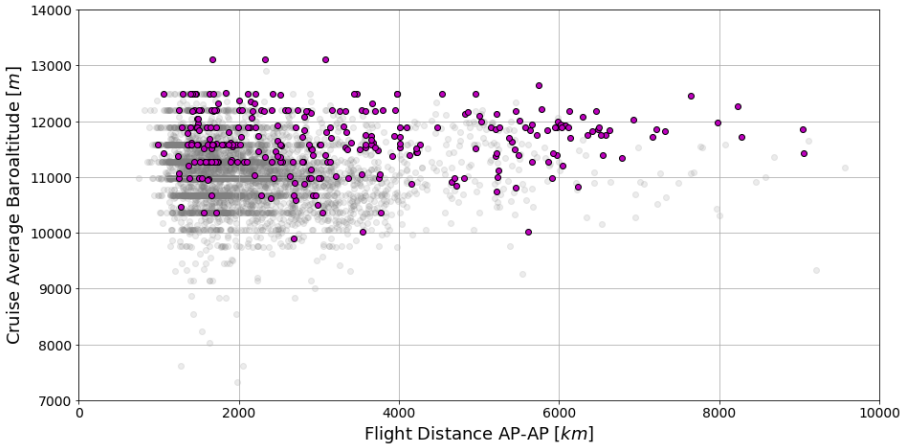

Figure 4.39: Category 5 Flight Distance vs Cruise Altitude

Shown in Figure 4.40, the calculated fuel use is significantly higher than that of category 4 over the same ranges. As the flight distance increases so does the spread, with the overall trend showing an increasing fuel use. The method used has led to the majority of flights showing a higher fuel use than the WeCare average, which again can be caused by different calculation methods or the selection of aircraft included. The found NO_x emissions are much higher, increasing over distance, as shown in Figure 4.41.

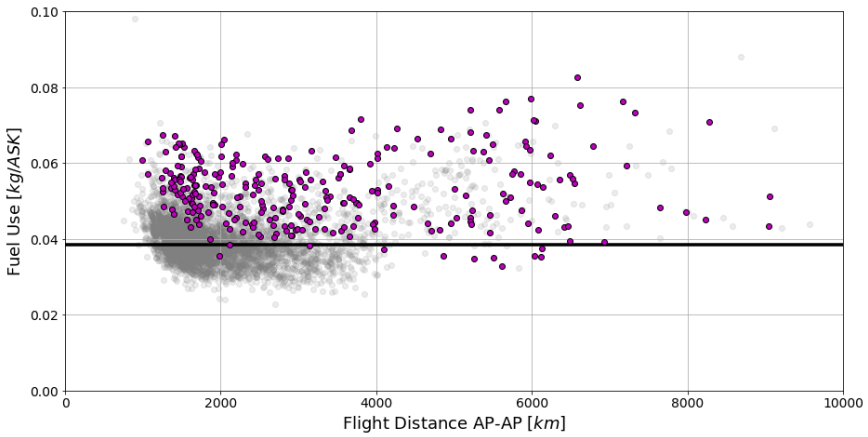

Figure 4.40: Category 5 Flight Distance vs Fuel Use

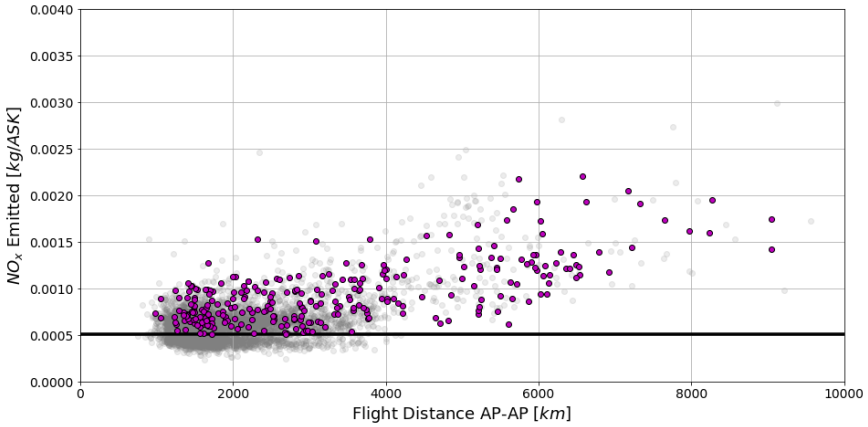

Figure 4.41: Category 5 Flight Distance vs NO_x Emission

In line with the flights found from ADS-B data, the fuel distribution of this category is completely different from the previous. The longer range makes that the aircraft are used for different missions, not being limited by crossing large areas without airports, such as the oceans. Flying in less busy areas directly explains the much higher impact of contrails for this category, due to the lower amount of cloud saturation in these areas.

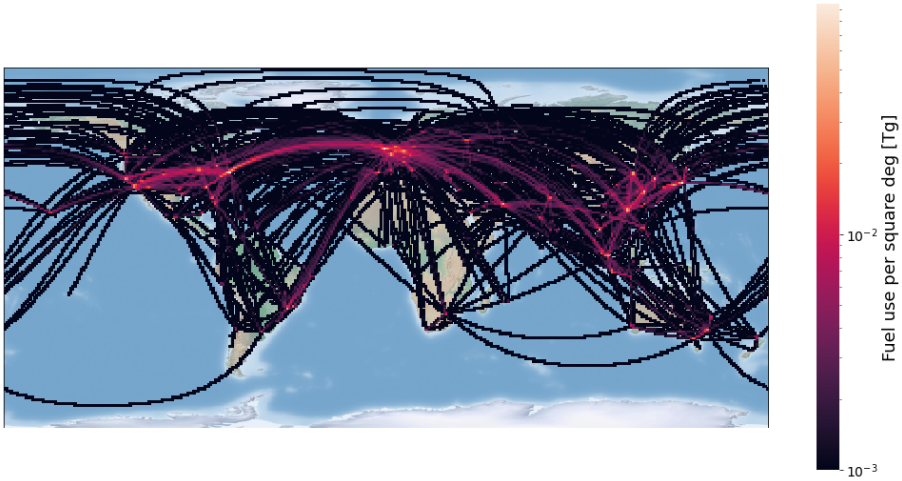

Figure 4.42: Category 5 Global Fuel Distribution in 2012

4.8. Category 6

Category 6 holds up to 301 passengers, being the second category in aircraft size. The overall impact ranks it in the middle of the categories, with a 23 mK temperature change by 2100. Per ASK the performance is slightly worse than the previous, ranking third behind categories 2 and 7. The variation of the species is quite similar to the previous category, with a slightly increased contrail effect.

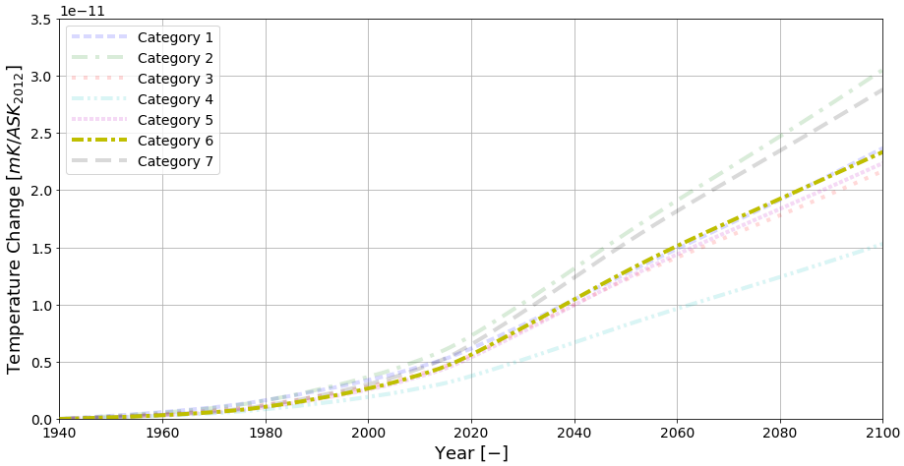

Figure 4.43: Category 6 Temperature Change per ASK in 2012

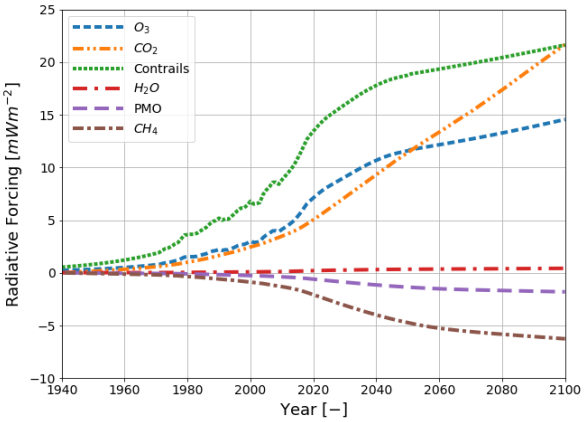

Figure 4.44: Category 6 Radiative Forcing by Species

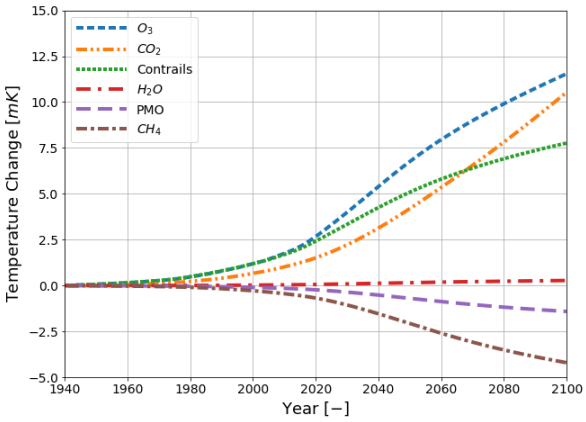

Figure 4.45: Category 6 Temperature Change by Species

On 01/09/2019 148 flights were found using these aircraft, mostly going overseas between the US and Europe, and between Europe and Asia, as shown in Figure 4.46.

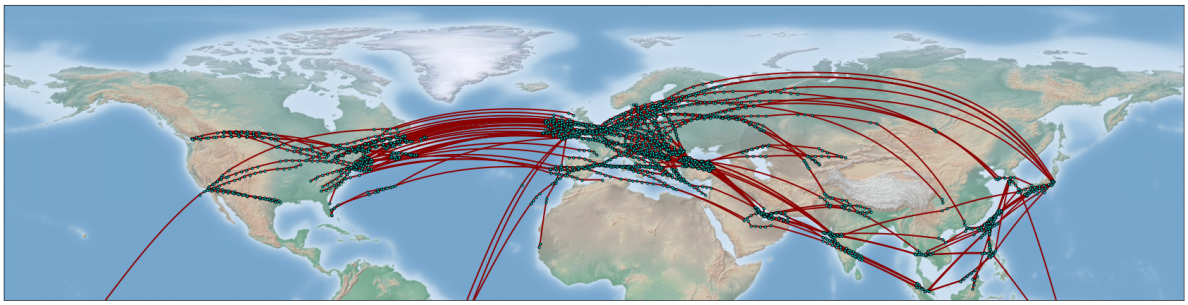

Figure 4.46: Category 6 01/09/2019 Identified Flights

Even though these aircraft have ranges up to 10,000 km, still roughly half of the identified flights are shorter than 4000 km, overlapping missions with much smaller aircraft, as shown in Figure 4.47. This matches the effects shown earlier in Figure 2.7, as for busy routes often large aircraft are used to increase capacity rather than solely increasing the flight frequency of smaller aircraft. The altitudes flown are higher than other aircraft, similar to the previous category. Due to its size, the fuel use per ASK, displayed in Figure 4.48, is significantly worse than the smaller aircraft for the same routes and per ASK the fuel use is lowest around 3500 km. The calculated fuel use for most flights is higher than the WeCare average. The NO_x increases over flight distance, similar to the previous category.

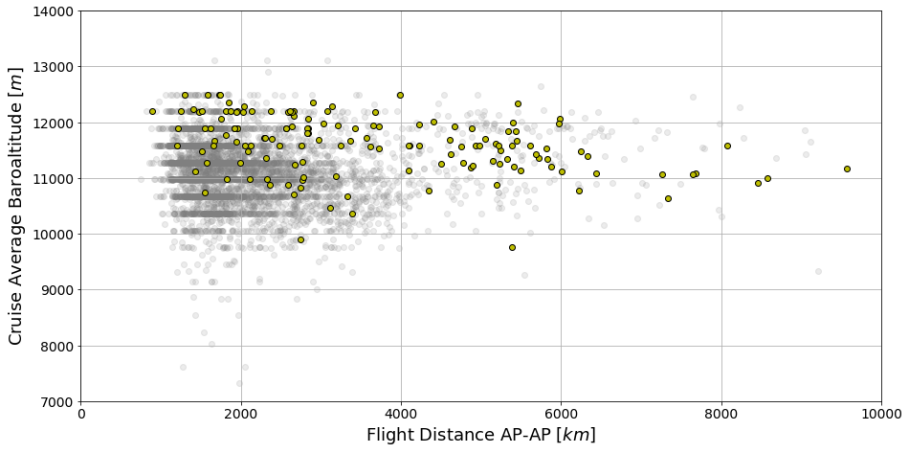

Figure 4.47: Category 6 Flight Distance vs Cruise Altitude

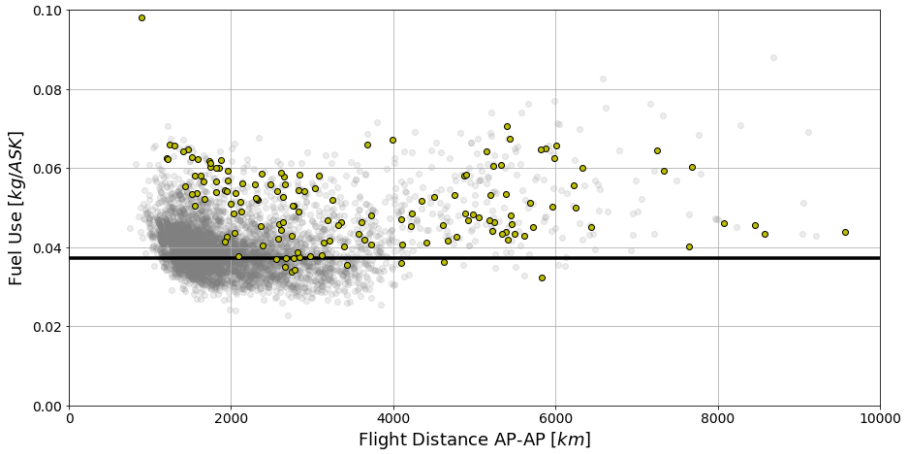

Figure 4.48: Category 6 Flight Distance vs Fuel Use

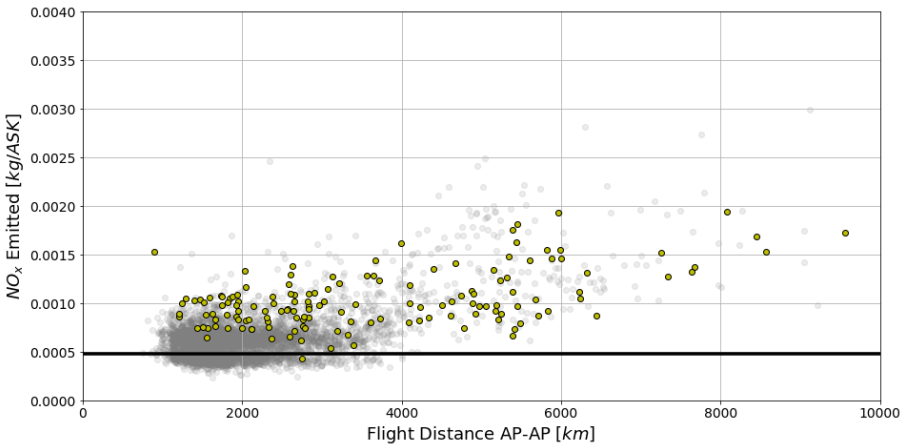

Figure 4.49: Category 6 Flight Distance vs NO_x Emission

At first sight, the fuel distribution in Figure 4.50 is equal to that of category 5. As the aircraft can operate in similar ranges, they are being used for the same routes. Looking more closely it shows that for this category the fuel use is distributed more evenly over the globe. The peaks at areas such as Europe and the US east coast are smaller compared to the overseas routes, which means that these aircraft are used more for inter-continental flights and less for shorter flights within the continent. This increases the time spent flying in less busy areas, with a lower cloud saturation and thus a higher contrail sensitivity. This causes the category to have an increased temperature change due to contrails and ultimately a higher impact overall.

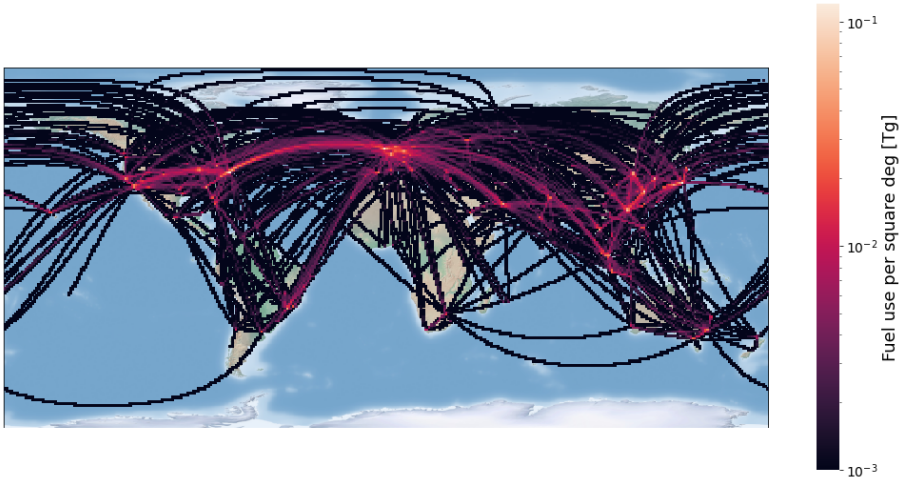

Figure 4.50: Category 6 Global Fuel Distribution in 2012

4.9. Category 7

Category 7 makes up the very largest aircraft, containing over 301 seats. Whereas the other categories each cover a range of ~50 seats, this covers much more, meaning there is also a larger variation between aircraft within this category. This category has the largest climate impact overall, as well as having the second largest impact per ASK, as displayed in Figure 4.51. The impact is largely made up by ozone and CO_2, as shown in Figure 4.52 and Figure 4.53. The relative importance of contrails is much lower for this category, as the impact of a single contrail does not scale with aircraft size within the employed model.

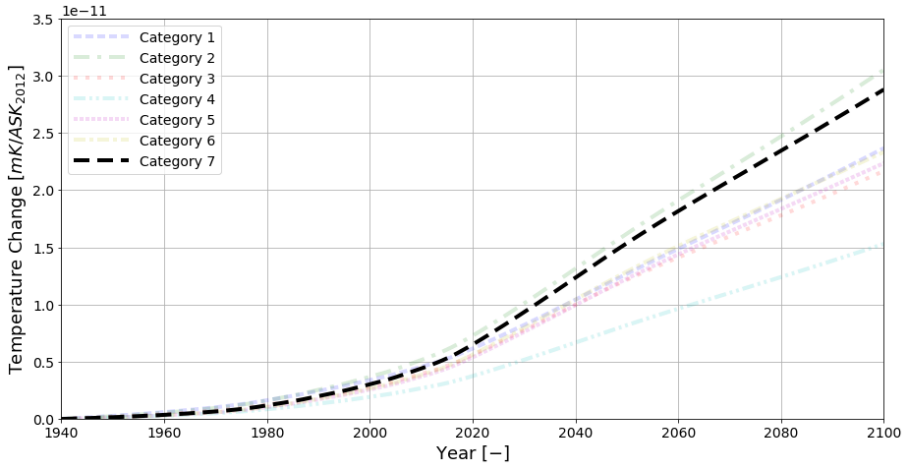

Figure 4.51: Category 7 Temperature Change per ASK in 2012

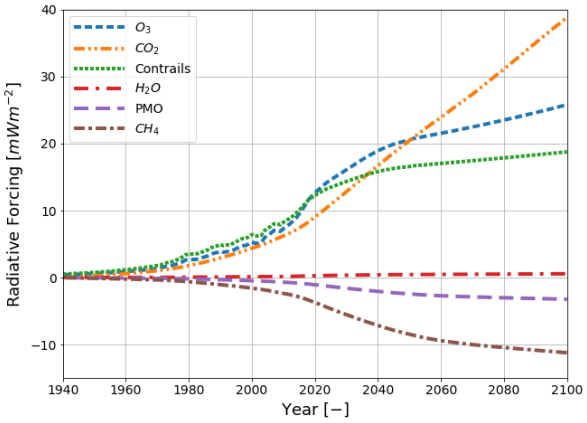

Figure 4.52: Category 7 Radiative Forcing by Species

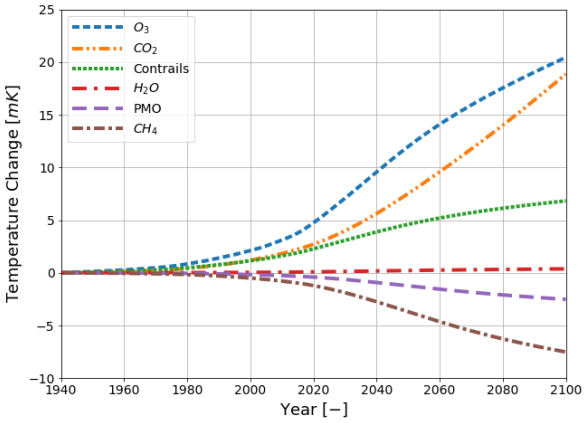

Figure 4.53: Category 7 Temperature Change by Species

215 flights have been found and this is the only category to have flights identified crossing the Pacific Ocean. In general, the routes flown are the same as for the previous 2 categories, which have a similarly long range.

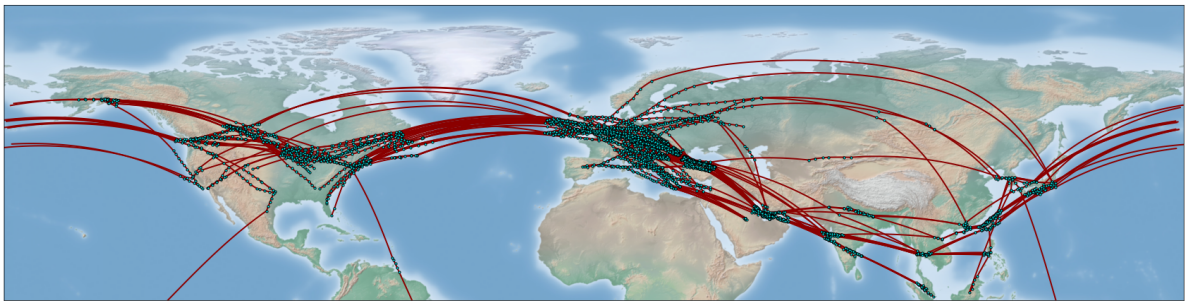

Figure 4.54: Category 7 01/09/2019 Identified Flights

Figure 4.55 shows the altitudes of these aircraft are much lower than the ones in category 6, with a larger spread. This explains why the impact of ozone relative to CO_2 for this category is the same as for the previous two, despite having an increase in NO_x emission. The effect of NO_x is smaller at lower altitudes, offsetting the increased emission resulting in a similar impact.

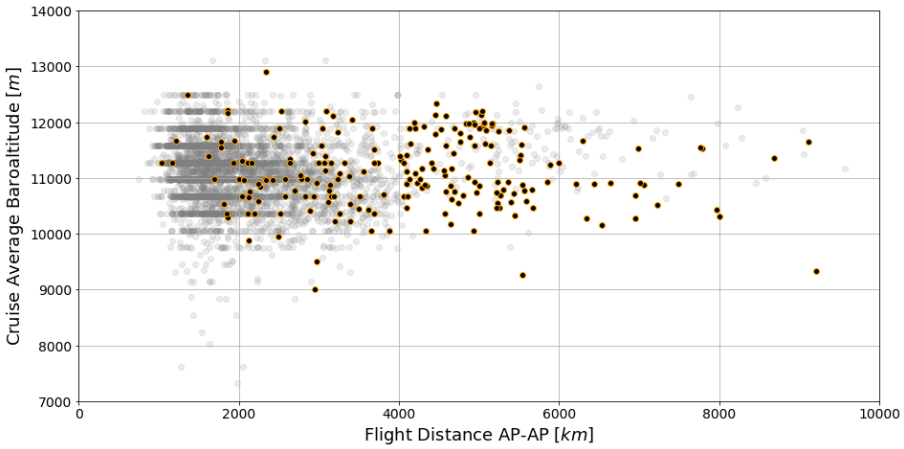

Figure 4.55: Category 7 Flight Distance vs Cruise Altitude

The average fuel use for this category closely matches that of the WeCare database, as seen in Figure 4.56. The spread is relatively small, with most values around the 0.05 kg per ASK mark. There is still a significant number of flights going short distances, even though these aircraft have a longer range. At these shorter distances the fuel use for this category is higher than for the other categories. Again the NO_x emissions are significantly higher than calculated within the WeCare database, due to differences in calculation methods.

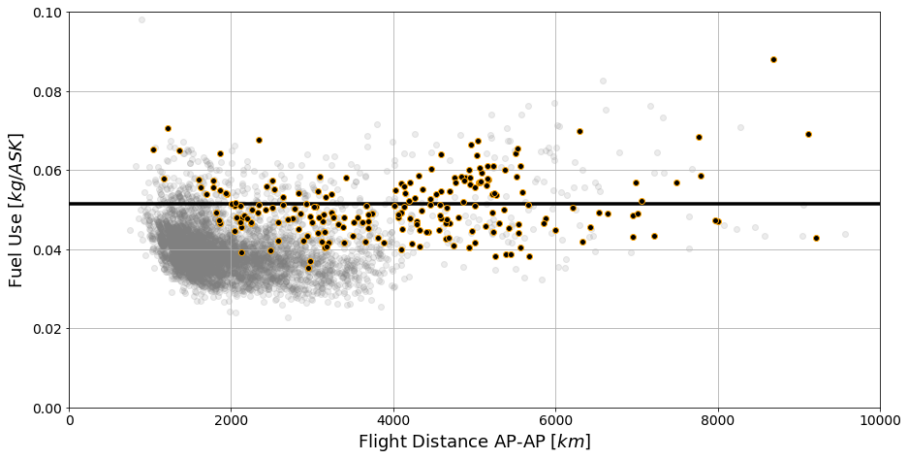

Figure 4.56: Category 7 Flight Distance vs Fuel Use

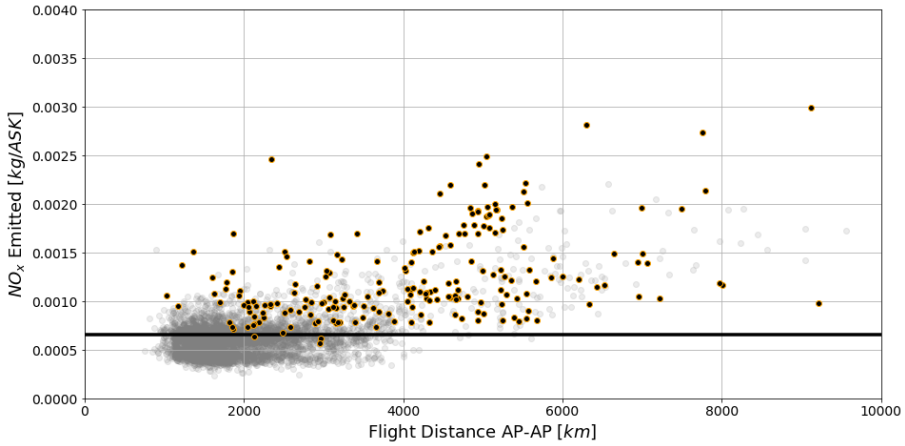

Figure 4.57: Category 7 Flight Distance vs NO_x Emission

The distribution of fuel globally shows only minor differences compared to the previous category, with a relatively smaller presence in Africa, and a smaller difference between the peak fuel locations and the fuel burned on routes going overseas.

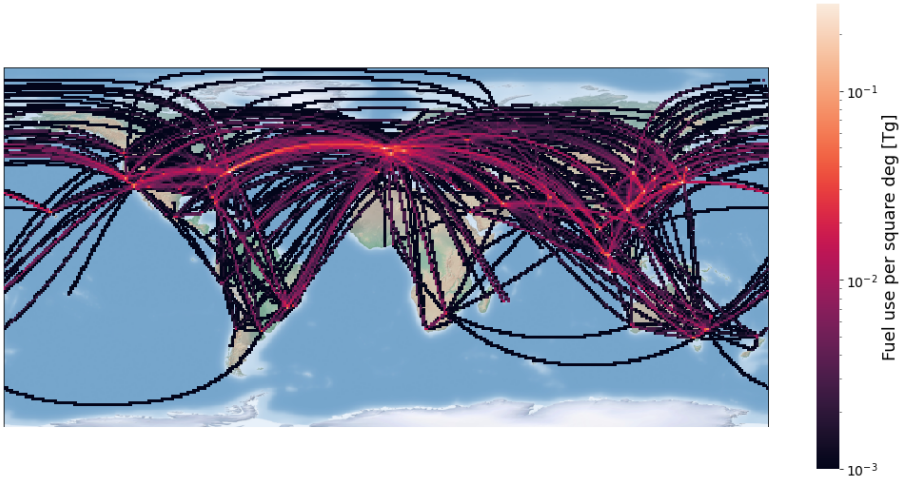

Figure 4.58: Category 7 Global Fuel Distribution in 2012

4.10. Adjusting Seating Capacity

So far clear differences between the aircraft types have been found, with the general climate impact described in terms of temperature change per ASK. Whereas when comparing the aircraft, ASKs can be used as a neutral factor of capacity, it is not fair to say that each seat flying a kilometre has the same value. Smaller aircraft, which are used for shorter flights, are often characterised by being less comfortable for the passenger. Seats are typically spaced closer together, thus more efficiently filling the aircraft. Long range aircraft typically assign more space per passenger, for example by providing beds for first class passengers. Ultimately, for the flights going the same distance it has been shown that the fuel use per ASK of a category 4 aircraft is superior to that of any larger category. However, these aircraft generally provide a less comfortable flight than the larger aircraft, and ASKs of these aircraft cannot be interchanged one-on-one.

In order to quantify the potential performance of the different aircraft providing a similar experience, an additional fuel use calculation is performed assuming equal seating density between aircraft. This is done by assuming the number of seats on the aircraft to be equal to the single-class maximum seating for each model. [31] This leads to an increase of capacity for each aircraft, but percentually the highest difference is found for the largest aircraft. The operating empty weight of the aircraft is assumed to remain the same, and an increase in overall weight is caused by the additional number of passengers on board, using the same load factor as before. Whereas this assumption will lead to a higher fuel use overall, the amount of ASKs generated will also increase with a more dense seating arrangement.

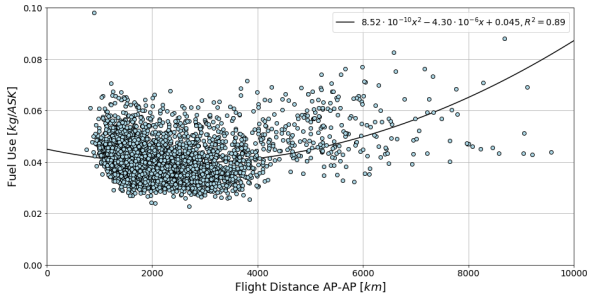

Figure 4.59: Fuel Use vs Flight Distance - Conventional

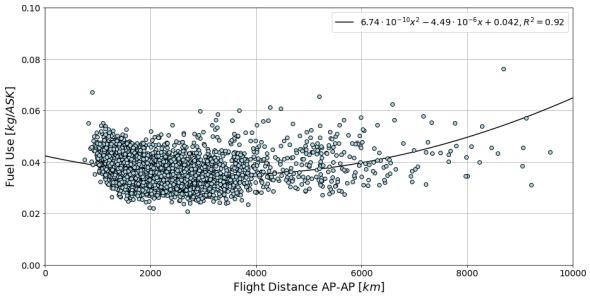

Figure 4.60: Fuel Use vs Flight Distance - Single Class Seating

The two figures above show the fuel use per ASK for the initial analysis (left) and that for the increased seating capacity (right). In general, the average fuel use for a given distance has improved. This is caused by an improvement for the points with the highest fuel use, which have shown to be flights from the three largest aircraft categories. The flights with the lowest fuel use, originating from the smaller aircraft, have barely changed in fuel use per ASK. Together, this leads to a reduction in overall spread. The flights of the long range aircraft are now closer to overlapping those of the shorter range aircraft, while the optimal flight distance has not changed. The initial jump in fuel use around the category 4 maximum range (~4000 km) has been reduced and is not clearly present in the new results.

The change in seating capacity has mixed effects on the NO_x emission. By being heavier, the thrust setting of the engines in flight is higher, leading to a higher NO_x emission index. At the same time, the fuel burned per ASK is reduced, positively affecting the NO_x per ASK. Ultimately, the same effect as for the fuel use is predominant, reducing the spread and the overall NO_x emission, with the exception of a small number of flights. The larger aircraft still make up the flights with the highest NO_x emission per ASK.

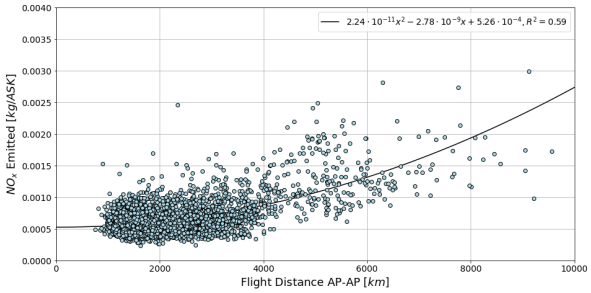

Figure 4.61: NO_X Emission vs Flight Distance - Conventional

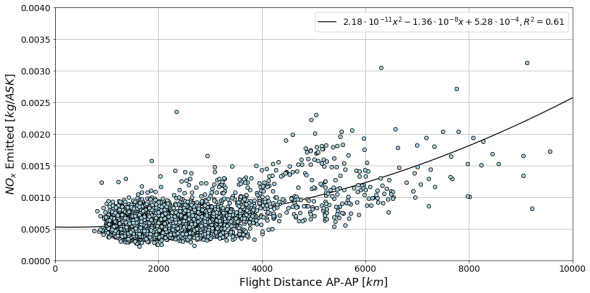

Figure 4.62: NO_X Emission vs Flight Distance - Single Class Seating

In the end the performance, especially of long range aircraft, can be significantly improved by increasing the seating density. The aircraft with a shorter range have a capacity that is closer to the maximum, leaving less room for improvement. Even though the smaller aircraft outperform the largest in terms of fuel use and NO_X emission per ASK, part of this difference can be attributed to the higher level of comfort provided by these large aircraft.

4.11. Adjusting Cruise Speed

The differences in cruise speed strongly divide the aircraft categories, with a jump in Mach number between categories 4 and 5. The exact effect of this difference is hard to quantify, as the optimal cruise speed is very much a result of the choices made in the aircraft design. Whereas alterations in aircraft design are out of scope, the direct effect of lowering the cruise speed for the largest aircraft category is investigated by re-performing the fuel calculations assuming a cruise Mach number of 0.77, matching that of category 4 aircraft. The graphs below compare the fuel use for the flights of category 7. It becomes clear that a reduction in cruise Mach number leads to an increase of fuel use, independent of the distance flown. The negative effect of the additional time being in the air outweighs the benefit of flying at a lower thrust.

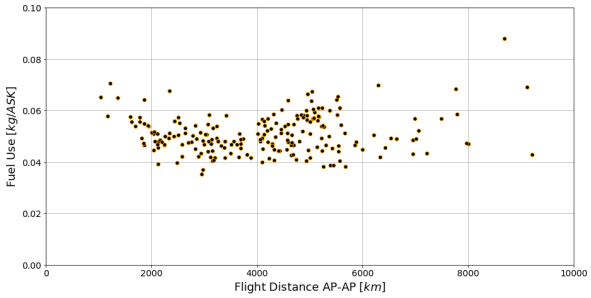

Figure 4.63: Fuel Use vs Flight Distance - Conventional

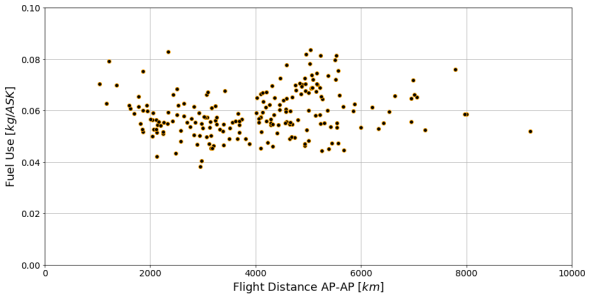

Figure 4.64: Fuel Use vs Flight Distance - Cruise Mach 0.77

The same effect is seen in the emissions of NO_X. Flying at a lower speed has the potential to reduce the thrust setting and decrease NO_X emission. However, the increase in fuel burn has resulted in a higher NO_X emission, due to the increase in aircraft take-off mass.

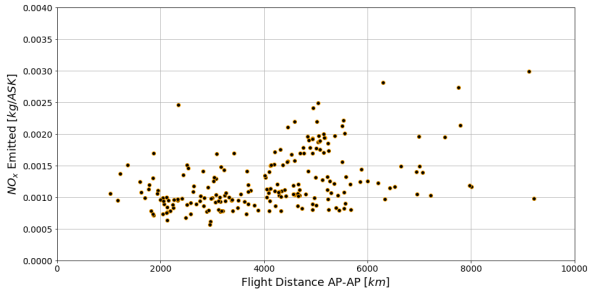

Figure 4.65: NO_X Emission vs Flight Distance - Conventional

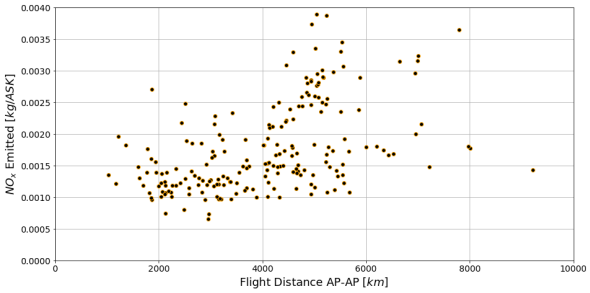

Figure 4.66: NO_X Emission s Flight Distance - Cruise Mach 0.77

It has become clear that only reducing the cruise speed of larger aircraft to match category 4 does not reduce the difference in fuel burn and emission. Doing so only has downsides, as the increased flight time and moving away from the design optimal speed leads to an increase in fuel burn and NO_X emission. A reduction in cruise speed could still improve the performance of large aircraft, but this would require a change in design, as shown in the analysis of the Airbus A330-200 performance. [6]

5

Uncertainty Analysis

Throughout the analyses various assumptions have been made in order to get to a result. Since these assumptions are often not a certainty and directly affect the results, the impact of the most important assumptions will be assessed with the aim to address the robustness of the given results.

In assessing the climate impact of the different categories the provided WeCare database has been used combined with the AirClim climate response model. Uncertainties are present in the additional assumptions made to combine these, for example in the assumed development scenarios of fuel and background emissions. Additionally, assumptions are already present within the creation of both the database and the AirClim model, as these only represent reality, in contrast to real-life measurements. The assumptions expected to influence the outcome the most, will be altered individually to investigate their effects.

5.1. Background Emission Scenarios

The assumed background emission scenario for the period up to 2100 is the RCP4.5 scenario, as it seems to be the middle of the road. In order to see what happens in a situation where the background emission levels are either significantly higher or lower, the changes in results assuming a more extreme scenario are investigated.

5.1.1. RCP2.6

In the RCP2.6 scenario the background emissions are at a lower level, with a roughly stagnant level of CO_2 from the year 2030 onward, and decreasing levels of methane. The differences in the original results (Figure 5.1) and when assuming the RCP2.6 scenario (Figure 5.2) are shown below. The main difference is an increase in the impact of CO_2. Due to the lowered background level of CO_2, the temperature change due to aviation's CO_2 has increased. This is caused by the decreasing sensitivity in CO_2 radiative forcing for increasing concentrations. [39] The magnitude of the cooling effect due to methane destruction has decreased. As background levels of methane are lower, the pace of the reaction between NO_x and CH_4 is reduced. Overall, by 2100 the temperature change has increased from 145 mK to 165 mK due to the lower level of background emissions.

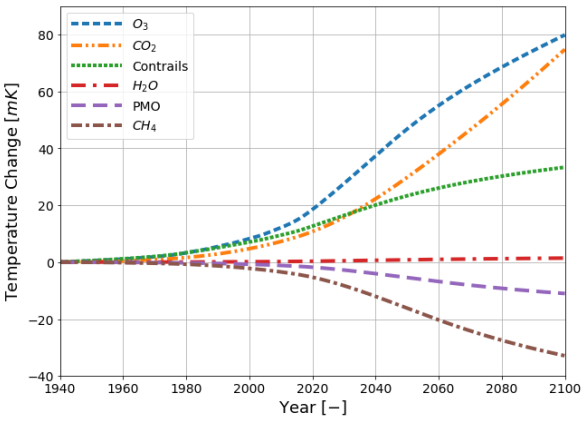

Figure 5.1: Base Temperature Change by Species

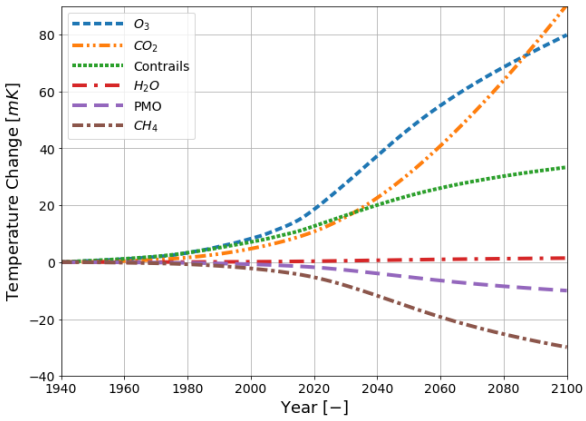

Figure 5.2: RCP2.6 Temperature Change by Species

The differences in temperature change caused by the individual categories have not changed significantly. The temperature change per ASK has increased for each category, but the categories have not changed in comparative performance. The categories which showed to have a relatively high share of CO_2 temperature change, mainly categories 1 and 2, experience the largest increase due to the increased CO_2 effects, but the findings discussed still hold for all categories. In this situation in which the background emission levels are lower than initially assumed, no significant changes are found which would affect the conclusions that can be drawn when comparing the categories. Having lower background levels of CO_2 and CH_4 does increase the climate impact the aviation industry has as a whole.

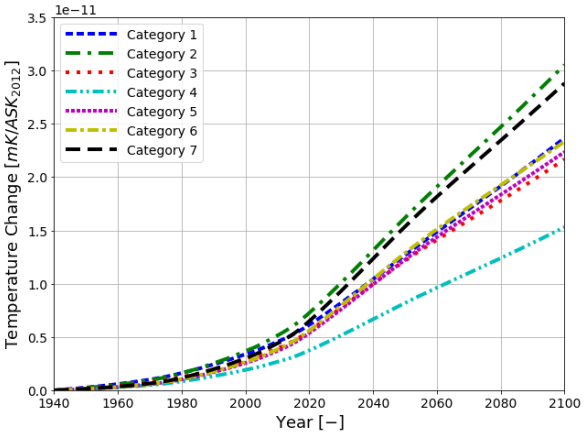

Figure 5.3: Base Temperature Change by Category

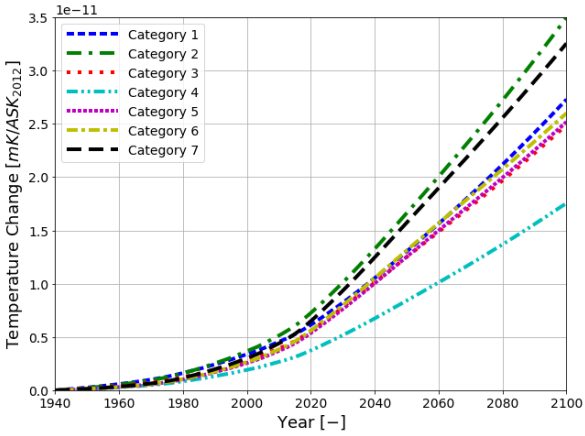

Figure 5.4: RCP2.6 Temperature Change by Category

5.1.2. RCP8.5

In the RCP8.5 scenario the background emissions of CO_2 and CH_4 are increasing within the period up to 2100. CO_2 in the atmosphere is accumulating at an increasing rate, and the increase in methane is accelerating up to 2040, after which it grows at a slower rate. By 2100 the methane levels are more than double that of 2000. Compared to the RCP4.5 scenario the CO_2 concentration is 74% higher by 2100, whereas the CH_4 concentration is more than double as high.

The result from increasing background emission levels is exactly the opposite of what happened by decreasing these levels. The effect of CO_2 is significantly reduced, and the slope of the temperature change due to CO_2 starts decreasing after 2050. The cooling effect due to methane destruction is much larger and now also a clear magnitude increase of primary mode ozone temperature change can be observed. The overall temperature change by 2100 will have been reduced to 113 mK.

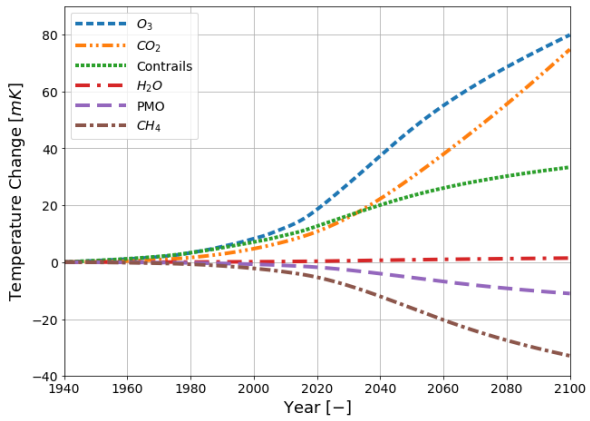

Figure 5.5: Base Temperature Change by Species

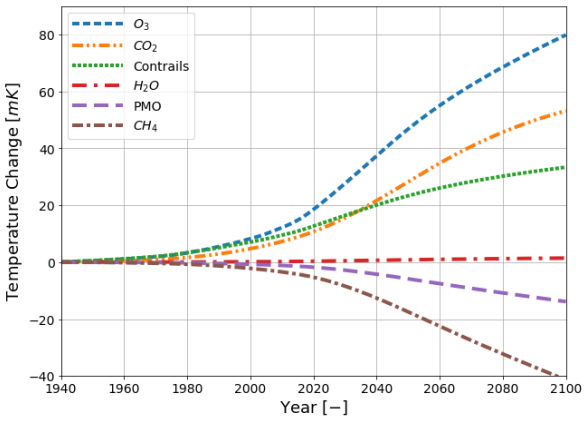

Figure 5.6: RCP8.5 Temperature Change by Species

Due to the reduction of CO_2 effects, the climate impact of all categories has been reduced. The overall shape of the development has changed, and due to the much higher background emission level achieved, the impact of the different categories normalised to the ASKs flown in 2012, has a decreasing slope after 2050, matching the overall decelerating temperature change of aviation as a whole. The main differences between the categories remain, with small alterations due to the aircraft having a different dependence on the various species. Still, the findings with respect to how the categories compare remains, but the overall picture in terms of development of the contribution of aviation to climate change varies as the background emission levels are higher.

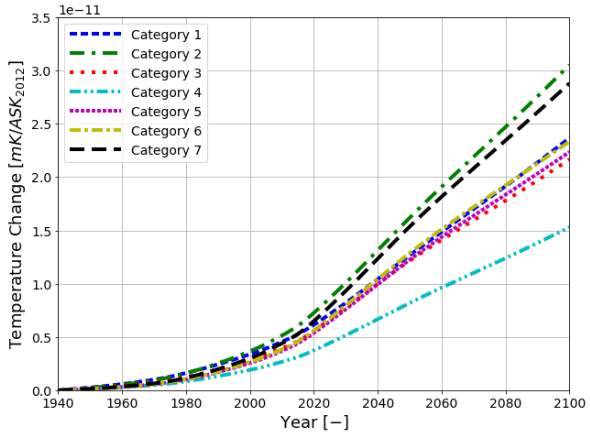

Figure 5.7: Base Temperature Change by Category

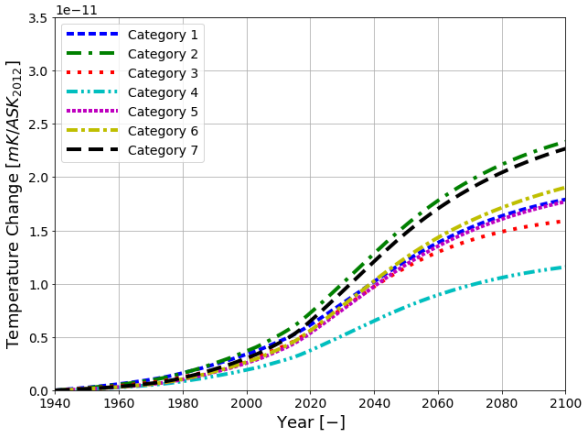

Figure 5.8: RCP8.5 Temperature Change by Category

5.2. Fuel Development Scenario

5.2.1. Increase and Decrease in Fuel Use

The fuel development scenario is used to scale the fuel use, distance flown and emissions over time. In order to see the effect of a different development, the assumed fuel use has been increased and decreased by 10% from the original starting point from the year 2013, the first year after the emission inventory year. As everything is scaled by the fuel use, there is very little variance in the emissions' relative importance. The overall impact changes with the fuel development, but no relative changes can be observed between the individual emissions nor between the different categories. The internal relations in the outcome show a low sensitivity to the overall fuel development, given that the emissions scale with the same factor.

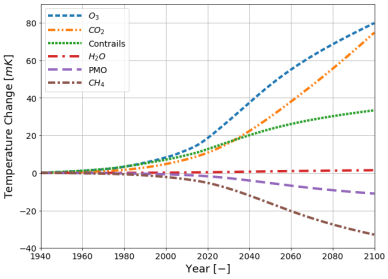

Figure 5.9: Base Temperature Change by Species

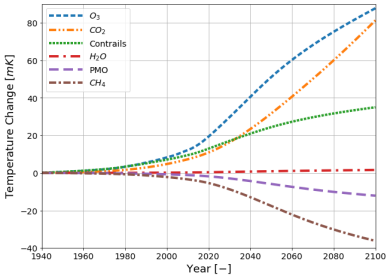

Figure 5.10: Increased Fuel Use Temperature Change by Species

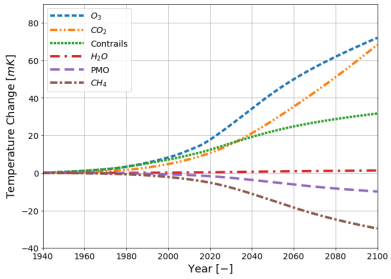

Figure 5.11: Decreased Fuel Use Temperature Change by Species

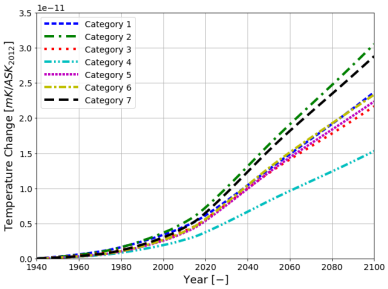

Figure 5.12: Base Temperature Change by Category

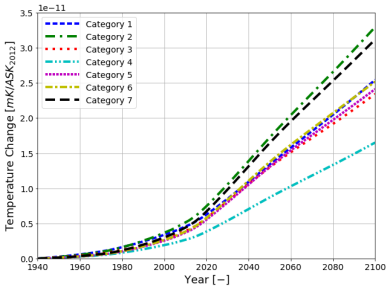

Figure 5.13: Increased Fuel Use Temperature Change by Category

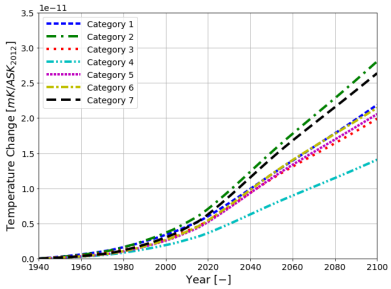

Figure 5.14: Decreased Fuel Use Temperature Change by Category

5.2.2. Biofuel

In the future there could be a shift of aviation towards making more use of bio-fuels, reducing the net emissions of aviation. In order to see how the increased use of bio-fuels affects the results, two scenarios are considered, in which the adoption of bio-fuels start in the year 2021, with the percentual share increasing linearly up to 50% and 100% of the total fuel use by 2100.

Within AirClim the effect of biofuel use is included by reducing CO_2 emission. Both scenarios cause a significant decrease in the temperature change by CO_2. In the most extreme case it is assumed that all burned fuel is bio-fuel by 2100, causing the curve to flatten towards this year. As CO_2 accumulates in the atmosphere the temperature change of CO_2 does not directly decrease from the reduction in emission. In the case of a bio-fuel share of 50% by 2100 the slope of the CO_2 curve has been reduced, resulting in a close to linear temperature development.

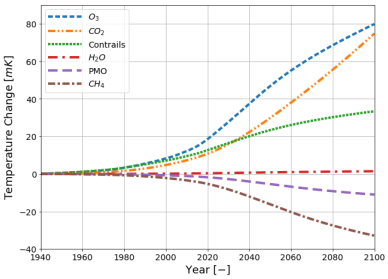

Figure 5.15: Base Temperature Change by Species

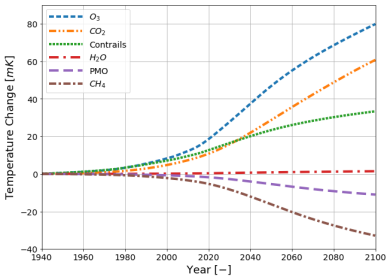

Figure 5.16: Bio-fuel up to 50% Temperature Change by Species

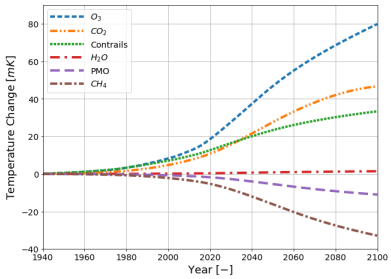

Figure 5.17: Bio-fuel up to 100% Temperature Change by Species

Since the CO_2 emission plays a significant role for all aircraft categories, the change mostly causes a different development overall, with minor changes in comparing the different categories. The extreme case has led to 19% reduction in temperature by 2100 (to 117 mK) and is clearly visible in the reduced slope of the overall temperature change. The categories for which CO_2 made up the largest share of overall impact benefit the

most from the adoption of bio-fuels, with the largest change observed in category 1. Overall, the differences between categories shows little sensitivity to an adoption of bio-fuels over an 80-year period.

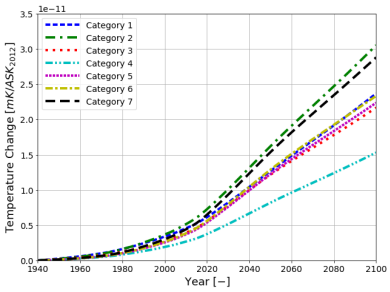

Figure 5.18: Base Temperature Change by Category

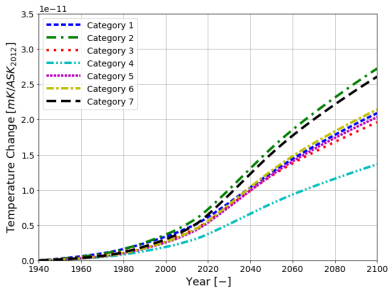

Figure 5.19: Bio-fuel up to 50% Temperature Change by Category

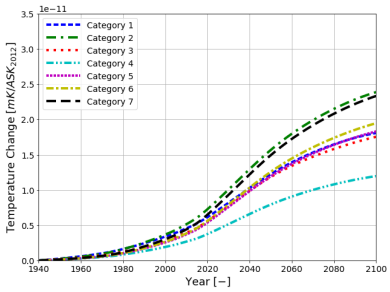

Figure 5.20: Bio-fuel up to 100% Temperature Change by Category

5.3. Contrail Size

Part of the climate impact calculated using AirClim consists of the contribution of contrails. The method in which AirClim accounts for these contrails is by using the distance flown by the aircraft, and applying the local sensitivity to find the radiative forcing and ultimately the temperature change. In this method no distinction is made between the contrails of the different aircraft, even though these can vary in size and thickness. In order to assess the uncertainty in this calculation method, a weighing is applied to the contrail distance to account for the differences between aircraft. Other work shows that the total extinction of Airbus A380-produced contrails are about 1.5 to 2.5 times higher than those from a Bombardier CRJ. [58] This total extinction measures the disturbance of shortwave flux, and can serve as a metric for contrail significance. [58]

Based on this, a new distribution is formed by scaling the distance flown of each individual category within the 2012 inventory. It is assumed that category 7 contrails are double as effective as those originating from category 1 aircraft, based on the given 1.5-2.5 range for the given examples. A linear increase over the categories is assumed for this factor, in this way a scaling factor is found for each category.. The total distance flown, which is solely used for contrail effects within AirClim, is assumed to remain the same in the new scenario, such that the overall contrail saturation will not significantly change and the main effect is a shift between the categories. To achieve this, the ratio between initial and adjusted distances is applied to all adjusted distances. The final scaling is applied to all distances of the categories within the emission inventory, after which the climate response is re-calculated. Table 5.1 shows how the scaling factor is determined, by applying the assumed effectiveness scaling between 1-2, adjusting the overall distance by this factor and ultimately scaling down to match the overall flown distance. The final scaling is applied to all distances flown in the inventory by each category to adjust for the effect of aircraft size on contrails.

Table 5.1: Contrail Scenario Scaling Factor

	Cat 1	**Cat 2**	**Cat 3**	**Cat 4**	**Cat 5**	**Cat 6**	**Cat 7**	Total
Effectiveness	1.00	1.17	1.33	1.50	1.67	1.83	2.00	-
Distance Flown [$10^9 km$]	3.84	4.99	15.8	20.9	5.02	5.74	6.12	62.4
Adjusted Distance [$10^9 km$]	3.84	5.82	21.1	31.3	8.37	10.5	12.2	93.1
Scaled Distance [$10^9 km$]	2.57	3.90	14.1	21.0	5.60	7.04	8.19	62.4
Final Scaling	0.67	0.78	0.89	1.00	1.12	1.23	1.34	1.00

The increase in effectiveness of contrail for larger aircraft shifts the 3 smallest aircraft categories towards a smaller impact, while the impact of the largest aircraft increases. The impact of category 4 remains equal, which matches the contrail scaling factor of 1 for this category. Due to contrails having a sizeable influence on the total climate impact of a category, the assumed change in effectiveness does affect how the individual categories compare overall. Category 7 now has a worse performance climate-wise than category 2, and also category 6 is at a distance from the middle cluster. As the total amount of contrails has not changed, the

overall temperature change due to aviation contrails shows little change. It is not exactly equal, due tot the change in global contrail distribution having more presence in areas where the largest aircraft are operated. In the end the results do show a relevant sensitivity towards the modelling of contrails, which is one of the more uncertain factors in aviation's climate change. Adjusting the contrail effectiveness to a rough estimate giving a category 7 a factor double of category 1 has resulted in a sizeable shift when comparing the climate impact of the various categories.

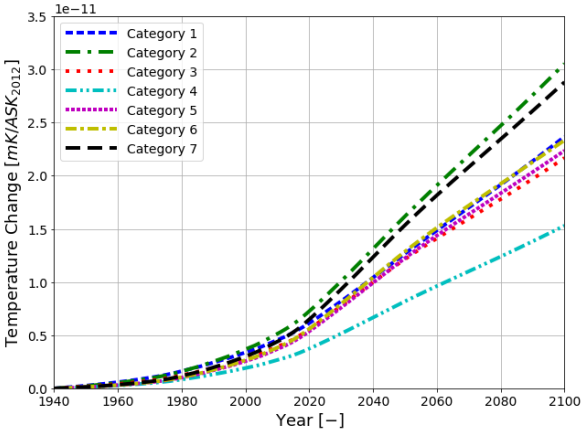

Figure 5.21: Base Temperature Change by Category

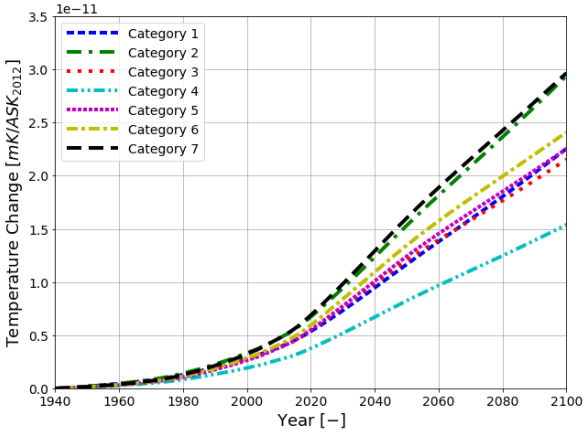

Figure 5.22: Contrail Adjusted Temperature Change by Category

5.4. NO_x Emission

Throughout the results section it was shown that the average NO_x emissions of the categories show significant differences between the used approach and the WeCare inventory. In order to address how a change in NO_x emissions would affect the results, an additional simulation was performed, in which the average NO_x emissions index matches those found from analysing the flight data. Table 5.2 shows with which factor the NO_x emissions within the database have been scaled, such that they match those of the used approach. As no fuel and emission calculations have been performed for aircraft within categories 1 and 2, their emissions have not been altered. Only for category 3 has a reduction in NO_x emission has been applied, whereas all other categories have seen an increase, up to a factor 2.2 for category 7.

Table 5.2: Average NO_x Emission Index Scaling Factor

	Cat 1	**Cat 2**	**Cat 3**	**Cat 4**	**Cat 5**	**Cat 6**	**Cat 7**
WeCare NO_x $[g/kg]$	10.6	11.8	20.8	12.3	13.1	12.9	12.7
Fuel Model NO_x $[g/kg]$	-	-	13.3	16.0	20.4	22.5	27.6
Scaling Factor	1.0	1.0	0.64	1.3	1.6	1.7	2.2

Since the NO_x emission overall has significantly increased, the magnitude of all NO_x related effects is larger. The overall temperature change by 2100 has increased to 163 mK, of which ozone alone accounts for 115 mK.

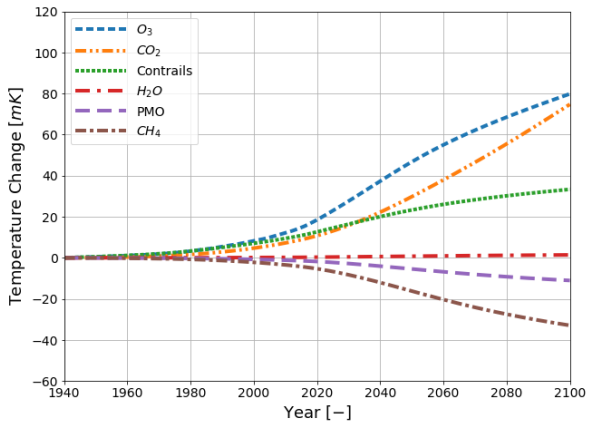

Figure 5.23: Base Temperature Change by Species

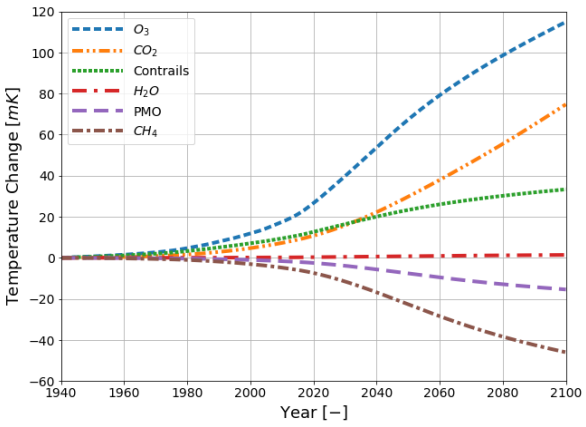

Figure 5.24: NO_x Adjusted Temperature Change by Species

As a result, there is a very large shift between the categories, affecting mostly the largest aircraft categories. The impact of category 7 by 2100 has increased by 34%. The gap between category 3 and 4 has tightened as category 3 improves while category 4 performs worse.

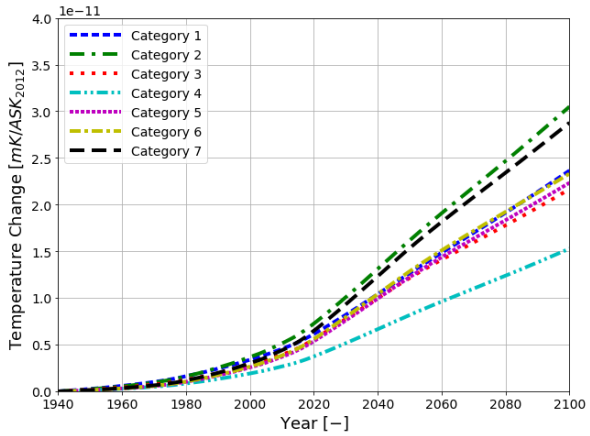

Figure 5.25: Base Temperature Change by Category

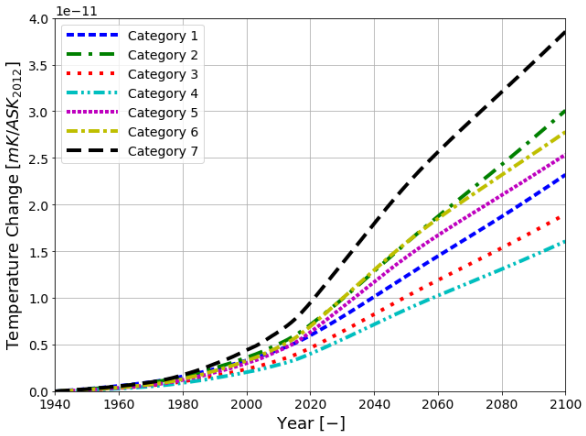

Figure 5.26: NO_x Adjusted Temperature Change by Category

It is clear that the actual emission levels of NO_x are uncertain, a fact which has a strong influence on the outcome. Adjusting the average NO_x emissions indices, those found from the fuel and emission model affect the performance of the larger aircraft, while they reduce the impact of category 3. Still, the climate impact per ASK is lowest for category 4, now at a smaller distance from category 3. While these changes show that the results in which categories are doing best hold up, the overall impact as well as that of the largest aircraft might have been considerably underestimated. However, this approach assumes the engine technology to be at the level of the aircraft that have been included when creating the OpenAP model. Since then improvements have been made, with the performance of the A320neo and 737-MAX being especially relevant. These are not yet part of this adjusted NO_x emissions.

6

Conclusion

In this work two approaches have been employed to compare the climate impact of different aircraft types. The overall impact in terms of temperature change is found by applying a climate response model to a set of emissions, which allows for a direct comparison between the impact of the categories. Flight data is used in combination with an aircraft performance model to investigate the influence of individual effects such as flight distance on the aircraft fuel use and emissions. This allows to draw conclusions on how individual factors affect the climate impact of an aircraft category.

The aircraft carrying 152-201 seats have the lowest climate impact per ASK and are outperforming other aircraft on multiple levels. These aircraft are used for flights with a distance close to the fuel optimal flight distance of ~2500 km, resulting in a lower fuel use for this category. For other aircraft flying the same distance this category also shows a better fuel efficiency. This is partially caused by the more efficient use of the capacity within the aircraft, as an assumed increase of seating density has been shown to reduce the difference. Moreover, the aircraft operate at a Mach number close to 0.77, which is lower than for the larger aircraft. This reduces the required thrust and is expected to positively affect fuel use and NO_x emission. Additionally, the aircraft within category 4 fly at a lower cruise altitude, which lowers the effective impact of the emitted NO_x. Lastly, the range of this category limits the aircraft in where it can fly. It is the category with the largest aircraft that has shown not to cross the Atlantic and almost exclusively stay within a continent. This means the aircraft fly in areas with a high contrail saturation and thus the impact of this category's contrails is small.

The two categories with the smallest aircraft, having a capacity of up to 100 seats, have a small total climate impact, but normalised to the ASKs are not performing well. The short distances for which these aircraft are used are expected to cause a higher relative fuel use. Additionally, due to the small size the effect of single contrail made by the aircraft is accounted for by a small number of seats, inflating relative importance. For these categories NO_x plays a smaller role, as the emission index is lower for smaller aircraft engines with a low rated thrust.

Category 3 is used for missions similar to category 4, but has a larger climate impact. The fuel efficiency is slightly worse and the higher cruise altitude increases the impact of NO_x. The analysis of the sensitivity of NO_x emissions showed that by adjusting the emission inventory to match the outcome of the performance model significantly improves category 3's relative performance which is then close to that of category 4.

The three categories with the largest aircraft have a great climate impact, with the highest for category 7. The aircraft have a longer range and the long-distance flights affect fuel efficiency. By flying in less busy areas, there is a smaller level of cloud saturation, increasing the impact of flown distance for these categories. Categories 5 and 6 have the highest average cruise altitudes, which increases the impact of NO_x emissions, which is already higher due to the increased engine size. The aircraft operate at the highest Mach numbers, affecting fuel use and emissions. A direct reduction in Mach number does not improve this however, as this would require adjusting the design. The higher comfort these aircraft provide in terms of space per seat increases the fuel use and NO_x emission per ASK; therefore an increase in seating density would reduce both.

7

Discussion and Recommendations

This research has the aim to show how the different aircraft compare in terms of climate impact, which can be used to formulate a strategy on how to mitigate the climate impact of aviation. Whereas aircraft manufacturers and airlines would want to reduce the climate impact of aircraft to gain a competitive advantage, any change leading to an increase in costs has little chance to be implemented unless required. It is therefore deemed important that governing bodies employ an effective policy on reducing the climate impact of aviation.

The Dutch government has announced to be looking to introduce a flight tax due to aviation's environmental effects, while there are also talks of a Europe-wide policy. [17, 18] This flight tax could consist of a €7 tax per departing passenger, to make the aviation sector more sustainable by flying cleaner with less CO_2 emissions. [18] Based on this research, it is suggested that a tax could be applied more fairly by taking into account the differences between flights. A long-distance flight with an aircraft carrying over 302 seats would not only have the largest impact overall, but even in terms of temperature change per ASK the impact is nearly double that of a flight with an aircraft carrying 152-201 seats.

Recently research has been done towards understanding the possibilities to include aviation's full climate impact in international policies. [49] It is suggested that a global emissions trading scheme for both CO_2 and non-CO_2 emissions would be best from an economic and environmental standpoint. By means of the average temperature response of a certain emission with specified location, an equivalent CO_2 mass is calculated for which a trading scheme can be used.

The difficulty in applying any climate-impact related policy is expected to lie in how this impact can effectively and fairly be quantified. Including all details of a given flight would lead to the most fair evaluation of its impact, but this can be excessively complex. For example, applying a statistical chance of contrail formation to the flown distance is easier to incorporate than measuring the actual formation of contrails. At the same time, this simplification would take away the incentive for airlines to adjust their routes to avoid contrail formation, as this would not be taken into account when quantifying their climate impact. This could be one of the reasons why the suggested policy on climate impact taxation is so superficial.

Even though it might be impossible to directly implement a policy that is completely fair, due to the uncertainties and complexity of the problem, this should not be a reason for not taking action. Moving towards the most effective policy can be done in multiple steps, iterating as the industry adapts. Based on the findings in this project, it is suggested that any proposed flight tax, such as the constant tax per departing passenger, would be adjusted to reflect the actual temperature response originating from each flight. The average temperature response per ASK for each category could be taken as a baseline to formulate a fair taxation. A continuous relation between aircraft size and ATR is suggested to be formulated, as this prevents the misuse by solely making use of aircraft which fall at the very edge of a category. The estimated ATR of a flight can simply be found by multiplying the appropriate ATR/ASK value by the distance flown and number of seats. The ATR-aircraft size relation should be updated occasionally to reflect the changes made by the industry. In order to keep the incentive for airlines to reduce their climate impact, any proven improvement not captured

by this metric should be rewarded accordingly. Ultimately, this would be only a first step towards a comprehensive policy, which takes into account the detailed emissions and temperature response of each individual flight.

In order to mitigate the climate impact of aviation, there are various options such as changes in aircraft design and operational use. What this research hopes to have shown is that direct gains can be achieved simply by employing the most efficient aircraft type for a given mission. For flight distances below 4000 km there is a large overlap in uses of the different aircraft types, even though aircraft with 152-201 seats have both the lowest fuel use and NO_x emission. Much larger aircraft are being used for the same missions, despite the higher fuel use. It is suggested to reduce the unnecessary usage of these aircraft, as this affects the climate impact. Only for flights exceeding 4000 km are these larger aircraft needed because of their longer range. This adjustment would require a higher frequency of flights, due to the smaller capacity, but would not affect the routes flown. Additional gains could be found by replacing long distance flights by several short distance flights with smaller aircraft, as long as this would not require significant deviations from the original flight path.

For any further analysis on this topic, it is recommended to reduce the uncertainty in the mass of the emitted NO_x. The adjustment that was made in terms of NO_x emission when analysing the uncertainty has shown that this is an important factor dividing the different categories. Narrowing the uncertainty range of the emissions will make it possible to better justify the results when going into the more detailed differences between the aircraft categories. Furthermore, it is suggested to use more recent data on aviation's global emissions and include newer aircraft models, such as the A320neo and 737-MAX, in assessing the aircraft performance, to ensure a higher relevance of the results considering aviation's current state.

Bibliography

[1] Airbus. Global market forecast 2019-2038, 2019.

[2] H. Appleman. The Formation of Exhaust Condensation Trails by Jet Aircraft. *Bulletin of the American Meteorological Society*, 34(1):14–20, 1953. ISSN 0003-0007. doi: 10.1175/1520-0477-34.1.14.

[3] BBC. France moves to ban short-haul domestic flights, 2021. URL https://www.bbc.com/news/world-europe-56716708.

[4] Tom Cooper, John Smiley, Chad Porter, and Chris Precourt. Global Fleet & MRO Market Forecast Commentary 2018-2028. *Oliver Wyman*, page 51, 2018. URL https://www.oliverwyman.com/content/dam/oliver-wyman/v2/publications/2018/January/2018-2028_Global_Fleet_MRO_Market_Forecast_Commentary_Public_Final_web.pdf.

[5] Katrin Dahlmann. Eine Methode zur effizienten Bewertung von Maßnahmen zur Klimaoptimierung des Luftverkehrs. 2012.

[6] Katrin Dahlmann, Alexander Koch, Florian Linke, Benjamin Lührs, Volker Grewe, Tom Otten, Doreen Seider, Volker Gollnick, and Ulrich Schumann. Climate-compatible air transport system-Climate impact mitigation potential for actual and future aircraft. *Aerospace*, 3(4):1–25, 2016. ISSN 22264310. doi: 10.3390/aerospace3040038.

[7] Eurocontrol. Aviation's recovery from the COVID-19 crisis will be a long-haul flight, 2020. URL https://www.eurocontrol.int/article/aviations-recovery-covid-19-crisis-will-be-long-haul-flight.

[8] FAA. Enr 1.5 holding, approach, and departure procedures. URL https://www.faa.gov/air_traffic/publications/atpubs/aip_html/part2_enr_section_1.5.html.

[9] FAA. Advisory Circular- Aircraft Weight and Balance Control. *Aviation*, AC 120-27E, 2005. ISSN 0047-2875. URL http://www.faa.gov/airports/resources/advisory_circulars/media/150-5345-51A/150_5345_51a.doc.

[10] David W Fahey and David S Lee. Aviation and Climate Change: A Scientific Perspective. 10(2):97–104, 2019.

[11] Christine Fichter. Climate impact of air traffic emissions in dependancy of the emission location and altitude. 2009.

[12] CAPA Centre for Aviation. World aviation: back to the last century, 2021. URL https://centreforaviation.com/analysis/reports/world-aviation-back-to-the-last-century-551095.

[13] Jan S. Fuglestvedt, Terje K. Berntsen, Odd Godal, Robert Sausen, Keith P. Shine, and Tora Skodvin. Metrics of climate change: Assessing radiative forcing and emission indices. *Climatic Change*, 58(3):267–331, 2003. ISSN 01650009. doi: 10.1023/A:1023905326842.

[14] M. Gauss, I.S.A. Isaksen, D.S. Lee, and O.A. Søvde. Impact of aircraft NO_x emissions on the atmosphere - Tradeoffs to reduce the impact. *Atmospheric Chemistry and Physics*, 6(6):1529–1548, 2006. doi: 10.5194/acp-6-1529-2006.

[15] A. Gettelman and C. Chen. The climate impact of aviation aerosols. *Geophysical Research Letters*, 40(11):2785–2789, 2013. ISSN 00948276. doi: 10.1002/grl.50520.

[16] Klaus Gierens. Contrails and contrail cirrus. *Encyclopedia of Aerospace Engineering*, 2010. doi: 10.1002/9780470686652.eae352.

[17] Dutch Government. Dutch government tables national flight tax bill, 2019. URL https://www.government.nl/latest/news/2019/05/14/dutch-government-tables-national-flight-tax-bill.

[18] Dutch Government. Plannen invoering nationale vliegbelasting, 2019. URL https://www.rijksoverheid.nl/onderwerpen/milieubelastingen/vliegbelasting.

[19] Brandon Graver, Kevin Zhang, and Dan Rutherford. CO_2 emissions from commercial aviation, 2018. *Working Paper 2019-16*, (September):13, 2019.

[20] V. Grewe and A. Stenke. AirClim: An efficient tool for climate evaluation of aircraft technology. *Atmospheric Chemistry and Physics*, 8(16):4621–4639, 2008. ISSN 16807324. doi: 10.5194/acp-8-4621-2008.

[21] Volker Grewe and Katrin Dahlmann. How ambiguous are climate metrics ? And are we prepared to assess and compare the climate impact of new air traffic technologies ? *Atmospheric Environment*, 106: 373–374, 2015. ISSN 1352-2310. doi: 10.1016/j.atmosenv.2015.02.039. URL http://dx.doi.org/10.1016/j.atmosenv.2015.02.039.

[22] Volker Grewe, Martin Dameris, Christine Fichter, and Robert Sausen. Impact of aircraft NO_x emissions. Part 1: Interactively coupled climate-chemistry simulations and sensitivities to climate-chemistry feedback, lightning and model resolution. *Meteorologische Zeitschrift*, 11(3):177–186, 2002. ISSN 09412948. doi: 10.1127/0941-2948/2002/0011-0177.

[23] Volker Grewe, Katrin Dahlmann, Jan Flink, Christine Frömming, Robin Ghosh, Klaus Gierens, Romy Heller, Johannes Hendricks, Patrick Jöckel, Stefan Kaufmann, Katrin Kölker, Florian Linke, Tanja Luchkova, Benjamin Lührs, Jesper van Manen, Sigrun Matthes, Andreas Minikin, Malte Niklaß, Martin Plohr, Mattia Righi, Simon Rosanka, Angela Schmitt, Ulrich Schumann, Ivan Terekhov, Simon Unterstrasser, Margarita Vázquez-Navarro, Christiane Voigt, Kai Wicke, Hiroshi Yamashita, Andreas Zahn, and Helmut Ziereis. Mitigating the climate impact from aviation: Achievements and results of the DLR WeCare project. *Aerospace*, 4(3), 2017. ISSN 22264310. doi: 10.3390/aerospace4030034.

[24] Volker Grewe, Sigrun Matthes, and Katrin Dahlmann. The contribution of aviation NO_x emissions to climate change: are we ignoring methodological flaws? *Environmental Research Letters*, 14(12):14–18, 2019. ISSN 17489326. doi: 10.1088/1748-9326/ab5dd7.

[25] R. Hein, M. Dameris, C. Schnadt, C. Land, V. Grewe, I. Köhler, M. Ponater, R. Sausen, B. Steil, J. Landgraf, and C. Brühl. Results of an interactively coupled atmospheric chemistry - General circulation model: Comparison with observations. *Annales Geophysicae*, 19(4):435–457, 2001. ISSN 09927689. doi: 10.5194/angeo-19-435-2001.

[26] IATA. Air passenger market analysis, 2013.

[27] IPCC. Special Report on Emission Scenarios. *International Panel on Climate Change*, (Emissions Scenarios):1–27, 2000. URL https://www.ipcc.ch/report/emissions-scenarios/.

[28] IPCC. *Climate Change 2013. www.climatechange2013.org*. 2013. ISBN 9781107661820.

[29] IPCC. Climate change 2014 synthesis report. 2014.

[30] KFW IPEX-Bank. The correlation between GDP growth and the increase in airline passengers 2001-2015. *Flash Analysis Credit Analysis*, (December):1–2, 2016. URL https://www.kfw-ipex-bank.de/pdf/Analyses-and-views/Market-analyses/2017-01-26-Blitz-Licht-Flughäfen-BIP-Faktor.pdf.

[31] L.R. Jenkinson, P. Simpkin, and D. Rhodes. *Civil Jet Aircraft Design*. Elsevier Ltd, 1999. ISBN 034074152X.

[32] Katrin Kölker, Peter Bießlich, and Klaus Lütjens. From passenger growth to aircraft movements. *Journal of Air Transport Management*, 56(Part B):99–106, 2016. ISSN 09696997. doi: 10.1016/j.jairtraman.2016.04.021.

[33] NOAA Global Monitoring Laboratory. Trends in atmospheric carbon dioxide, 2021. URL https://gml.noaa.gov/ccgg/trends/.

[34] D S Lee, G Pitari, V Grewe, K Gierens, J E Penner, A Petzold, M J Prather, U Schumann, A Bais, T Berntsen, D Iachetti, L L Lim, and R Sausen. Transport impacts on atmosphere and climate : Aviation. *Atmospheric Environment*, 44(37):4678–4734, 2010. ISSN 1352-2310. doi: 10.1016/j.atmosenv.2009.06.005. URL http://dx.doi.org/10.1016/j.atmosenv.2009.06.005.

[35] D. S. Lee, D. W. Fahey, A. Skowron, M. R. Allen, U. Burkhardt, Q. Chen, S. J. Doherty, S. Freeman, P. M. Forster, J. Fuglestvedt, A. Gettelman, R. R. De León, L. L. Lim, M. T. Lund, R. J. Millar, B. Owen, J. E. Penner, G. Pitari, M. J. Prather, R. Sausen, and L. J. Wilcox. The contribution of global aviation to anthropogenic climate forcing for 2000 to 2018. *Atmospheric Environment*, 244(February 2020), 2021. ISSN 18732844. doi: 10.1016/j.atmosenv.2020.117834.

[36] David S Lee, David W Fahey, Piers M Forster, Peter J Newton, Ron C N Wit, Ling L Lim, Bethan Owen, and Robert Sausen. Aviation and global climate change in the 21st century. *Atmospheric Environment*, 43(22-23):3520–3537, 2009. ISSN 1352-2310. doi: 10.1016/j.atmosenv.2009.04.024. URL http://dx.doi.org/10.1016/j.atmosenv.2009.04.024.

[37] D.S. Lee, I. Köhler, E. Grobler, F. Rohrer, R. Sausen, L. Gallardo-Klenner, J.G.J. Olivier, F.J. Dentener, and A.F. Bouwman. Estimations of global NO(x) emissions and their uncertainties. *Atmospheric Environment*, 31(12):1735–1749, 1997. ISSN 13522310. doi: 10.1016/S1352-2310(96)00327-5.

[38] Th J. Mulder and G. J.J. Ruijgrok. On the reduction of NO_x-emission levels by performing low NO_x flights. *ICAS Secretariat - 26th Congress of International Council of the Aeronautical Sciences 2008, ICAS 2008*, 2:3226–3235, 2008.

[39] Gunnar Myhre, Cathrine Lund Myhre, Piers M. Forster, and Keith P. Shine. Halfway to doubling of CO2 radiative forcing. *Nature Geoscience*, 10(10):710–711, 2017. ISSN 17520908. doi: 10.1038/ngeo3036.

[40] Angela Nuic, Damir Poles, and Vincent Mouillet. BADA: An advanced aircraft performance model for present and future ATM systems. *International Journal of Adaptive Control and Signal Processing*, 24 (10):850–866, 2010. ISSN 08906327. doi: 10.1002/acs.1176.

[41] International Civil Aviation Organization. Aircraft engine emissions databank, 2020.

[42] International Civil Aviation Organization. Future of Aviation, 2020. URL https://www.icao.int/Meetings/FutureOfAviation/Pages/default.aspx.

[43] Yongha Park and Morton E. O'Kelly. Fuel burn rates of commercial passenger aircraft: Variations by seat configuration and stage distance. *Journal of Transport Geography*, 41:137–147, 2014. ISSN 09666923. doi: 10.1016/j.jtrangeo.2014.08.017. URL http://dx.doi.org/10.1016/j.jtrangeo.2014.08.017.

[44] Michael Ponater, Marius Bickel, Lisa Bock, and Ulrike Burkhardt. Towards Determining the Contrail Cirrus Efficacy. *Aerospace*, 8(2):42, 2021. ISSN 2226-4310. doi: 10.3390/aerospace8020042.

[45] J. Roskam. *Airplane Design: component weight estimation (Part V)*. 1999.

[46] Robert Sausen and Ulrich Schumann. Estimates of the climate response to aircraft CO_2 and NO(x) emissions scenarios. *Climatic Change*, 44(1-2):27–58, 2000. ISSN 01650009. doi: 10.1023/a:1005579306109.

[47] Matthias Schäfer, Martin Strohmeier, Vincent Lenders, Ivan Martinovic, and Matthias Wilhelm. Bringing up OpenSky: A large-scale ADS-B sensor network for research. *IPSN 2014 - Proceedings of the 13th International Symposium on Information Processing in Sensor Networks (Part of CPS Week)*, pages 83–94, 2014. doi: 10.1109/IPSN.2014.6846743.

[48] Matthias Schäfer, Martin Strohmeier, Matthew Smith, Markus Fuchs, Vincent Lenders, and Ivan Martinovic. OpenSky report 2018: Assessing the integrity of crowdsourced mode S and ADS-B data. *AIAA/IEEE Digital Avionics Systems Conference - Proceedings*, 2018-September, 2018. ISSN 21557209. doi: 10.1109/DASC.2018.8569833.

[49] Janina D. Scheelhaase, Katrin Dahlmann, Martin Jung, Hermann Keimel, Hendrik Nieße, Robert Sausen, Martin Schaefer, and Florian Wolters. How to best address aviation's full climate impact from an economic policy point of view? – Main results from AviClim research project. *Transportation Research Part D: Transport and Environment*, 45:112–125, 2016. ISSN 13619209. doi: 10.1016/j.trd.2015.09.002. URL http://dx.doi.org/10.1016/j.trd.2015.09.002.

[50] P. Schulte, H. Schlager, H. Ziereis, U. Schumann, S. L. Baughcum, and F. Deidewig. NO_x emission indices of subsonic long-range jet aircraft at cruise altitude: In situ measurements and predictions. *Journal of Geophysical Research Atmospheres*, 102(17):21431–21442, 1997. ISSN 01480227. doi: 10.1029/97jd01526.

[51] Seatguru. Airline seat maps. URL https://www.seatguru.com/.

[52] Keith P. Shine. Radiative forcing of climate change. *Space Science Reviews*, 94(1-2):363–373, 2000. ISSN 00386308. doi: 10.1023/A:1026752230256.

[53] Keith P. Shine, Terje K. Berntsen, Jan S. Fuglestvedt, Ragnhild Bieltvedt Skeie, and Nicola Stuber. Comparing the climate effect of emissions of short- and long-lived climate agents. *Philosophical Transactions of the Royal Society A: Mathematical, Physical and Engineering Sciences*, 365(1856): 1903–1914, 2007. ISSN 1364503X. doi: 10.1098/rsta.2007.2050.

[54] Junzi Sun. *Open Aircraft Performance Modeling Based on an Analysis of Aircraft Surveillance Data*. 2019. ISBN 9789055841745. doi: 10.4233/uuid.

[55] Junzi Sun, Jacco M. Hoekstra, and Joost Ellerbroek. OpenAP: An open-source aircraft performance model for air transportation studies and simulations. *Aerospace*, 7(8), 2020. ISSN 22264310. doi: 10.3390/AEROSPACE7080104.

[56] Junzi Sun, Jacco M. Hoekstra, and Joost Ellerbroek. Estimating aircraft drag polar using open flight surveillance data and a stochastic total energy model. *Transportation Research Part C: Emerging Technologies*, 114(May):391–404, 2020. ISSN 0968090X. doi: 10.1016/j.trc.2020.01.026.

[57] E. Torenbeek. *Optimum cruise performance of subsonic transport aircraft*. 1995.

[58] S. Unterstrasser and N. Görsch. Aircraft-type dependency of contrail evolution. *Journal of Geophysical Research*, 119(22):14,015–14,027, 2014. doi: 10.1002/2014JD022642.

[59] Detlef P. van Vuuren, Jae Edmonds, Mikiko Kainuma, Keywan Riahi, Allison Thomson, Kathy Hibbard, George C. Hurtt, Tom Kram, Volker Krey, Jean Francois Lamarque, Toshihiko Masui, Malte Meinshausen, Nebojsa Nakicenovic, Steven J. Smith, and Steven K. Rose. The representative concentration pathways: An overview. *Climatic Change*, 109(1):5–31, 2011. ISSN 01650009. doi: 10.1007/s10584-011-0148-z.

[60] C.W.C. van Woensel. Integration of a Liquid Hydrogen Fuel Tank into the Concept of the Flying-V. 2021.

[61] Donata K Wasiuk, Anwar H Khan, Dudley E Shallcross, and Mark H Lowenberg. A Commercial Aircraft Fuel Burn and Emissions Inventory for 2005 – 2011. (June), 2016. doi: 10.3390/atmos7060078.

[62] Joda Wormhoudt, Scott Hemdon, Paul Yelvington, and Richard Miake-Lye. Nitrogen oxide (no/no2/hono) emissions measurements in aircraft exhausts. *Journal of Propulsion and Power*, 23(5), 2007. doi: 10.2514/1.23461.